Geoenvironmental Management of Excavated Earthen Materials with Geogenic Contamination

2024

Tomohiro KATO

ABSTRACT

Many construction projects involving large-scale earth excavation and cutting have generated a lot of excavated soil. Since transporting and disposing of soil is highly costly, and landfill space is limited in Japan, surplus soil should be utilized as geomaterials for sustainable development. However, since geogenic contaminants, such as arsenic (As) and fluorine (F), are widely distributed in Japan, excavated soils often contain heavy metals or metalloids slightly exceeding the environmental standard values due to natural resources. Therefore, environmental safety must be paid attention to the risks of soil groundwater contamination when using excavated earthen materials with geogenic contamination. The proper countermeasures are required to establish the utilization of excavated earthen materials with geogenic contamination. As one of the promising countermeasures, the attenuation layer method is considered. Evaluating the leaching behavior of geogenic contaminants closer to the on-site condition and the sorption performance of the attenuation layer are vital issues to design. Therefore, this dissertation conducted batch leaching tests modifying temperature conditions, shaking conditions, and soil-water contact time were conducted. Column leaching tests also obtained concentration profiles to discuss the interpretation of the results. As for column sorption tests, soil amended with a stabilizing agent was compacted in the acrylic column to evaluate the sorption performance against fluoride. An immobilized amount was proposed as an index to evaluate how much contaminant was captured in the attenuation layer. As for the numerical analysis, the safer design obtaining underestimated partition coefficients was discussed because of the limitation of the conventional advection-dispersion analysis for soil amended with a stabilizing agent because of its complex chemical reaction. Finally, the linkage of the results obtained in each chapter was discussed regarding the environmental management of excavated earthen materials with geogenic contamination.

The leaching behavior of arsenic and boron is evaluated in this work through two types of excavated earthen materials with geogenic contamination under different temperatures. The materials with geogenic contamination are expected to be usable for embankments, while the leaching behavior might change because of changes in the ground temperature. However, the effects of temperature on the leaching behavior of such rocks have not been well examined. Herein, batch leaching tests at temperatures between 5 and 60°C were performed under shaking and nonshaking conditions. Mudstone and shale rock were crushed into particles smaller than 2 mm, which were required for the tests. The tests were carried out for durations ranging from 6 h to 15 days because changes in leaching kinetics also require careful evaluation. After conducting the nonshaking tests for 15 days at 40°C, the mudstone sample leached arsenic and boron at concentrations of ~0.7 mg/L and ~1.0 mg/L, respectively. The arsenic and boron concentrations were about 20 and 40% higher than those of the sample leached at a temperature of 20°C. Elevated temperatures were seen to increase the leaching kinetics of the toxic elements. For the shale rock sample, the leaching rate for arsenic was 7.7×10^{-2}/h at 40°C, which was about 2.5 times greater than the value at 30°C. The nonshaking tests showed higher leaching amounts of arsenic and boron than the shaking tests, especially at elevated temperatures. As unrealistic estimations should be avoided, nonshaking tests are suggested. Moreover,

nonshaking tests lasting longer than 6 h are necessary due to the relatively slow dissolution of minerals.

Up-flow column percolation tests were conducted to discuss the rigor interpretations and the engineering applications, adequate descriptions of which have been limited. Two types of marine sediments were tested using the two different sizes of columns (ϕ 5 cm × h 10 or 30 cm) with a flow rate of 12 or 36 mL/h. Trends in concentrations with pore volumes of flow (PVF) were examined. Since the concentration trends of selenium provided a monotonous decrease and showed the maximum value of approximately 0 PVF, and showed half of the maximum value less than 1 PVF, their leaching was considered to diminish immediately. On the other hand, arsenic and fluorine concentrations showed initial increases and consequent decreases, therefore their leaching continued after 10 PVF. Since monotonous decreasing leaching contaminants show the maximum concentration of approximately 0 PVF, a more realistic risk analysis can be conducted to obtain the maximum concentration from column tests. To investigate the trends in concentrations, column tests should be carried out at least 2 PVF.

Sorption-desorption column tests using acrylic columns (ϕ 5 cm × h 10 cm) evaluated the sorption performance of the attenuation layer against geogenic contamination. The attenuation layer material was silica sand amended with 1, 5, or 10% of a stabilizing agent. The main component of the agent was magnesium oxide. The sorption behaviors of the materials were determined using a fluoride solution (C_0 = 80 mg/L F^-), while the desorption behaviors were determined using distilled water. Breakthrough (C/C_0 > 0.05) occurred after approximately 1, 20, and 50 PVF for 1, 5, and 10% of stabilizing agent content, respectively. The one-dimensional advection-dispersion equation modelled the breakthrough curves from the tests. The predictions gave unrealistic estimates, especially for the breakthrough point where C/C_0 = 0.05. For a 1% agent content, approximately 20% of the sorbed mass, S_s, was desorbed, but the percentage of desorbed mass, S_d, was much smaller for a higher agent content. The difference between the sorbed and desorbed mass was defined as the immobilized fraction, S_s - S_d. For a 5% agent content, S_s - S_d = 4.0 mg/g. The results suggest that when silica sand is amended with magnesium oxide as an agent, the mixture can immobilize fluoride in the attenuation layer.

Breakthrough curves which are assumed to be obtained from column sorption tests are simulated using numerical analysis. Four different methods to obtain partition coefficients from breakthrough curves are discussed to investigate the evaluation of attenuation layer. The one-dimensional advection-dispersion analysis was conducted considering attenuation layer of 30 cm thickness using these obtained partition coefficients. Partition coefficients were determined within approximately 40% differences. The partition coefficient obtained using inverse analysis to fit numerical solution provided the lowest determination, and earlier breakthrough than the parameters determined by Freundlich parameters.

As practical imprecations, since categorizing the leaching behavior of readily soluble toxic chemicals is essential to the robust design of the attenuation layer, column leaching tests with even small scale and short duration are recommended. On the other hand, the contaminants whose leaching is expected to continue should investigate the equilibrium concentrations. Finally, the promising countermeasures against excavated earthen materials with geogenic contamination were discussed with the linkage between evaluating the leaching behavior of geogenic contaminants closer to the on-site condition and the sorption performance of the attenuation layer.

ACKNOWLEDGEMENTS

The research shown herein is mainly organized when the author studied and did research at Kyoto University. I am fortunate to have had great support and guidance from professors, friends, and family during these days. It is a pleasure to express gratitude to all these people.

First and foremost, I would like to express profound gratitude and appreciation to my supervisor, Professor Takeshi Katsumi, Graduate School of Global Environmental Studies (GSGES), Kyoto University, for his continuous and generous support throughout my studies and carriers, starting research as an undergraduate student in April 2017. His insightful advice and support always inspired me and broadened my horizons. Based on his deep insight and experiences as a professor, I completed the present work with his guidance. In particular, I appreciate that he gives me many opportunities to go on business trips regarding site investigation, attend conferences and technical committees, and meet with the experts. Through these unique activities, I can learn many things and realize that the life of a professor in civil engineering, especially in the geotechnical engineering field, is wonderful and exciting. The best memory is the discussion when I started writing my first journal paper in April 2020. Although busy, he took the time to check my writing and showed me the crucial points in journal papers. Thanks to his guidance, I can start my career smoothly and enjoy my life every day.

Special thanks to Professor Hideaki Yasuhara, Graduate School of Engineering, Kyoto University, for his help, advice, and suggestions. I would like to contribute more as a member of the geotechnical teams at Kyoto University. Since I am interested in ground improvement using biogeotechnics, I would be happy to study reading his publications. Sincere thanks are also extended to Professor Masashi Kawasaki and Professor Shinya Echigo, GSGES, Kyoto University, for their review of the author's scholarship.

I would also like to offer my sincere gratitude to my other supervisor, Associate Professor Atsushi Takai, GSGES, Kyoto University, for his warm support and encouragement throughout my studies and carriers. This research work is only complete with his valuable suggestions and kind cooperation. The author could learn a great deal about experiments and how to write academic theses and applications for research funds. The best memory is insightful teaching how to prepare the application for JSPS scholarships. When I decided to enter the doctoral course in April 2019, he took the time to check my documents and carefully explained what the highlight was. Based on this experience, I have been continuing the researcher's life. Also, my presentation skills are matured by his patient guidance.

The author wishes to express his heartfelt gratitude to Professor Masashi Kamon, Professor Emeritus of Kyoto University. Since I can learn a lot about the history of geoenvironmental engineering and the future perspective from him, it is a great pleasure to have opportunities to spend time with him.

The author acknowledges to Professor Toru Inui, Graduate School of Engineering, Kyoto University. Thanks to his technical guidance on my bachelor's research, I realized the fun of research and acquired the skills.

Special thanks are also extended to Professor Ryosuke Uzuoka, Disaster Prevention Research

Institute (DPRI), Kyoto University, and Professor Yosuke Higo, Graduate School of Engineering, Kyoto University, for his kind encouragement. I appreciate that both professors often visit our laboratory and give me kind advice. Also, I would like to thank Dr. Ryunosuke Kido, Assistant Professor, Graduate School of Engineering, Kyoto University, for his kind support.

The author would like to express appreciation to Dr. Gathuka Lincoln Waweru, Researcher, National Institute for Environmental Studies (NIES). We had worked together for six years, from April 2017 to March 2023. He is both my senior researcher and a kind of good friend. I learned many things from him, such as writing research papers, chemical measurements, and international perspectives. Although we sometimes had conflicts regarding the research direction or life values, we finally had a best relationship to overcome the honest discussion. Currently, we are in different places, but I hope to keep in touch continuously and write more journal papers.

The author wishes to extend sincere appreciation to Dr. Tetsuo Yasutaka, Dr. Yukari Imoto, Dr. Kazuya Morimoto, and Ms. Miu Nishikata, Researchers at the Research Institute for Geo-Resources and Environment of National Institute of Advanced Industrial Science and Technology (AIST). Since my supervisor recommended joining the project of standardizing the batch and column sorption tests for evaluating the stabilizing agent for the attenuation layer, the author has been learning many things from them. I usually respect Dr. Tetsuo Yasutaka's decision-making speed and finding through the essence. When I struggled to write the first journal paper, he showed me how to write a straightforward introduction. This experience changed my research life. I have never forgotten the incredible time I spent studying numerical analysis, writing papers, and discussing new research plans with Dr. Yukari Imoto in AIST in August 2020, March 2021, and August 2021. Since she gave me many unique research approaches, I would like to expand my research topics in the future. I am grateful and appreciate the kindness and encouragement given by Dr. Kazuya Morimoto. Although our study fields are slightly different, he patiently explains the stabilizing agent's sorption mechanisms from the geochemistry perspective. He also teaches me how enjoyable the mineralogy is when we have a meal. When I was tired in Tsukuba, he invited me to dinner and cheered me up. Since Ms. Miu Nishikata and I are in the same generation, I am inspired by her hard work. Also, she kindly taught me about X-ray diffraction analysis. This research has never been completed without their kind cooperation and guidance.

The author would like to express appreciation to all members of the Environmental Engineering Laboratory at Kyoto University. Ms. Kaoru Hijino, Ms. Yuki Kadowaki, and Ms. Miho Yasumoto, Administrative Assistant in the laboratory, helped the author with many administrative works. Thanks to their kind cooperation, I can focus on my research. Special thanks are also extended to Mr. Yusuke Iwata, Ms. Haruka Kasai, Mr. Takaomi Okada, Mr. Yosuke Kinoshita, and Mr. Yusuke Masaki for their kind support for many experimental works, especially during the author's student days. When I decided to go on the doctoral course in April 2019, I worried about whether I could survive because I did not expect new human relations. However, my thinking needed to be corrected. I was surrounded by many grateful junior lab members, not only mentioned above but also all of my lab mates. The time spent with my lovely juniors is my treasure. Although I started my career in October 2021, and the position differed from the previous one, I am happy because current junior members still invite me to lunch. During the time I was preparing this dissertation,

both Dr. Zhang Yu and Ms. Aye Cho Cho Zaw encouraged me. I appreciate her kind support. Especially for Cho Cho, since we have spent both good and bad times together in the six years, I am happy to submit the dissertation simultaneously.

I would like to express my appreciation to my friends in the doctoral program, Dr. Jun Kurima, Assistant Professor, The University of Tokyo and Dr. Akihiko Sato, JSPS research fellowship, Kyoto University. Thanks to them, I had never felt alone, and kept my research motivations.

Many thanks are also extended to the members of the committees the author is joining, the Technical Committee on Geoenvironmental Engineering (Japanese Geotechnical Society). It was my pleasure to discuss the geoenvironmental issues with the members. Especially, I would like to extend sincere appreciation to Dr. Yoshikazu Otsuka, Okumura Corporation Co., Ltd., for his energetic support. Since I was a master's student in 2019, he has kindly treated me as one of the researchers and given me many opportunities to visit construction sites. I would like to extend thanks to Mr. Shinji Miyaguchi, OYO Corporation Co., Ltd., for his constructive discussions. I am happy to work with him in our laboratory starting in 2023. Finally, I sincerely thank Dr. Atsushi, Ogawa, Okumura Corporation Co., Ltd., for his kind encouragement. Since we have spent time with him since I was a master course student, I have many memories with him.

Finally, my most deeply felt gratitude goes to my family, namely, my parents, Kinichi and Naoko, and my young sister Ayumi, for all their love, support, and faith. I dedicate this dissertation to them.

February 2024

Tomohiro KATO

TABLE OF CONTENTS

Chapter 1

Introduction

1.1 Background

A large amount of excavated soil has been generated, as shown in Fig. 1.1. For example, there are many projects involving large-scale earth excavation and cutting, such as the construction of the Hokuriku Shinkansen (scheduled to open in March 2024 between Kanazawa and Tsuruga), the Hokkaido Shinkansen (scheduled to open in FY 2030 between Shin-Hakodate-Hokuto and Sapporo), the maglev train (scheduled to open in FY 2027 between Tokyo-Nagoya), the underground highway expresses in the Tokyo metropolitan area, and the 2025 Osaka Expo. Because linearity is important for Shinkansen trains and expressways, the frequency of tunnel excavation, such as a mountain tunnel, a shield tunnel, is increasing compared to conventional infrastructure development.

Excavated soil in Japan is generally divided into surplus soil and sludge. Since transporting and disposing of soil is highly costly, and landfill space is limited in Japan (e.g., Katsumi et al., 2017), the surplus soil should be utilized as geomaterials for the sustainable development. Also, a balance between cutting and filling should be provided (Katsumi, 2017). In other words, using the soil generated from cutting and tunnel excavation (hereafter surplus soils) as much as possible for embankments or filling materials is necessary (Magnusson et al., 2019). According to the Ministry of Land, Infrastructure, Transport, and Tourism (MLIT), the material recycling ratio of surplus soil in fiscal 2018 was as low as 80% and has yet to progress (MLIT 2020). To increase the utilization of surplus soil, MLIT has set a target value of 80% in FY 2024 for the material recycling of surplus soils, and various kinds of efforts are conducted (Sumikura and Katsumi, 2022).

(a)  (b) 

Figure 1.1 The source of excavated soil (a) the mountain tunnel, or (b) the shield tunnel.

Geogenic contaminants, such as arsenic (As), fluorine (F), and lead (Pb), are widely distributed in Japan (e.g., Tabelin et al., 2013; Ito and Katsumi, 2020). Excavated soils often contain heavy metals or metalloids exceeding the environmental standard values due to natural resources, such as the geological process (e.g., Tamoto et al., 2015; Tabelin, 2018). Therefore, when using large volumes of excavated soils, environmental safety must be paid attention to the risks of containing and leaching the toxic chemicals (e.g., Naka et al., 2016; Gathuka et al., 2021; Tang et al., 2023). In Japan, the Soil Contamination Countermeasures Act Law (SCCL) was enacted in 2002 to prevent soil groundwater contamination. Although SCCL initially targeted only anthropological contamination, the law was revised in 2010 to include geogenic contamination. Due to the strict standard value, surplus soil containing a slight amount of geogenic toxic chemicals exceeding the limits became challenging to utilize.

However, most geogenic contaminants are contained in low concentrations even if geogenic heavy metals or metalloids do not meet the standards (Ito and Katsumi, 2020). In addition, they are only distributed in specific geological regions (Katsumi, 2017). Therefore, the dealing was pointed out as an excessive response. In 2017, SCCL reforming made it possible to move and utilize the excavated soils and rocks with geogenic contamination under proper management. In other words, soils are expected to be utilized while taking risks into account (Katsumi, 2019). In 2020, MLIT established the "Construction Recycling Promotion Plan 2020 - Towards recycling that emphasizes quality." Among these goals, a target value has been set for increasing the material recycling ratio of surplus soil to more than 80% by 2024 (MLIT, 2020). To achieve this goal, the proper countermeasures for the utilization of geogenically contaminated soils while considering their naturally occurring properties.

A proper countermeasure that meets both workability and economics should be established to increase the material recycling ratio of geogenically contaminated soils. First, the leaching behavior of heavy metals or metalloids from excavated soil must be precisely elucidated to achieve this goal. Batch and column tests are often applied to evaluate the leaching behavior of solid materials (e.g., Grathwohl and Susset, 2009; Tang et al., 2023).

The SCCL specifies a batch test of 6 hours of shaking at room temperature. This test called the Environmental Agency Notification No.46: Leaching Test Method for Soils (hereafter JLT46) test, determines whether the leaching concentration exceeds the regulatory limit. However, since the test targeted anthropology contamination, the evaluation may be far from the reality of geogenic contamination (Katsumi, 2017). Basic parameters such as shaking time and liquid-solid ratio have yet to be studied sufficiently. Furthermore, considering that excavated soil is used in shallow ground such as embankments, the temperature should also be considered a parameter (e.g., Menberg et al., 2013; Saito et al., 2018; Takai et al., 2020; Ogawa et al., 2023). The fundamental parameters of temperature, shaking condition, and soil-water contact time should be evaluated.

Column testing is a more realistic evaluation than batch testing. Standardization of column testing methods has progressed in recent years, and the International Organization for Standardization (ISO) and Japanese Industrial Standards (JIS) standards have been completed. Although the test method has been established, there needs to be more discussion about how column test results can be used to design countermeasures for the excavated soils and rocks with geogenic contamination. Challenges include utilizing

column test results and considering the linkage between lab tests and construction sites.

One of the simple countermeasures for utilizing soil containing heavy metals or metalloids is the attenuation layer method. This method has a soil layer for stabilizing contaminants. The attenuation layer is constructed beneath the excavated soils and rocks with geogenic contamination, and when pore water containing contaminants permeates, they are immobilized. Compared to containment methods that use geomembranes or clay liners to prevent infiltrating water completely, geogenic contaminants might leach out. However, the attenuation layer has the advantage of workability and economics. Various studies have evaluated the sorption performance of the attenuation layer materials, including material development and natural ground sorption performance (e.g., Tatsuhara et al., 2015; Mo et al., 2020; Nishikata et al., 2022).

On the other hand, a method for determining the partition coefficient, K_d, a parameter indicating sorption performance, from column tests has yet to be fully established. Also, a design method for the sorption layer method has yet to be established. In particular, few studies target specimens that are a mixture of soil (called as a parent material, a natural material) and a stabilizing agent (an artificial material). More fundamental knowledge regarding sorption performance is required. Therefore, it is necessary to conduct basic column experiments and advection-dispersion analysis to evaluate whether the conventional models regarding the chemical reaction between soils and chemicals can be applied to the soil-stabilizing agent mixture.

1.2 Objectives

The main objective of the present study was to investigate the leaching behavior of geogenic contaminants closer to the on-site condition using modified batch leaching tests and column leaching tests. In addition, the sorption performance of the attenuation layer was evaluated using column sorption experiments and the advection-dispersion analysis. Finally, the linkage between evaluating leaching behavior and sorption performance was discussed to elucidate the effectiveness of the attenuation layer method against geogenic contamination. The parameters for modified batch leaching tests were the temperature effect, leaching kinetics under different soil-water contact times, and shaking effect. As for column leaching tests, the column's height, the permeation's flow rate, and soil types were considered as the parameters, and the difference in the shape of the concentration profile was discussed. Mainly, the leaching behavior of the chemicals whose concentration was monotonously decreasing was focused on determining the boundary condition for the advection-dispersion analysis. As for column sorption tests, soil amended with a stabilizing agent was compacted in the acrylic column to evaluate the sorption performance against fluoride. An immobilized amount was proposed as an index to evaluate how much contaminant was captured in the attenuation layer. As for the numerical analysis of the advection-dispersion equation, since the limitation of the conventional advection-dispersion analysis for soil amended with a stabilizing agent because of its complex chemical reaction, the safer design obtaining underestimated partition coefficients was demonstrated.

Figure 1.2 shows that a schematic diagram of the objectives of the present study. This study plays

an important role in interpreting the leaching behavior closer to the reality and evaluating the sorption performance of the attenuation layer. The novelty of the present study is the challenge to deepen investigation for the batch leaching tests against geogenic contaminated soils, discussing the interpreting the results of column leaching tests, evaluating the applicability of advection-dispersion analysis for column sorption tests using soil amended with the stabilizing agent.

1.3 Structures of the thesis

This dissertation covers the following five subjects:

(1) Evaluation of leaching behavior of geogenic contaminants using modified batch leaching tests to evaluate the temperature effect, leaching kinetics, and effects of shaking conditions;

(2) Classification of leaching behavior of geogenic contaminants focusing on the shape of the concentration profiles obtained from column tests to consider the utilization of the test results;

(3) Investigation of the applicability of the advection-dispersion analysis for the soil amended with the stabilizing agent;

(4) Discussion of how to obtain the partition coefficients, K_d to design the attenuation layer as a safe side using the numerical analysis of the advection-dispersion equation;

(5) Giving the practical implications as the linkage of the evaluation of leaching behavior and sorption performance towards the robust design of the attenuation layer method based on subjects (1)-(4).

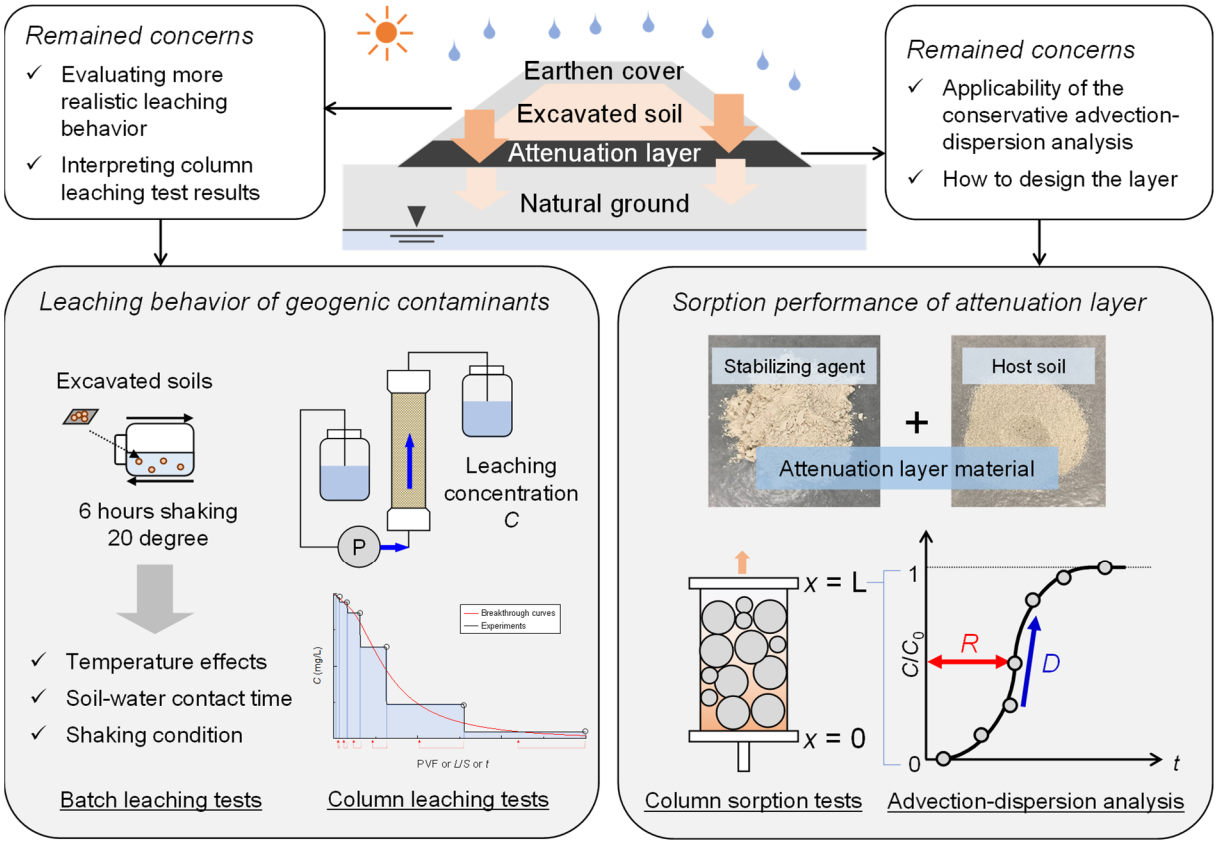

Figure 1.2 Schematic diagram of objectives of thesis.

In order to approach the above subjects, a series of the investigations were provided in this dissertation as shown in Fig. 1.3. Outlines of Chapter 2 to 8 are summarized below.

Chapter 2 presents a literature review regarding soil utilization, evaluating the leaching behavior of geogenic contaminants and countermeasures against geogenic contamination. The current status of soil utilization in Japan was explained, and material recycling was emphasized. Regarding the leaching behavior of geogenic contaminants, various testing methods and parameters that previous research focused on were presented. The characteristics of the attenuation layer method were mainly explained for the countermeasures, and how to currently evaluate the sorption performance was shown.

In Chapter 3, The leaching behavior of arsenic and boron is evaluated through two types of excavated rocks with geogenic contamination under different temperatures. Excavated rocks with geogenic contamination are expected to be usable for embankments after appropriate countermeasures have been taken against the risks brought about by geogenic contamination. The leaching behavior might change because of changes in the ground temperature. However, the effects of temperature on the leaching behavior of such rocks have not been well examined. Herein, batch leaching tests at temperatures between 5 and 60°C were performed under shaking and nonshaking conditions. Mudstone and shale rock were crushed into particles smaller than 2 mm, which were required for the tests. The tests were carried out for durations ranging from 6 h to 15 days because changes in leaching kinetics also require careful evaluation.

In Chapter 4, up-flow column percolation tests were conducted to discuss the rigor interpretations and the engineering applications, adequate descriptions of which have been limited. Two types of marine sediments were tested using the two different sizes of columns (ϕ 5 cm× h 10 or 30 cm) with a flow rate of 12 or 36 mL/h. Trends in concentrations with pore volumes of flow (PVF) were examined.

In Chapter 5, sorption-desorption column tests using acrylic columns (ϕ 5 cm× h 10 10 cm) were employed to evaluate the sorption performance of an attenuation layer against geogenic contamination. The attenuation layer material was silica sand amended with 1, 5, or 10% of a stabilizing agent. The main component of the agent was magnesium oxide. The sorption behavior of the materials was determined by a fluoride solution (C_0 = 80 mg/L F^-), while the desorption behavior was determined by distilled water.

In Chapter 6, towards the discussing the design of the attenuation layer, breakthrough curves which are assumed to be obtained from column sorption tests are simulated using numerical analysis. Four different methods to obtain partition coefficients from breakthrough curves are discussed to investigate the evaluation of attenuation layer. The one-dimensional advection-dispersion analysis was conducted considering attenuation layer of 30 cm thickness using these obtained partition coefficients, K_d.

In Chapter 7, practical implications regarding the utilization of the excavated soils and rocks with geogenic contamination are discussed based on the findings of Chapters 3-6. Since most previous research focuses on the leaching behavior of geogenic contaminants and sorption performance separately, this dissertation contributes to designing the proper countermeasures against geogenic contamination.

In Chapter 8, the conclusions of this thesis and recommendations for future directions were provided.

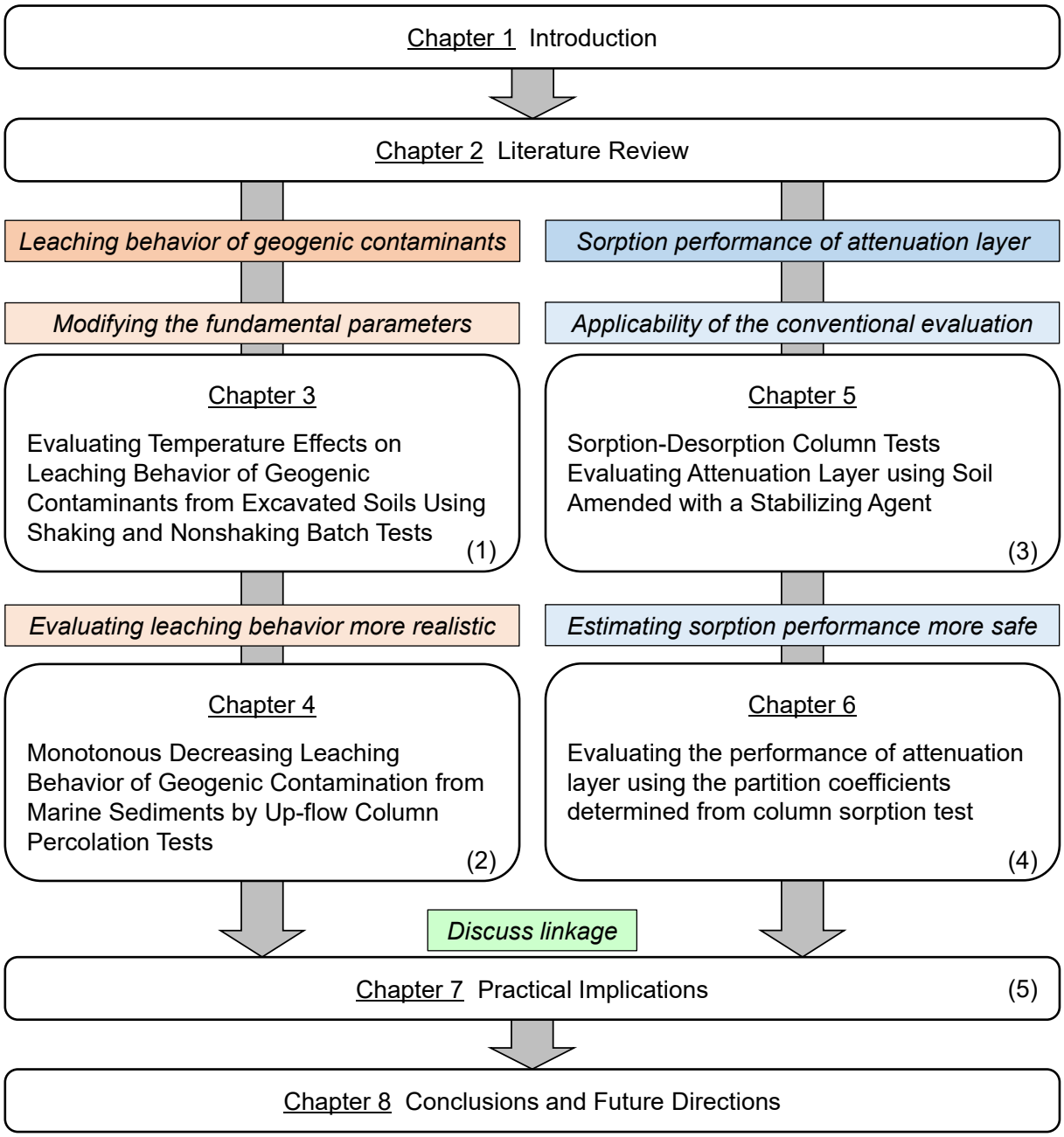

Figure 1.3 Structure of thesis and corresponding subjects.

References for Chapter 1

Grathwohl, P. and Susset, B., 2009. Comparison of percolation to batch and sequential leaching tests: theory and data. *Waste Management* 29, 2681–2688. https://doi.org/10.1016/j.wasman.2009.05.016.

Gathuka L.W., Kato, T., Takai, A., Flores, G., Inui, T. and Katsumi, T., 2021. Effect of acidity on attenuation performance of sandy soil amended with granular calcium-magnesium composite. *Soils and Foundations* 61(4), 1099-1111. https://doi.org/10.1016/j.sandf.2021.05.007.

ISO 21268-3, 2019. Soil Quality—Leaching Procedures for Subsequent Chemical and Ecotoxicological Testing of Soil and Soil Materials—Part 3: Up-Flow Percolation Test. *International Standardization Organization*.

Ito, H. and Katsumi, T., 2020. Leaching characteristics of naturally derived toxic elements from soils in the western Osaka area: considerations from the analytical results under the Soil Contamination Countermeasures Act. *Japanese Geotechnical Journal* 15(1), 119–130. https://doi.org/10.3208/jgs.15.119 (in Japanese).

Katsumi, T., 2017. Use of excavated soils with natural contamination. *Japanese Geotechnical Society Magazine*. 65 (11/12), 1–3 (in Japanese).

Katsumi, T., 2019. “Countermeasures against geogenic Contaminations”, *The Foundation Engineering & Equipment*, 47(6), 2-5 (in Japanese).

Magnusson, S., Johansson, M., Frosth, S., and Lundberg, K., 2019. Coordinating soil and rock material in urban construction—scenario analysis of material flows and greenhouse gas emissions. *Journal of Cleaner Production* 241, 118236. https://doi.org/10.1016/j.jclepro.2019.118236.

Menberg, K., Bayer, P., Zosseder, K., Rumohr, S., and Blum, P., 2013. Subsurface urban heat islands in German cities. *Science of the Total Environment* 442, 123–133. https://doi.org/10.1016/j.scitotenv.2012.10.043.

Ministry of Land, Infrastructure, and Transport, Japan, 2020. Material Reuse and Recycling Promotion Plan in Construction Works 2020 “Towards Recycling with an Emphasis on Quality. https://www.mlit.go.jp/report/press/sogo03_hh_000247.html (in Japanese) (accessed 3 July 2022).

Ministry of Land, Infrastructure, and Transport, Japan, 2020. Results of the Survey on Construction By-products in FY2018. https://www.mlit.go.jp/report/press/sogo03_hh_000233.html (accessed 3 July 2022) (in Japanese).

Ministry of Land, Infrastructure, and Transport, Japan, 2023. Technical Manual on the Countermeasure Against Soils and Rocks Containing Naturally Occurring Heavy Metals in Construction Works. https://www.mlit.go.jp/sogoseisaku/region/recycle/d11pdf/recyclehou/manual/shizenyurai2023.pdf (accessed 1 December 2023) (in Japanese).

Ministry of Environment, 1995. Environmental Agency Notification No.46: Leaching Test Method for Soils. http://www.env.go.jp/kijun/dojou.html (in Japanese) (accessed 27 October 2021).

Ministry of Environment, 2017. “Soil Contamination Countermeasure Law”, enacted in 2017 (accessed 3 July 2022) www.env.go.jp/water/dojo/dojogl2021_3.pdf. (in Japanese).

Mo, J., Flores, G., Inui, T., and Katsumi, T., 2020. Hydraulic and sorption performances of soil amended

with calcium-magnesium composite powder against natural contamination of arsenic. *Soils and Foundations* 60(5), 1084–1096. https://doi.org/10.1016/j.sandf.2020.05.007.

Naka, A., Yasutaka, T., Sakanakura, H., Kalbe, U., Watanabe, Y., Inoba, S., Takeo, M., Inui, T., Katsumi, T., Fujikawa, T., Sato, K., Higashino, K., and Someya, M., 2016. Column percolation test for contaminated soils: key factors for standardization. *Journal of Hazardous Materials* 320, 326–340. https://doi.org/10.1016/j.jhazmat.2016.08.046.

Nishikata, M., Yasutaka, T., Morimoto, K., and Imoto, Y., 2022. Evaluation of water contact influence on adsorbents by water immersion pretreatment and serial batch tests, *Japanese Geotechnical Journal* 17(2), 195–204. https://doi.org/10.3208/jgs.17.195 (in Japanese).

Ogawa, A., Takai, A., Sakanakura, H., and Katsumi, T., 2023. Evaluating temperature effects on diffusive releases from clay particles. *Proceedings of the 9th International Congress on Environmental Geotechnics (ICEG2023)* 1, 115–124. https://doi.org/10.53243/ICEG2023-162.

Saito, T., Hamamoto, S., Ueki, T., Ohkubo, S., Moldrup, P., Kawamoto, K., and Komatsu, T., 2016. Temperature change affected groundwater quality in a confined marine aquifer during long-term heating and cooling. *Water Research* 94, 120–127. https://doi.org/10.1016/j.watres.2016.01.043.

Sumikura, Y., and Katsumi, T., 2022. Material reuse and recycling in construction works in Japan, *Journal of Material Cycles and Waste Management*, 24, 1216–1227. https://doi.org/10.1007/s10163-022-01411-y.

Tabelin, C.B., Igarashi, T., Yoneda, T., and Tamamura, S., 2013. Utilization of natural and artificial adsorbents in the mitigation of arsenic leached from hydrothermally altered rock. *Engineering Geology* 156, 58–67. https://doi.org/10.1016/j.enggeo.2013.02.001.

Tabelin, C.B., Igarashi, T., Villacorte-Tabelin, M., Park, I., Opiso, E.M., Ito, M., and Hiroyoshi, N., 2018. Arsenic, selenium, boron, lead, cadmium, copper, and zinc in naturally contaminated rocks: a review of their sources, modes of enrichment, mechanisms of release, and mitigation strategies. *Science of the Total Environment* 645, 1522–1553. https://doi.org/10.1016/j.scitotenv.2018.07.103.

Takai, A., Iwata, Y., Gathuka, L.W., and Katsumi, T., 2020. Laboratory tests on arsenic leaching from excavated shale rock by elevated temperatures. *E3S Web of Conferences* 205, 09006. https://doi.org/10.1051/e3sconf/202020509006.

Tamoto, S., Tabelin, C.B., Igarashi, T., Ito, M., and Hiroyoshi, N., 2015. Short and long term release mechanisms of arsenic, selenium and boron from a tunnel-excavated sedimentary rock under in situ conditions. *Journal of Contaminant Hydrology* 175–176, 60-71. https://doi.org/10.1016/j.jconhyd.2015.01.003.

Tang, J., Sakanakura, H., Takai, A., and Katsumi, T., 2023. Effect of dry-wet cycles on leaching behavior of recovered soil collected from tsunami deposits containing geogenic arsenic. *Soils and Foundations* 63(1), 101271. https://doi.org/10.1016/j.sandf.2022.101271.

Tatsuhara, T., Jikihara, S., Tatsumi, T., and Igarashi, T., 2015. Effects of the layout of adsorption layer on immobilizing arsenic leached from excavated rocks. *Japanese Geotechnical Journal* 10(4), 635–640. https://doi.org/10.3208/jgs.10.635 (in Japanese).

Chapter 2

Literature Review

2.1 Current status of material recycling of surplus soils in Japan

Much excavated soil has been generated due to construction projects involving tunnel excavation. As explained in Section 1.1, many projects involve large-scale earth excavation and cutting, such as the construction of the Shinkansen, the maglev train, and the underground highway. Because linearity is important for Shinkansen trains and expressways, the frequency of tunnel excavation, such as a mountain tunnel or a shield tunnel, is increasing compared to conventional infrastructure development.

Excavated soil in Japan is generally divided into surplus soil and sludge. Since transporting and disposing of soil is highly costly, and landfill space is limited in Japan, surplus soil should be utilized as geomaterials for sustainable development. Also, a balance between cutting and filling should be provided (Katsumi, 2017). In other words, using the soil generated from cutting and tunnel excavation as much as possible for embankments or filling materials is necessary (Magnusson et al., 2019).

The status of the volume of the surplus soils generated in Japan is explained. In the survey by MLIT in 2012, the utilization ratio was as low as 65%. However, since many efforts are conducted in the construction society, such as establishing the matching system of the surplus soils, the utilization ratio has increased to approximately 80% in 2018, as shown in Table 2.1 (MLIT 2020; Sumikura and Katsumi, 2022). As mentioned earlier, the amount of soil used at construction sites was 61% in 2000 since many new materials were used. The amount of soil used at construction sites has increased to 83% in 2002 and 89% in 2018, respectively. This indicates that the use of excavated soil on site is enhanced. However, the recycling or utilization of excavated soils is remained to be lower than other categories; the utilization of the surplus soils is a crucial issue for the material recycling society. To increase the utilization ratio, MLIT has set a target value of more than 80% in FY 2024 for the material recycling of surplus soils.

Excavated soils can be dealt with in three ways. First, high quality surplus soil can be utilized as filling or for embankments without any treatment. Second, other kinds of surplus soil are reused after improvements have been made to them. Third, some surplus soil is not being used at all, but simply disposed of, with/without treatment. A classification for excavated soil has been established by MLIT as shown in Table 2.2 to promote the reuse of excavated soil. If slurry or sludge on the bottom line is not improved by applying the improvement method, slurry or sludge is regarded as industrial waste.

Figure 2.1 presents the material flow for excavated soils (Sumikura and Katsumi, 2022). Approximately 290 million m^3 of soil was excavated, while approximately 160 million m^3 was used on site.

Approximately 130 million m^3 of excavated soil was transported to different sites. The amount of excavated soil transported to inland reclamation was approximately 60 million m^3, which accounted for more than 40% of the excavated soil transported from the sites. This percentage includes the soil transported to the soil reclamation sites and the soil not yet used in construction works. Some of the surplus soil may have the potential for illegal dumping (Sumikura and Katsumi, 2022). Appropriate transportation and reclamation methods for excavated soils, as well as their traceability, are strongly demanded (Sumikura and Katsumi, 2022). Some excavated soils may be illegally dumped and cause environmental issues.

In conclusion to the explanations mentioned above, the utilization of the surplus soils is still halfway. More effort is required to increase the utilization ratio and reduce the mining of new soils from mountainous areas as much as possible. However, since some surplus soils contain geogenic contaminants as naturally occurring sources, and the leaching concentration of the toxic chemicals often slightly exceeds the environmental standards regulated by Soil Contamination Countermeasures Low (SCCL; MOE, 2017), the utilization of the surplus soils remains challenging. The issue regarding the leaching behavior of geogenic contaminants and the promising countermeasures towards the utilization of surplus soils containing geogenic contamination are shown in Sections 2.2 and 2.3.

Table 2.1 Target values described in "Material Reuse and Recycle Promotion Plan in Construction Works 2020 “Towards Recycling with an Emphasis on Quality" (Sumikura and Katsumi, 2022).

Category		Index	2018 target value	2018 actual value	2024 target value
	Asphalt-concrete waste	Recycling and reduction ratio	> 99%	99.5%	> 99%
	Concrete waste	Recycling and reduction ratio	> 99%	99.3%	> 99%
	Construction wood waste	Recycling and reduction ratio	> 95%	96.2%	> 97%
	Construction sludge	Recycling and reduction ratio	> 90%	94.6%	> 95%
	Construction mixed waste	Discharge ratio	< 3.5%	3.1%	< 3.0%
Construction waste		Recycling and reduction ratio	> 96%	97.2%	> 98%
Excavated soil		Utilization ratio	> 80%	79.8%	> 80%
(Reference value)					
Construction mixed waste		Recycling and reduction ratio	> 60%	63.2%	-

Table 2.2 Classification of excavated soil from construction works set by MLIT, with the selected properties (Sumikura and Katsumi, 2022).

Class of soil	Content (type and state)	Cone penetration strength, q_c (kPa)	Water content (%)
1st-class soil	Sand or gravel; improved soil	-	-
2nd-class soil	Sandy soil or gravely soil; improved soil	> 800	-
3rd-class soil	Sandy, silty or clay soil which can easily executed on; improved soil	> 400	< 40% (except for volcanic cohesive soil)
4th-class soil	Clay soil, expect for 3rd-class soil; improved soil	> 200	40-80%
Sludge	Slurry state soil or sludge	< 200	> 80%

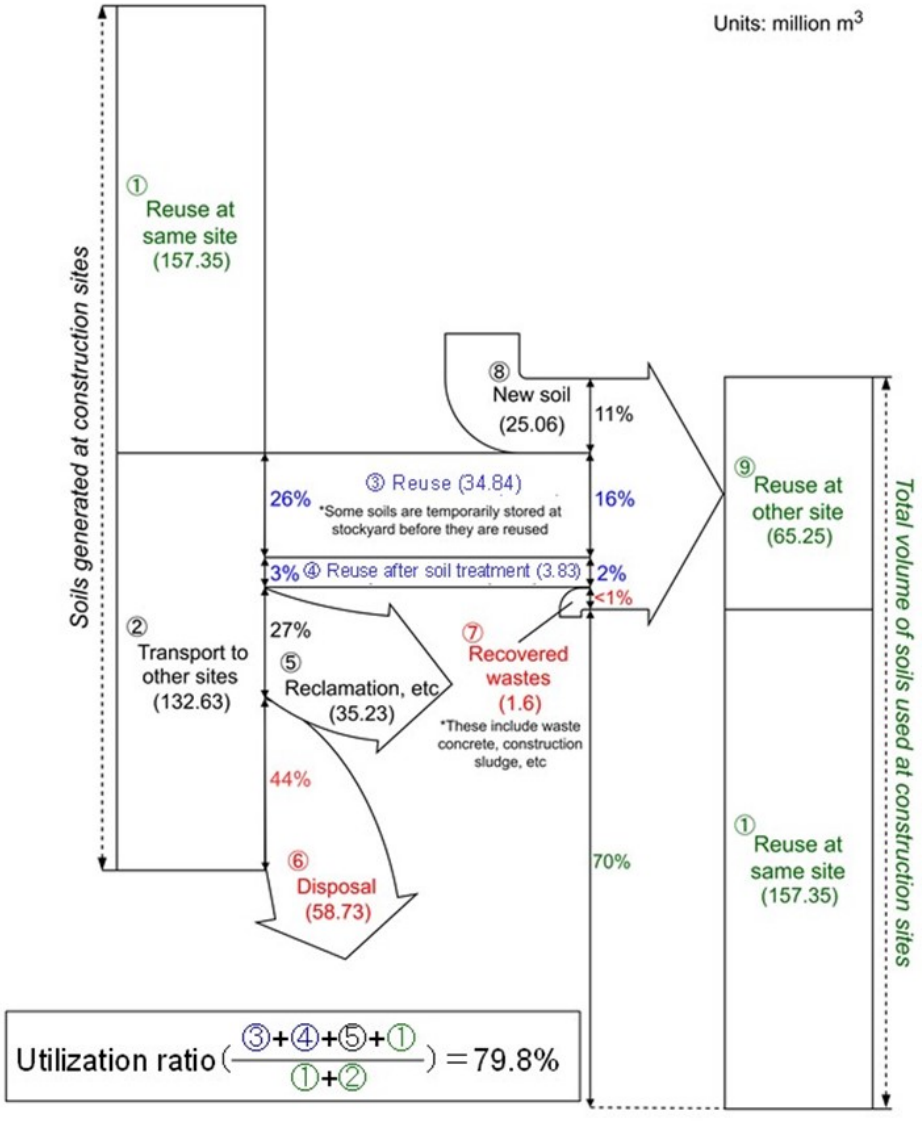

Figure 2.1 Material flow of excavated soil surveyed in FY 2018 (Sumikura and Katsumi, 2022).

2.2 Previous studies on leaching behavior of geogenic contaminants

2.2.1 Leaching tests regulated by Soil Contamination Countermeasures Low

Since many plates gather in Japan, the activity of geological processes, such as hydrothermal alteration, volcanic eruption, etc., is significant due to crustal deformation. Therefore, naturally existing heavy metals and metalloids, such as arsenic (As), fluorine (F), and lead (Pb), are widely distributed in Japan (e.g., Tabelin et al., 2013; Ito and Katsumi, 2020). In this dissertation, such toxic chemicals are called geogenic contaminants. The Clark number represents the proportion of elements present near the earth's surface in terms of mass percent concentration. In Japan, the Clark number of As is higher than the average value in the world (Katsumi, 2017).

Excavated soils often contain heavy metals or metalloids exceeding the environmental standard values due to natural resources, such as the above-mentioned geological process (e.g., Tamoto et al., 2015; Tabelin, 2018). Therefore, when using excavated soils, environmental safety must be paid attention to the risks of containing and leaching the toxic chemicals (e.g., Naka et al., 2016; Tang et al., 2023). In Japan, the Soil Contamination Countermeasures Act Law (SCCL) was enacted in 2002 to prevent soil groundwater contamination. Although SCCL initially targeted only anthropological contamination, the law was revised in 2010 to include geogenic contamination. Due to the strict standard value, surplus soil containing a slight amount of geogenic toxic chemicals exceeding the limits became challenging to utilize. After 2010, the fact that most geogenic contaminants are contained in lower concentrations compared to anthropological contamination, even if the leaching concentration of geogenic contaminants does not meet the standards, was revealed (Ito and Katsumi, 2020). In addition, geogenic contaminants are often distributed in specific geological regions (Katsumi, 2017). Therefore, the deal enacted in 2010 was pointed out as an excessive response. In 2017, SCCL reforming made it possible to move and utilize the excavated soils and rocks with geogenic contamination under proper management. In other words, soils are expected to be utilized while taking risks into account (Katsumi, 2019). However, as presented in Section 2.1, the utilization of the surplus soils has not yet been enough. To achieve a soil material recycling society, a proper countermeasure that meets workability, economics, and environmental safety should be established to increase the material recycling ratio of the excavated soils and rocks with geogenic contamination. As a primal issue, the leaching behavior of geogenic heavy metals or metalloids from excavated soil must be precisely elucidated because the countermeasures should be designed based on the levels of the leaching concentration.

Batch and column tests are often applied to evaluate the leaching behavior of solid materials (e.g., Grathwohl and Susset, 2009; Tang et al., 2023). One of the most basic leaching tests described by the Ministry of Environment MOE) Japan is shown herein. As illustrated in Fig. 2.2, SCCL specifies a batch test of 6 hours of shaking at room temperature. This test is called the Environmental Agency Notification No.46: Leaching Test Method for Soils (MOE, 1995; hereafter, JLT46). However, this test was established for the evaluation of anthropological contamination. Therefore, the applicability of geogenic contamination has yet to be elucidated. In addition, this test aims to judge whether the leaching concentration exceeds the regulatory limit. Therefore, the obtained concentration is not considered to be used to design the countermeasures against the utilization of the excavated soils and rocks with geogenic contamination.

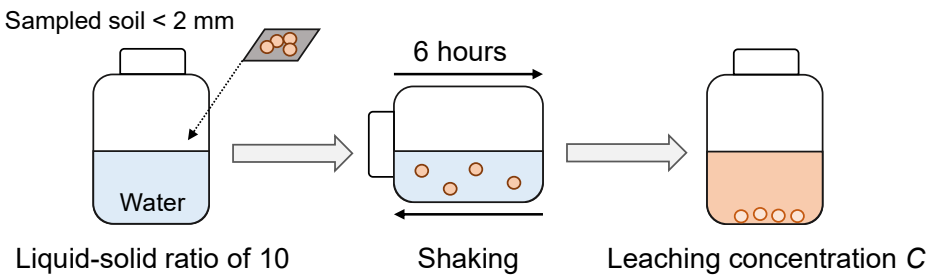

Figure 2.2 Schematic image of the batch leaching test called as JLT46.

2.2.2 Batch leaching tests evaluating leaching behavior of geogenic contaminants

A batch test is one of the fundamental leaching tests. Herein, a certain amount of soil and water are usually in contact with a shaking condition. Since evaluating the leaching behavior of contaminants is essential for environmental safety, numerous researchers conducted batch leaching tests to elucidate the soil-ground contamination of such as organic compounds, and anthropological contamination of heavy metals (e.g., Dalgren et al., 2011; Badea et al., 2013; Balseiro-Romero et al., 2016). Also, batch tests evaluated environmental safety for utilization of by-products or wastes such as incineration bottom ash, coal ash, brick, and concrete aggregate, etc. (e.g., Gwenzi and Mupatsi, 2016; Schafer et al., 2019; Shinohara et al., 2020; Ershadi, et al., 2023). Since numerous studies exist, the topic regarding evaluation of leaching behavior of geogenic contaminants from excavated soils is presented here.

Research regarding the leaching behavior of geogenic contaminants has increased in the 21st century. When the Tohoku Shinkansen was extended to Shin-Aomori, geogenic contamination, and acid drainage were severe problems during the Hakkoda tunnel excavation (Hattori et al., 2007; Shimada, 2014). In addition, as mentioned above, geogenic contamination was also regulated when SCCL was revised in 2010. However, since the regulatory test of JLT46 was established for anthropology contamination, some research pointed out that the evaluation may be far from the reality of geogenic contamination (Shimada, 2014; Katsumi, 2017). Based on such problems, MLIT presented the tentative version of the manual of testing methods evaluating the leaching behavior of geogenic contaminants and countermeasures in 2010. In the twenty years, many findings of the leaching behavior of geogenic contaminants have been obtained through batch tests, column tests, lysimeter tests, and field tests, and the MLIT manual has been revised in 2023 (MLIT. 2023). This section briefly summarizes the previous research evaluating the leaching behavior of geogenic contaminants from excavated soils using batch leaching tests.

Batch leaching tests have been conducted to evaluate the mechanisms of the leaching behavior of contaminants from earthen materials in previous studies. As for the leaching of arsenic, various testing from the perspective of geology, resource engineering, environmental engineering, and geoenvironmental engineering has been conducted (e.g., Masscheleyn et al., 1991; Tabelin and Igarashi, 2009; Saito et al., 2016; Li et at., 2018; Kamata and Katoh, 2019; Adachi and Katoh, 2020; Ogawa et al., 2022; Tang et al., 2023). Herein, one of the possible leaching mechanisms of As is presented because exceeding As is frequently reported in Japan. Figure 2.3 illustrates the schematic images of arsenic leching and acid drainage generation.

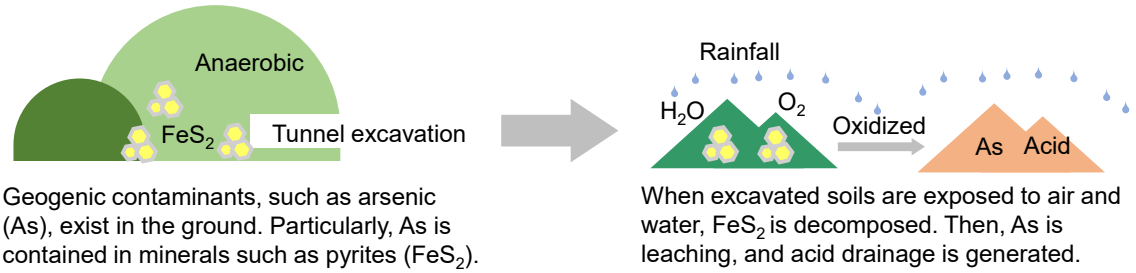

Figure 2.3 Schematic image of arsenic leching and acid drainage generation.

As explained in Section 2.2.1, geogenic contaminants, such as As, F, and B, are widely contained in Japanese ground. When they are in the original ground, the contamination is not a problem. However, once they are excavated and exposed to the outside environment, the leaching of the contaminants is promoted (Shimada, 2011; Atsuta et al., 2019). Many researchers have pointed out that As is contained in some minerals such as pyrite (FeS_2), and pyrite is easy to decompose by oxidation. When the mineral decomposes, contaminants are released from the earthen materials. In addition, since sulfide (S) is also released as sulfuric acid (H_2SO_4), acid drainage should be considered. Therefore, acid drainage from the earthen materials has been investigated by batch leaching tests in previous research (e.g., Sasaki, K., 1998; Igarashi et al., 2002; Hattori et al., 2007; Tabelin et al., 2012). As for other contaminants such as F, B, and Se, the leaching behavior will be discussed in Chapter 4.

Each research has decided parameters for batch leaching tests to clarify the research's focus. Since the earthen materials are considered weathered at a construction site, sample preparation methods were considered parameters (Kamata and Katoh, 2019; Tang et al., 2023). The sequential batch leaching tests changing the extracting solution were applied to elucidate which minerals contain contaminants (Li et al., 2018). Further, some research focuses on the filtration step after batch leaching tests (Yasutaka et al., 2017; Imoto et al., 2018; Someya et al., 2021). Since geogenic contaminants are bonded with a small particle of soil and exist in a colloidal state (Shimada, 2010), the applied membrane filter might affect the result of chemical analysis. Although JLT46 describes the use 0.45-μm membrane filter before chemical analysis, the research mentioned above showed that both centrifugal intensity and filtration volume per filter affected the reproducibility of batch leaching tests. A comparison of the filtration tests using 0.10 and 0.45 μm membrane filters showed significant differences in turbidity and concentration of contaminants. As demonstrated in Fig. 2.3, since the redox condition significantly affects the leaching behavior of geogenic contaminants (Shimada, 2014), batch leaching tests under different redox conditions or anaerobic conditions have been conducted (Tamoto and Kurahashi, 2017, 2018; Kato et al., 2021).

However, batch tests regulated by JLT46 have been established to evaluate anthropological contamination, as shown in Section 2.1.2. Therefore, the applicability of the test for geogenic contamination has yet to be investigated. Fundamental investigations considering parameters such as shaking time and liquid-solid ratio have yet to be studied sufficiently. Furthermore, considering that excavated soil is used in shallow ground such as embankments, the temperature should also be considered a parameter (e.g., Menberg et al., 2013; Saito et al., 2016; Takai et al., 2020; Ogawa et al., 2023). Therefore, the fundamental parameters of temperature, shaking condition, and soil-water contact time should be evaluated.

2.2.3 Column leaching tests evaluating leaching behavior of contaminants

Column leaching test can be a more realistic evaluation than batch leaching testing. Although the testing protocol of the column test is more complex than the batch test, and the testing duration of the column test is more prolonged than the batch test, the concentrations in the effluents can be monitored for several *L*/*S* ratios, including much smaller ratios than in the batch test. The smaller *L*/*S* ratios can better represent the in-field conditions. Although the leaching test is often called the column percolation test, since this dissertation presents both column leaching and sorption tests, it is called a column leaching test to clarify it.

Standardization of column testing methods has progressed in recent years because testing methods have not been established. Toward the standardization, the fundamental parameters such as the height of the column, saturation time, flow rate, compaction method, and dry density of the specimen have been investigated (e.g., Kalbe et al., 2007, 2008; Meza et al., 2010; Susset and Grathwohl, 2011; Nakamura et al., 2014, 2016; Naka et al., 2016). Also, the reproducibility of the column leaching test has been evaluated (Kalbe et al., 2007, 2008; Naka et al., 2016; Yasutaka et al., 2017). Consequently, the International Organization for Standardization (ISO 21268-3, 2019) and Japanese Industrial Standards (JIS A 1231, 2023) standards have been enacted, and the test results can be compared. Although the testing method has been established, there needs to be more discussion about how column test results apply to the design of countermeasures for excavated earthen materials with geogenic contamination. Challenges include utilizing column test results and considering the linkage between lab tests and construction sites.

Column leaching tests have often been applied to discuss the leaching behavior of geogenic contaminants closer to practical conditions. Since excavated earthen materials are often utilized for embankment over groundwater, column leaching tests with unsaturated conditions are closer to reality. Therefore, tests with a rainfall simulator are often applied (e.g., Tamoto et al., 2015; Inui et al., 2020). Herein, down-flow seepage is applied in the unsaturated specimen with a larger scale (ϕ 15 cm× h 70 cm) than the condition in ISO protocol. Arsenic concentrations differed in each depth, and the leaching was significant in the low saturation area (Inui et al., 2020). Further review of the column tests will be shown in Chapter 4.

As leaching tests are closer to reality than batch tests, tank leaching tests simulated the diffusion leaching of heavy metals or metalloids (e.g., Ogawa et al., 2022; Nasahara et al., 2023). Since column tests focus on the advection, the combination research of tests is expected towards the detailed discussion.

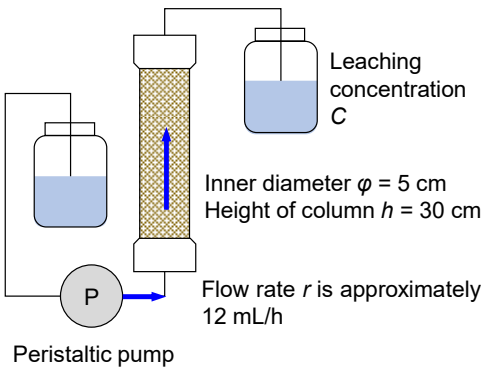

Figure 2.4 Schematic image of column leaching test.

2.3 Countermeasures against excavated earthen materials with geogenic contamination

2.3.1 Several types of countermeasures

Figure 2.5 illustrates examples of the schematic images of countermeasures against excavated earthen materials with geogenic contamination. The concepts of these methods are shown in the published manual (MLIT, 2023). The most conservative method is containment with a geomembrane or clay liner because seepage into the excavated soil layer is prevented. Since the boundary between the geomembrane or clay liner and natural soil might become a slip surface, it is necessary to pay attention to the mechanical stability of the embankment (Katsumi et al., 2017).

The second method is immobilization. Herein, excavated earthen materials are mixed with stabilizing agents such as calcium oxide (CaO), magnesium oxide (MgO), or iron oxide (FeO) to immobilize geogenic contaminants (e.g., Oyama, 2022). Since the methods shown in Fig. 2.5 (b)~(d) are proposed these days, the knowledge needs to be gathered. For example, if many agents are mixed with the excavated soils, economics becomes an issue. On the other hand, if more than the mixing ratio of agents is needed, immobilization performance becomes challenging due to the heterogeneity of the soil-agent mixture. Also, the workability to mix a certain amount of soils and agents is expected to take time and effort. The third method is an attenuation layer explained in Section 2.3.2. If the sorption performance of the natural ground can be expected to prevent groundwater contamination, no countermeasure is also considered as one measure.

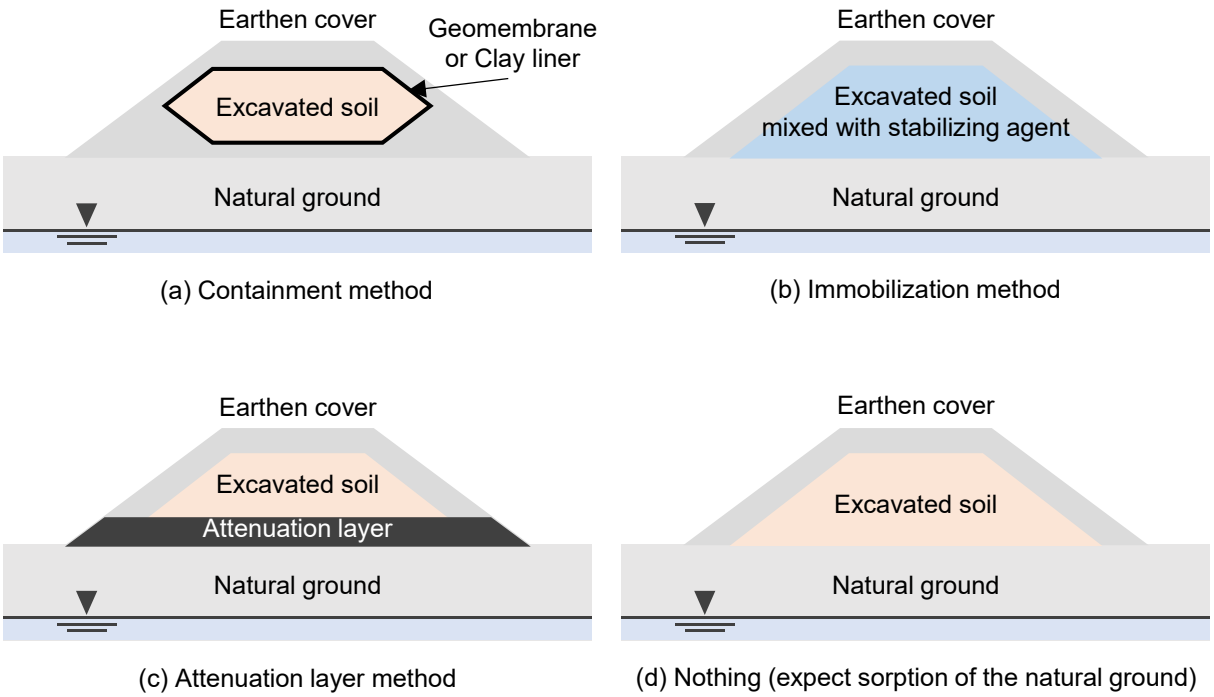

Figure 2.5 Schematic images of countermeasures against excavated earthen materials with geogenic contamination: (a) Containment using geomembrane or clay liner, (b) Immobilization using the stabilizing agent, (c) Attenuation layer method, and (d) no countermeasure is installed, but sorption performance of the natural ground is expected.

2.3.2 Attenuation layer method

One of the simple countermeasures for utilizing excavated soils with geogenic contamination is the attenuation layer method (e.g., Tabelin et al., 2013; Mo et al., 2020). This method has a soil layer for stabilizing contaminants. As the attenuation layer, natural soil or soil-agent mixture is applied (e.g., Arima et al., 2011; Gathuka et al., 2021). The attenuation layer is constructed beneath the excavated soils, and when pore water containing contaminants permeate, they are immobilized. The attenuation layer has the advantage of workability and economics. However, geogenic contaminants might leach out a certain amount compared to containment methods that use geomembranes or clay liners to prevent infiltrating water completely. On the other hand, since the leaching concentrations of geogenic contaminants are not high (Ito and Katsumi, 2020), even though the concentration exceeds the regulatory limit, the concept of the attenuation layer might be acceptable. The challenge is whether it can be expected to have mechanical stability and environmental compatibility as an earth structure. Evaluating leaching behavior from contaminated soil is essential because the leaching burden from the excavated earthen materials on the attenuation layer determines the required sorption performance.

Previous studies have evaluated the sorption performance of the attenuation layer materials, including material development and natural ground sorption performance. As the stabilizing agent, various kinds of materials such as magnesium oxide (MgO) (e.g., Sasaki et al., 2011; Nozaki et al., 2013; Wada and Morishita, 2013; Zhen et al., 2015), and MgO-calcium carbonate ($CaCO_3$) mixture (e.g., Mo et al., 2020; Itaya and Kuninishi, 2020; Gathuka et al., 2021, 2022) have been developed. The difference of the type of the stabilizing agent is comprehensively studied (Nishikata et al., 2022). Also, since sorption performance of the natural soils are widely investigated (e.g., Igarashi and Shimogaki, 1998; Tatsuhara et al., 2015), the applicability of the natural soils is promising.

Although the attenuation layer concept looks simple, the design method has yet to be established. The effectiveness of the attenuation layer was investigated by the column sorption test with ϕ 5.2 cm× h 50 cm (Tatsuhara et al., 2015). In the study, even a 3 cm height of the attenuation layer was performed to immobilize geogenic arsenic from the excavated soil layer with 30 cm. However, since the sorption performance of the attenuation layer has not been modeled, the sorption tests' experimental results cannot be applied to the design. Modeling the fate and transport in the attenuation layer is necessary for its robust design. Also, the hydraulic and mechanical performance of the attenuation layer have yet to be well discussed. Since the amendment of the stabilizing agent, which has high reactivity, might affect the geotechnical aspects of the embankment, further studies are required.

2.3.3 Evaluating sorption performance of attenuation layer

When the sorption performance of the soils or stabilizing agents is evaluated, a batch sorption test is usually applied (Nozaki et al., 2013; Wada and Morishita, 2013; Itaya and Kuninishi, 2020; Nishikata et al., 2022). The testing protocols of the batch and column leaching tests are established, while those of the sorption tests still need to be made. Therefore, each company evaluates each stabilizing agent arbitrarily. Standardization

of batch and column sorption tests is expected to support the constructors in selecting a stabilizing agent at the site.

A partition coefficient, K_d, is usually obtained from the sorption test as an index of the sorption performance. For the batch sorption test, sorbed mass, S, is calculated from the difference between the initial and equilibrium concentrations, C_{eq}. Then, sorption isotherms are drawn using S and C_{eq}. Then, K_d is obtained S divided by C_{eq}. For column tests, K_d is often obtained to fit the analytical solution of the advection-dispersion equation to the concentration profiles (experimental results). Previous studies focused on the sorption performance of natural soils against contaminants (e.g., Bouchard et al., 1988; Igarashi and Shimogaki, 1998; Wang and Liu et al., 2005; Martínez-Lladó et al., 2011). However, the method's applicability for determining K_d from column tests for the attenuation layer is still being determined because few studies target a mixture of soil and the stabilizing agent (an artificial material). Therefore, it is necessary to conduct basic column experiments and advection-dispersion analysis to evaluate whether the conventional models regarding the chemical reaction between soils and chemicals from both experimental and analytical approaches can be applied to the soil-stabilizing agent mixture.

2.4 Statement of novelty based on literature review

This section states the novelty of this dissertation based on the literature review from Section 2.1 to 2.3. The general goal of this study is the geoenvironmental management of excavated earthen materials with geogenic contamination to increase the utilization ratio of surplus soils, as mentioned in 2.1.2. Towards the material recycling of excavated soils with geogenic contamination, this dissertation focuses two aspects: evaluating leaching behavior of geogenic contamination closer to reality, and evaluating sorption performance of the attenuation layer to elucidate the applicability of the conventional advection-dispersion analysis model, as presented in Sections 2.2 and 2.3, respectively.

The first novelty of this dissertation is a deep investigation of the batch leaching tests against geogenic contaminated soils to address the issue stated in Section 2.2.2. The parameters for modified batch leaching tests were the temperature effect, leaching kinetics under different soil-water contact times, and shaking effect in Chapter 3. The second novelty is the discussion about interpreting the results of column leaching tests, as mentioned in Section 2.2.3. The column's height, the permeation's flow rate, and soil types were considered as the parameters, and the difference in the shape of the concentration profile was discussed in Chapter 4. The third novelty is evaluating the applicability of advection-dispersion analysis for column sorption tests using soil amended with the stabilizing agent, as described in Section 2.3.3. Soil amended with a stabilizing agent was compacted in the acrylic column to evaluate the sorption performance against fluoride in Chapter 5. Also, numerical analysis of the advection-dispersion equation was conducted in Chapter 6 to discuss the safer design obtaining underestimated partition coefficients was demonstrated. Finally, the linkage between evaluating leaching behavior and sorption performance was discussed to elucidate the effectiveness of the attenuation layer method against geogenic contamination in Chapter 7. Further detailed introductions and reviews regarding each chapter are presented in each chapter.

References for Chapter 2

Adachi, M, and Katoh, M., 2020. Arsenic accumulation leached from excavated mudstone into lower soil with different ability of arsenic sorption and its re-release by alteration of chemical environment. *Japanese Geotechnical Journal* 15(3), 487–496 (in Japanese). https://doi.org/10.3208/jgs.15.487.

Arima, T., Sato, D., Igarashi, T., Tamoto, S, and Tatsuhara, T., 2011. Reduction and retardation of arsenic and boron leached from excavated rocks by volcanic ash adsorption layer. *Journal of the Japan Society of Engineering Geology* 52(3), 88–96 (in Japanese). https://doi.org/10.5110/jjseg.52.88.

Atsuta, S., Sun, Y., and Ohta, T., 2019. Study on arsenic leaching mechanism in natural ground. *Journal of the Japan Society of Engineering Geology* 59(6), 430–445 (in Japanese). https://doi.org/10.5110/jjseg.59.430.

Badea, S-L., Lundstedt, S., Liljelind, P., and Tysklind, M., 2013. The influence of soil composition on the leachability of selected hydrophobic organic compounds (HOCs) from soils using a batch leaching test, *Journal of Hazardous Materials* 254–255(15), 26–35. https://doi.org/10.1016/j.jhazmat.2013.03.019.

Balseiro-Romero, M., Lundstedt, S., Liljelind, P., and Tysklind, M., 2013. Leachability of volatile fuel compounds from contaminated soils and the effect of plant exudates: A comparison of column and batch leaching tests, *Journal of Hazardous Materials* 304(5), 481–489. https://doi.org/10.1016/j.jhazmat.2015.11.017.

Bouchard, D.C., Wood, A.L., Campbell, M.L., Nkedi-Kizza, P. and Rao, P.S.C., 1988. Sorption nonequilibrium during solute transport. *Journal of Contaminant Hydrology* 2(3), 209–223. https://doi.org/10.1016/0169-7722(88)90022-8.

Dalgren, K.E., Düker, A, Arwidsson, Z, von Kronhelm, T, van Hees, P. A.W., 2011. Re-cycling of remediated soil – Evaluation of leaching tests as tools for characterization, *Waste Management* 31(2), 215–224. https://doi.org/10.1016/j.wasman.2009.12.021.

Ershadi, A., Finkel, M., Susset, B., and Grathwohl, P., 2023. Applicability of machine learning models for the assessment of long-term pollutant leaching from solid waste materials, *Waste Management* 31(2), 215–224. https://doi.org/10.1016/j.wasman.2023.09.001.

Gathuka L.W., Kato, T., Takai, A., Flores, G., Inui, T. and Katsumi, T., 2021. Effect of acidity on attenuation performance of sandy soil amended with granular calcium-magnesium composite. *Soils and Foundations* 61(4), 1099-1111. https://doi.org/10.1016/j.sandf.2021.05.007.

Gathuka L.W., Kasai, H., Kato, T., Takai, A., Inui, T. and Katsumi, T., 2022. Evaluating the arsenic attenuation of soil amended with calcium–magnesium composites of different particle sizes. *Soils and Foundations* 62(3), 101130. https://doi.org/10.1016/j.sandf.2021.05.007.Grathwohl, P. and Susset, B., 2009. Comparison of percolation to batch and sequential leaching tests: theory and data. *Waste Management* 29, 2681–2688. https://doi.org/10.1016/j.sandf.2022.101130.

Gwenzi, W., and Mupatsi, N.M., 2016. Evaluation of heavy metal leaching from coal ash-versus conventional concrete monoliths and debris, *Waste Management* 49, 114–123. https://doi.org/10.1016/j.wasman.2015.12.029.

Hattori, S., Ohta, T., and Kikuchi, Y., 2011. Assessment of judgment standard for acid water drainage from rock muck at the Hakkouda Tunnel. *Journal of the Japan Society of Engineering Geology* 47(6), 323–336 (in Japanese). https://doi.org/10.5110/jjseg.47.323.

Igarashi, T., and Shimogaki, H., 1998. Migration characteristics of boron by batch and column methods, *Journal of Groundwater Hydrology* 40(2), 121–132 (in Japanese). https://doi.org/10.5917/jagh1987.40.121.

Igarashi, T., Izutsu, T., and Oka, Y., 2002. Evaluation of pyrite dissolution rates by two-step leaching model. *Journal of the Japan Society of Engineering Geology* 43(4), 208–215 (in Japanese). https://doi.org/10.5110/jjseg.43.208.

Itaya Y., and Kuninishi, K., 2020. Development of selenium insolubilized material eluted from tunnel excavation rock. *Japanese Geotechnical. Journal* 15(3), 435–440 (in Japanese). https://doi.org/10.3208/jgs.15.435.

Imoto, Y., Yasutaka, T., Someya, M., and Higashino, K., 2018. Influence of solid-liquid separation method parameters employed in soil leaching tests on apparent metal concentration, *Science of The Total Environment* 624(15), 96–105. https://doi.org/10.1016/j.scitotenv.2017.12.048.

Inui, T., Hori, M., Katsumi, T., and Takai, A., 2020. Long-term leaching behavior of marine sediment by a large column percolation test. *Journal of the Society of Materials Science, Japan* 69(4), 53–56 (in Japanese). https://doi.org/10.2472/jsms.69.53.

ISO 21268-3, 2019. Soil Quality—Leaching Procedures for Subsequent Chemical and Ecotoxicological Testing of Soil and Soil Materials—Part 3: Up-Flow Percolation Test. International Standardization Organization.

Ito, H. and Katsumi, T., 2020. Leaching characteristics of naturally derived toxic elements from soils in the western Osaka area: Considerations from the analytical results under the Soil Contamination Countermeasures Act. *Japanese Geotech. Journal* 15(1), 119–130 (in Japanese). https://doi.org/10.3208/jgs.15.119.

JIS A 1231, 2023. Test method for leaching characteristics of geomaterials Up-flow percolation test. Japanese Standards Association.

Kalbe, U., Berger, W., Simon, F., Eckardt, J., and Christoph, G., 2007. Results of interlaboratory comparisons of column percolation tests, *Journal of Hazardous Materials* 148, 714–720, https://doi.org/10.1016/j.jhazmat.2007.03.039.

Kalbe, U., Berger, W., Eckardt, J., and Simon, F., 2008. Evaluation of leaching and extraction procedures for soil and waste, *Waste Management* 28, 1027–1038. https://doi.org/10.1016/j.wasman.2007.03.008.

Kamata, A. and Katoh, M., 2019. Arsenic release from marine sedimentary rock after excavation from urbanized coastal areas: Oxidation of framboidal pyrite and subsequent natural suppression of arsenic release. *Science of the Total Environment* 670, 752–759. https://doi.org/10.1016/j.scitotenv.2019.03.217.

Katsumi, T., 2017. Use of excavated soils with natural contamination. *Japanese Geotechnical Society Magazine*. 65 (11/12), 1–3 (in Japanese).

Katsumi, T., 2019. “Countermeasures against geogenic Contaminations”, *The Foundation Engineering & Equipment*, 47(6), 2-5 (in Japanese).

Kato, T., Masaki, Y., Gathuka, L.W., Takai, A., and Katsumi, T., 2021. Anaerobic batch leaching tests of shale rock grains, *Japanese Geotechnical Society Special Publication* 9(7), 374–379. https://doi.org/10.3208/jgssp.v09.cpeg153.

Li, J., Kosugi, T., Riya, S., Hashimoto, Y., Hou, H., Terada, A., and Hosomi, M., 2018. Investigations of water-extractability of As in excavated urban soils using sequential leaching tests: Effect of testing parameters. *Journal of Environmental Management* 217, 297–304.

Magnusson, S., Johansson, M., Frosth, S., and Lundberg, K., 2019. Coordinating soil and rock material in urban construction—scenario analysis of material flows and greenhouse gas emissions. *Journal of Cleaner Production* 241, 118236. https://doi.org/10.1016/j.jclepro.2019.118236.

Martínez-Lladó, X., Valderrama, C. M. Rovira, Martí, V., Giménez, J., and De Pablo, J., 2011. Sorption and mobility of Sb(V) in calcareous soils of Catalonia (NE Spain): batch and column experiments. *Geoderma* 160, 468–476. https://doi.org/10.1016/j.geoderma.2010.10.017.

Masscheleyn, P.H., Delaune, R.D., and Patrick, W.H., 1991. Effect of redox potential and pH on arsenic speciation and solubility in a contaminated soil. *Environmental Science & Technology* 25(8), 1414–1419. https://doi.org/10.1021/es00020a008.

Menberg, K., Bayer, P., Zosseder, K., Rumohr, S., and Blum, P., 2013. Subsurface urban heat islands in German cities. *Science of the Total Environment* 442, 123–133. https://doi.org/10.1016/j.scitotenv.2012.10.043.

Meza, S.L. Kalbe, U., Berger, W., and Simon, F.G., 2010. Effect of contact time on the release of contaminants from granular waste materials during column leaching experiments, *Waste Management* 30, 565–571. https://doi.org/10.1016/j.wasman.2009.11.022.

Ministry of Land, Infrastructure, and Transport, Japan, 2020. Material Reuse and Recycling Promotion Plan in Construction Works 2020 “Towards Recycling with an Emphasis on Quality. https://www.mlit.go.jp/report/press/sogo03_hh_000247.html (in Japanese) (accessed 3 July 2022).

Ministry of Land, Infrastructure, and Transport, Japan, 2020. Results of the Survey on Construction By-products in FY2018. https://www.mlit.go.jp/report/press/sogo03_hh_000233.html (accessed 3 July 2022) (in Japanese).

Ministry of Land, Infrastructure, and Transport, Japan, 2023. Technical Manual on the Countermeasure Against Soils and Rocks Containing Naturally Occurring Heavy Metals in Construction Works. https://www.mlit.go.jp/sogoseisaku/region/recycle/d11pdf/recyclehou/manual/shizenyurai2023.pdf (accessed 1 December 2023) (in Japanese).

Ministry of Environment, 1995. Environmental Agency Notification No.46: Leaching Test Method for Soils. http://www.env.go.jp/kijun/dojou.html (in Japanese) (accessed 27 October 2021).

Ministry of Environment, 2017. “Soil Contamination Countermeasure Law”, enacted in 2017 (accessed 3 July 2022) www.env.go.jp/water/dojo/dojogl2021_3.pdf. (in Japanese).

Mo, J., Flores, G., Inui, T., and Katsumi, T., 2020. Hydraulic and sorption performances of soil amended with calcium-magnesium composite powder against natural contamination of arsenic. *Soils and*

Foundations 60(5), 1084–1096. https://doi.org/10.1016/j.sandf.2020.05.007.

Naka, A., Yasutaka, T., Sakanakura, H., Kalbe, U., Watanabe, Y., Inoba, S., Takeo, M., Inui, T., Katsumi, T., Fujikawa, T., Sato, K., Higashino, K., and Someya, M., 2016. Column percolation test for contaminated soils: key factors for standardization. *Journal of Hazardous Materials* 320, 326–340. https://doi.org/10.1016/j.jhazmat.2016.08.046.

Nakamura, K., Ysutaka, T., Fujikawa, T., Takeo, M., Sato, K., Watanabe, Y., Inoba, S., Tamoto, S., and Sakanakura, H., 2014. Up-flow column tests to evaluate heavy metal leaching for standardization. *Japanese Geotechnical. Journal* 9(4), 697–706 (in Japanese). https://doi.org/10.3208/jgs.9.697.

Nakamura, K., Aoki, T., Watanabe, N., and Komai, T., 2016. Evaluation of porosity distributions within packed soil columns with X-ray CT based 3-D visualization. *Journal of Japan Society of Civil Engineers, Ser. C (Geosphere Engineering)* 72(2), 190–195 (in Japanese). https://doi.org/10.2208/jscejge.72.190.

Nasahara, T., Sakanakura, H., Kato, T., Takai, A., and Katsumi, T., 2023. Evaluating solute transport between soil particles and pore water considering intra-particle diffusion. *Japanese Geotechnical Journal* 18(4), 381–393 (in Japanese). https://doi.org/10.3208/jgs.18.381.

Nishikata, M., Yasutaka, T., Morimoto, K., and Imoto, Y., 2022. Evaluation of water contact influence on adsorbents by water immersion pretreatment and serial batch tests. *Japanese Geotechnical. Journal* 17(2), 195–204 (in Japanese). https://doi.org/10.3208/jgs.17.195.

Nozaki, F., Shimizu, Y., and Ito, K., 2013. Discussion on construction method of heavy metals adsorption layer. In: *Proceedings of the 19th Symposium on Groundwater and Soil Contamination and Countermeasures*, Kyoto, Japan (in Japanese).

Ogawa, S., Kinoshita, K., Katoh, T., Katoh, M., and Sakanakura, H., 2022. Leaching behavior observation of arsenic-containing soil from geogenic sources insolubilized with magnesium oxide-based material and preserved for a long term. *Japanese Geotechnical Journal* 17(3), 361–372 (in Japanese). https://doi.org/10.3208/jgs.17.361.

Ogawa, A., Takai, A., Sakanakura, H., Meguro, M., and Katsumi, T., 2022. Effect of temperature on diffusion leaching characteristics of clays containing geogenic substances. *Japanese Geotechnical Journal* 17(2), 181–194 (in Japanese). https://doi.org/10.3208/jgs.17.181.

Ogawa, A., Takai, A., Sakanakura, H., and Katsumi, T., 2023. Evaluating temperature effects on diffusive releases from clay particles. *Proceedings of the 9th International Congress on Environmental Geotechnics (ICEG2023)* 1, 115–124. https://doi.org/10.53243/ICEG2023-162.

Oyama, S, 2022. A Optimal stirring conditions in batch leaching tests for obtaining the leaching parameters of recycled geomaterials. *Japanese Geotechnical Journal* 17(3), 249–254 (in Japanese). https://doi.org/10.3208/jgs.17.249.

Saito, T., Hamamoto, S., Ueki, T., Ohkubo, S., Moldrup, P., Kawamoto, K., and Komatsu, T., 2016. Temperature change affected groundwater quality in a confined marine aquifer during long-term heating and cooling. *Water Research* 94, 120–127. https://doi.org/10.1016/j.watres.2016.01.043.

Sasaki, K., 1998. Experimental geochemical studies on oxidation of pyrite at ambient temperatures. *Journal of the Mineralogical Society of Japan* 27(2), 200–209 (in Japanese).

https://doi.org/10.2465/gkk1952.27.93.

Sasaki, K., Fukumoto, N., Moriyama, S., and Hirajima, T., 2011. Sorption characteristics of fluoride on to magnesium oxide-rich phases calcined at different temperatures. *Journal of Hazardous Materials* 191, 240–248. https://doi.org/10.1016/j.jhazmat.2011.04.071.

Schafer, M.L., Clavier, K.A., Townsend, T.G., Kari, R., and Worobel, R.F., 2019. Assessment of the total content and leaching behavior of blends of incinerator bottom ash and natural aggregates in view of their utilization as road base construction material, *Waste Management* 98, 92–101. https://doi.org/10.1016/j.wasman.2019.08.012.

Shimada, N., 2014. Naturally derived heavy metals and environmental pollution - Applied geological and geochemical data bank, ISBN 978-4-87256-423-5, 77–115 (in Japanese).

Shinohara, S., Kawai, T., Ishigami, D., Kawabata, J., Sato, T., Hisada, M., Minagawa, H., and Miyamoto, S., 2020. An evaluation of the long-term leaching behavior of heavy metals from granulated incineration ash. *Japanese Geotechnical Journal* 15(3), 471–478 (in Japanese). https://doi.org/10.3208/jgs.15.471.

Someya, M., Higashino, K., Imoto, Y., Sakanakura, H., and Yasutaka, T., 2021. Effects of membrane filter material and pore size on turbidity and hazardous element concentrations in soil batch leaching tests, *Chemosphere* 265, 128981. https://doi.org/10.1016/j.chemosphere.2020.128981.

Sumikura, Y., and Katsumi, T., 2022. Material reuse and recycling in construction works in Japan, *Journal of Material Cycles and Waste Management*, 24, 1216–1227. https://doi.org/10.1007/s10163-022-01411-y.

Susset, B. and Grathwohl, P., 2011. Leaching standards for mineral recycling materials – A harmonized regulatory concept for the upcoming German Recycling Decree, *Waste Management* 31, 201–214. https://doi.org/10.1016/j.wasman.2010.08.017.

Tabelin, C.B., and Igarashi, T., 2009. Mechanisms of arsenic and lead release from hydrothermally altered rock. *Journal of Hazardous Materials* 169(1–3), 980–990. https://doi.org/10.1016/j.jhazmat.2009.04.049.

Tabelin, C.B., Igarashi, T., Tamoto, S., and Takahashi, R., 2012. The roles of pyrite and calcite in the mobilization of arsenic and lead from hydrothermally altered rocks excavated in Hokkaido, Japan. *Journal of Geochemical Exploration* 119, 17–31. https://doi.org/10.1016/j.gexplo.2012.06.003.

Tabelin, C.B., Igarashi, T., Yoneda, T., and Tamamura, S., 2013. Utilization of natural and artificial adsorbents in the mitigation of arsenic leached from hydrothermally altered rock. *Engineering Geology* 156, 58–67. https://doi.org/10.1016/j.enggeo.2013.02.001.

Tabelin, C.B., Igarashi, T., Yoneda, T., and Tamamura, S., 2013. Utilization of natural and artificial adsorbents in the mitigation of arsenic leached from hydrothermally altered rock. *Engineering Geology* 156, 58–67. https://doi.org/10.1016/j.enggeo.2013.02.001.

Tabelin, C.B., Igarashi, T., Villacorte-Tabelin, M., Park, I., Opiso, E.M., Ito, M., and Hiroyoshi, N., 2018. Arsenic, selenium, boron, lead, cadmium, copper, and zinc in naturally contaminated rocks: a review of their sources, modes of enrichment, mechanisms of release, and mitigation strategies. *Science of the Total Environment* 645, 1522–1553. https://doi.org/10.1016/j.scitotenv.2018.07.103.

Takai, A., Iwata, Y., Gathuka, L.W., and Katsumi, T., 2020. Laboratory tests on arsenic leaching from excavated shale rock by elevated temperatures. *E3S Web of Conferences* 205, 09006. https://doi.org/10.1051/e3sconf/202020509006.

Tamoto, S., Tabelin, C.B., Igarashi, T., Ito, M., and Hiroyoshi, N., 2015. Short and long term release mechanisms of arsenic, selenium and boron from a tunnel-excavated sedimentary rock under in situ conditions. *Journal of Contaminant Hydrology* 175–176, 60-71. https://doi.org/10.1016/j.jconhyd.2015.01.003.

Tamoto, S. and Kurahashi, T., 2017. Preliminary study on batch leaching test method in reductive condition, In: *Proceedings of the 23rd Symposium on Soil and Groundwater Contamination and Remediation*, Okinawa, Japan, 559–560 (in Japanese).

Tamoto, S., and Kurahashi, T., 2018. Study on batch leaching test method in reductive condition. In: *Proceedings of the 53rd Symposium on Japanese Geotechnical Society*, Kyoto, Japan, 2173–2174 (in Japanese).

Tatsuhara, T., Jikihara, S., Tastumi, T., and Igarashi, T., 2015. Effects of the layout of adsorption layer on immobilizing arsenic leached from excavated rocks. *Japanese Geotechnical. Journal* 10(4), 635–640 (in Japanese). https://doi.org/10.3208/jgs.10.635.

Tang, J., Sakanakura, H., Takai, A., and Katsumi, T., 2023. Effect of dry-wet cycles on leaching behavior of recovered soil collected from tsunami deposits containing geogenic arsenic. *Soils and Foundations* 63(1), 101271. https://doi.org/10.1016/j.sandf.2022.101271.

Wang, X. and Liu, X., 2005. Sorption and desorption of radioselenium on calcareous soil and its solid components studied by batch and column experiments. *Applied Radiation and Isotopes* 62, 1–9. https://doi.org/10.1016/j.apradiso.2004.05.081.

Wada, S., and Morishita, T., 2013. Stabilization of heavy metals contaminated soils by magnesium oxide and related chemical and mineralogical reactions. *Journal of the Clay Science Society of Japan* 51, 107–117 (in Japanese). https://doi.org/10.11362/jcssjnendokagaku.48.1_9.

Yasutaka, T., Imoto, Y., Kurosawa, A., Someya, M., Higashino, K., Lalbe, U., and Sakanakura, H., 2017. Effects of colloidal particles on the results and reproducibility of batch leaching tests for heavy metal-contaminated soil, *Soils and Foundations* 57(5), 861–871. https://doi.org/10.1016/j.sandf.2017.08.014.

Yasutaka, T., Naka, A., Sakanakura, H., Kurosawa, A., Inui, T., Takeo, M., Inoba, S., Watanabe, Y., Fujiwara, T., Miura, T., Miyaguchi, S., Tatsuhara, T., Chida, T., Hirata, K., Ohori, K., Someya, M., Katoh, M., Umino, M., Negishi, M., Ito, K., Kojima, J., and Ogawa, S., 2017. Reproducibility of up-flow column percolation tests for contaminated soils, *PLoS ONE* 12(6), 1–17. https://doi.org/10.1371/journal.pone.0178979.

Zhen, J., Jia, Y., Luo, T., Kong, L.T., Sun, B., Shen, W., M, F.L. and Liu, J.H., 2015. Efficient removal of fluoride by hierarchical MgO microspheres: Performance and mechanism study. *Applied Surface Science* 357, 1080–1088. https://doi.org/10.1016/j.apsusc.2015.09.127.

Chapter 3

Evaluating Temperature Effects on Leaching Behavior of Geogenic Arsenic and Boron from Crushed Excavated Rocks Using Shaking and Nonshaking Batch Tests

3.1 General remarks

Many construction projects generate substantial amounts of excavated soils and rocks. A certain percentage of these soils and rocks contain toxic metals and metalloids that are derived from geological processes. Geogenic toxic metals and metalloids, such as arsenic (As) and boron (B), are widely distributed. They are found in different types of natural rocks and sediments, including marine clays, igneous rocks, and hydrothermally altered rocks. Such soils and rocks are expected to be used in embankments as a part of the ongoing efforts to achieve sustainable soil management. However, their proper use is sometimes a concern, especially because toxic elements can be released from the soils and rocks (Katsumi, 2015). Given the importance of developing economical and effective utilization methods for the excavated soils and rocks with geogenic contamination, evaluating the leaching behavior of these materials is important.

Working toward the aforementioned goal, researchers have used various batch tests to evaluate the leaching behavior of different soils and rocks with geogenic contamination (e.g., Tabelin and Igarashi, 2009; Li et al., 2018; Tabelin et al., 2018; Kamata and Katoh, 2019; Ito and Katsumi, 2020). When the soils and rocks are used in embankments or other shallow geostructures, the effects of the ground temperature on the leaching behavior of toxic elements are of technical concern because the daily and seasonal changes in temperature in shallow grounds can be much larger than those in deep grounds (Menberg et al., 2013; Alam et al., 2015; Saito et al., 2016). According to Menberg et al. (2013), the ground temperature can sometimes reach 60°C. In addition, various thermally active geosystems, introduced recently (e.g., thermal energy storage and ground-source heat pumps), involve changes in ground temperature (Wang et al., 2015; Başer et al., 2018), which might influence the leaching potential of the toxic elements in soils and rocks. Given these points, the effects of temperature on the behavior of geostructures need to also be clarified from a geoenvironmental perspective because the leaching behavior of such materials can change as a result of thermo-mechanical-chemical interactions. However, when the leaching concentrations of toxic elements are measured in laboratory tests, the tests are typically conducted at room temperature (approximately 15 to 20°C) because of the nearly constant ground temperature at depths greater than 10 to 15 m below the surface.

In addition, the leaching behavior of soils and rocks differs depending on how long the water has

been in contact with them. Japanese Leaching Test Method No. 46 (JLT46) is a standard leaching method used in Japan (MOE, 1995). For this test, the liquid obtained after shaking for six hours at a liquid-to-solid ratio (*L*/*S*) of 10 and separation with a 0.45-μm opening filter is analyzed to determine the concentration of the chemicals of concern. It should be noted that this leaching test was developed to test for artificial contamination. There is no certainty that it can be applied to geogenic contamination. The chemical forms and leaching processes differ between geogenic and artificial contamination contained in soils and rocks (Li et al., 2018). Thus, the standard leaching test may underestimate the risks of contamination if the leaching kinetics of the geogenic contamination is relatively slow. In order to assess the risks of geogenic contaminants with a higher level of safety, it is necessary to investigate their leaching kinetics. Moreover, any method employed to evaluate geogenic contamination must take into consideration the time needed for soil reactions to reach equilibrium.

The leaching behavior of As and B is evaluated in this work through two types of excavated rocks with geogenic contamination under different temperatures. The tests were performed under both shaking and nonshaking conditions to elucidate how shaking, which is applied in the standard leaching tests, affects the leaching behavior of the materials. Temperatures between 5 and 60°C were applied to account for the possible changes in temperature due to solar radiation and thermally active geosystems. The tests were conducted for 6 h to 15 days because changes in the leaching kinetics also require careful evaluation. A first-order kinetic model was used to fit the experimental results to investigate the leaching kinetics.

3.2 Methodologies for evaluating leaching behavior of geogenic contaminants

3.2.1 Materials

The shale rock and mudstone used in this work were excavated from tunnel construction sites. The rock samples were crushed into particles smaller than 2 mm for the batch leaching tests. Figure 3.1 shows the appearance of the rock samples after they were crushed and sieved through a 2-mm screen. The rock samples were then stored in sealed plastic bags to prevent their oxidation by air.

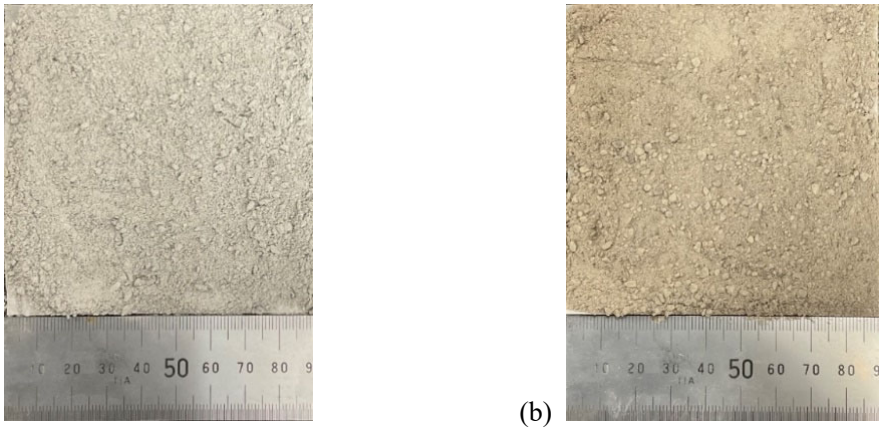

Figure 3.1 Appearance of the (a) shale rock sample and (b) mudstone sample after crushing and sieving through a 2-mm screen.

Table 3.1 highlights the fundamental physicochemical properties of the rock samples. Figure 3.2 shows the particle size distribution curves. The chemical composition and the total content of As were evaluated by X-ray fluorescence (XRF) analysis using a Shimadzu EDX 720 energy-dispersive X-ray spectrometer. The total content of B was determined by the acid digestion method.

Figure 3.3 shows the X-ray diffraction (XRD) patterns of the samples (PANalytical X'Pert PRO MPD, Cu Kα, 45 kV, 40 mA). Peaks of calcite were identified. The calcite in the rocks contributes to the sorption of toxic elements and neutralizes acidic solutions (Barton and Vatanatham, 1976; Niu and Lin, 2021). Toxic metals and metalloids can be leached via desorption from soil particles (e.g., Tabelin et al., 2018). As the pH level affects desorption reactions, the trends in pH should be carefully examined.

The zeta potential of the rock samples was measured to better understand how their surface charge changes with the pH level. A 0.1-g rock sample and 100 mL of water were poured into a beaker. A 100-W ultrasonic wave irradiated the beaker for 3 min. Next, the pH values of the solution were adjusted to pH levels of 2, 4, 6, 8, and 10 using hydrochloric acid or sodium hydroxide. Then, the solution was poured into a capillary cell, and the zeta potential was measured using the electrophoresis method (Malvern Zetasizer Nano ZS). The refractive index, dielectric constant, and viscosity of the solution were assumed to be the same as those of water. Figure 3.4 plots the zeta potential of the rock samples against the pH. The results show that the soil particles became more negatively charged as the pH increased. The isoelectric point of the shale rock sample was at pH 3.12. No isoelectric point was detected for the mudstone sample.

Table 3.1 Properties of the rock samples used in this study.

Parameter	Shale rock	Mudstone	Method of measurement
Particle density	2.73 g/cm^3	2.64 g/cm^3	JIS A 1202 (2009)
Particle size distribution			JIS A 1204 (2009)
Sand fraction [0.075–2 mm]	85.5%	94.5%	
Fines fraction [<0.075 mm]	14.5%	5.5%	
Average particle size	0.50 mm	0.52 mm	
Chemical composition			XRF analysis
SiO_2	24.7%	54.5%	
CaO	41.1%	7.2%	
Fe_2O_3	20.4%	17.3%	
Al_2O_3	7.1%	12.9%	
K_2O	2.5%	3.2%	
SO_3	0.9%	1.4%	
MgO	-	1.4%	
Others	3.3%	2.1%	
As content	20 mg/kg	27 mg/kg	XRF analysis
B content	29 mg/kg	150 mg/kg	Acid digestion method

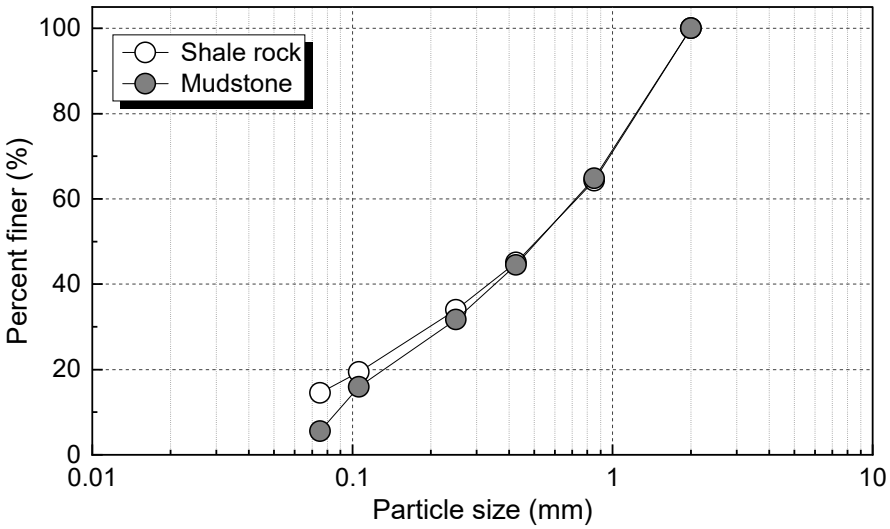

Figure 3.2 Particle size distribution curve of the rock samples.

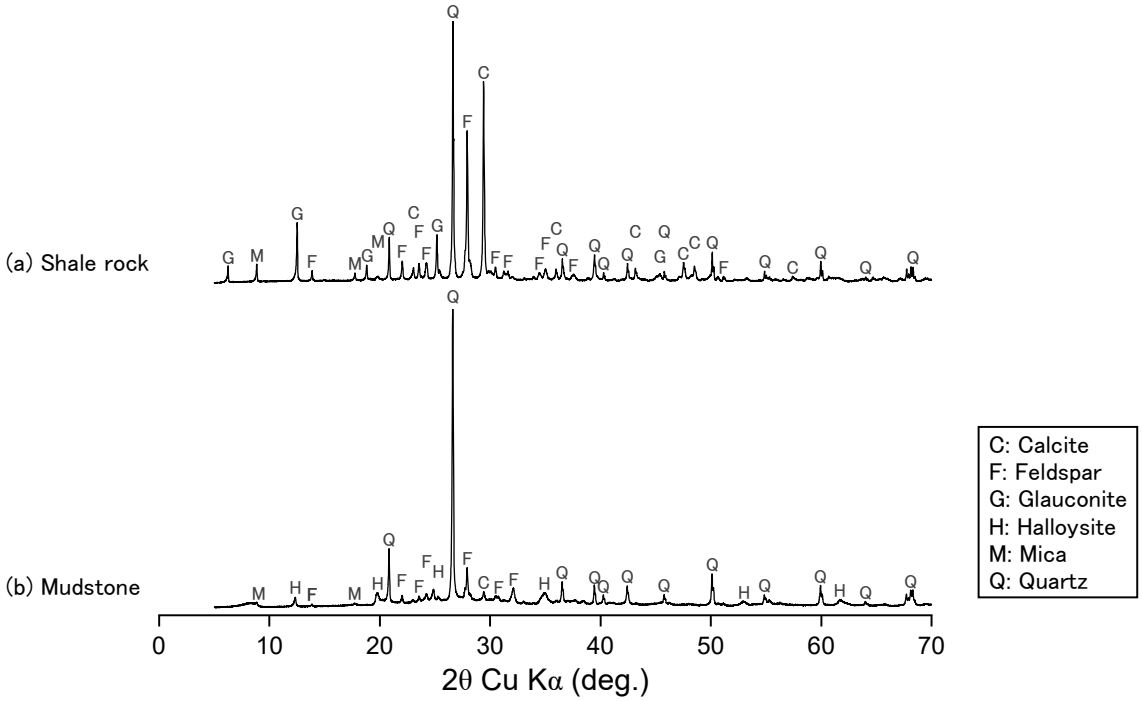

Figure 3.3 X-ray diffraction patterns of the rock samples.

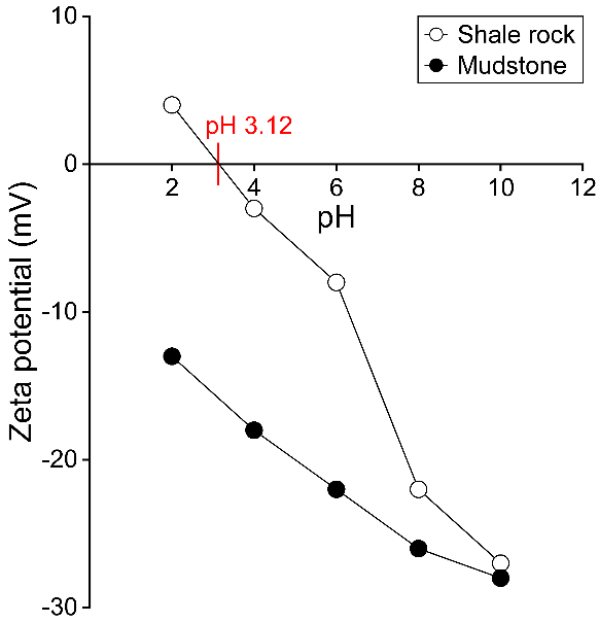

Figure 3.4 Zeta potential of the rock samples.

3.2.2 Batch leaching tests

3.2.2.1 Shaking conditions

Batch leaching tests were conducted under shaking conditions and at an *L*/*S* of 10. Figure 3.5 shows the test setup. Rubber heaters connected to a temperature control system were wrapped around plastic bottles. The rubber heaters heated the bottles during the tests. Distilled water was used as the solvent. After the water temperature was adjusted to the required temperature, the water was poured into the bottles. Temperatures between 20 and 60°C were used for the tests. The appropriate amount of each rock sample was then poured into the bottles to achieve an L/S of 10. Afterwards, the bottles were horizontally shaken for 6 h to 15 days at 200 rpm using a mechanical shaker (TAITEC NR-30) to evaluate the leaching kinetics. The test conditions are briefly summarized in Table 3.2.

3.2.2.2 Nonshaking conditions

Batch leaching tests were also conducted under nonshaking conditions. Shaking conditions are typically used to promote chemical reactions and to ensure homogeneous contact between soil and water. However, shaking conditions can lead to an inaccurate assessment of how the materials will leach. Thus, nonshaking conditions were also considered herein. Nonshaking tests can provide important information for properly evaluating the leaching behavior in practical situations because geomaterials in the ground or geostructures should make contact with rainwater and/or groundwater without disturbance or agitation. The nonshaking tests also used an *L*/*S* of 10. Temperatures between 5 and 60°C were used for the tests. Temperatures greater than 20°C were controlled via the rubber heaters wrapped around the bottles during the tests. The tests performed at 5°C were conducted in a refrigerator. The bottles containing the rock samples and distilled water were placed on a table or in a refrigerator and allowed to stand for 6 h to 15 days.

3.2.2.3 Chemical analyses

After the aforementioned tests, centrifugation at 3000 rpm for 10 min and filtration with a 0.45-μm membrane filter were carried out to separate the liquid from the solids. Chemical analyses were conducted the following methods. Figure 3.6 shows the machines for chemical analyses. The pH of the filtrate was measured using a pH/EC meter (Horiba F-54). The calibration was done using the standard solution of pH 4, 6, and 9, respectively. The As concentrations were measured using an atomic absorption spectrophotometer (Shimadzu AA-6800). The calibration was done using the standard solution of As 100 mg/L (Fujifilm Wako Pure Chemical Corporation). And then, As concentrations were adjusted to 0, 0.001, 0.005. 0.01, and 0.02 .mg/L using distilled water. The concentrations of cations (B, Ca, and Fe) were measured using an inductively coupled plasma optical emission spectrometer (Agilent Technologies ICP-OES 710). The calibration was done using the standard solution of Multielement Standard Solution W-VI for ICO analysis (Fujifilm Wako Pure Chemical Corporation). The concentrations of Ca and Fe were measured because they are key indices for evaluating the leaching behavior of As and B (Tabelin et al., 2018).

Table 3.2 Conditions of the batch leaching tests.

Sample form	Particles smaller than 2 mm
Solvent	Distilled water ($5.8 \leq pH \leq 6.3$)
Solvent temperature	5–60°C (5°C for nonshaking condition only)
Test duration	6–360 h
Liquid-to-solid ratio	10 L/kg
Filter type	0.45 μm membrane filter

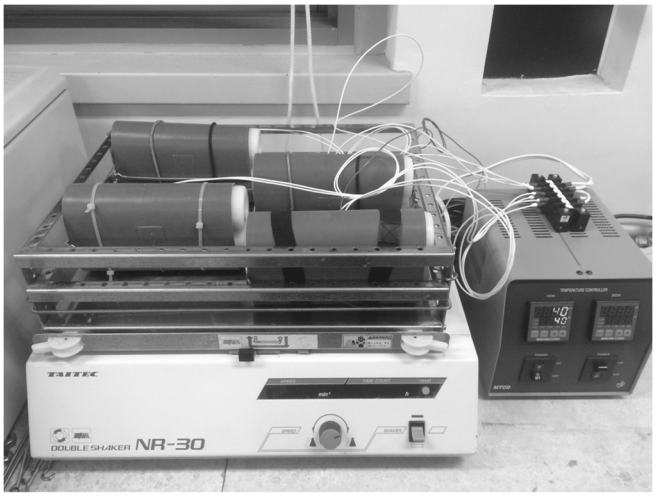

Figure 3.5 Batch leaching tests under the shaking conditions using a temperature control system.

(a) 

(b) 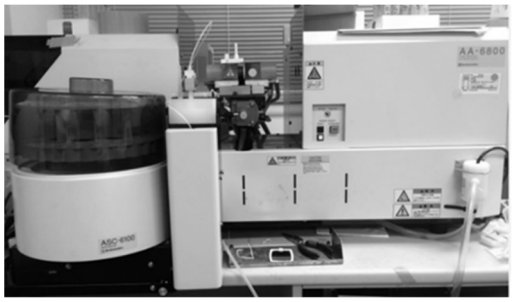

(c) 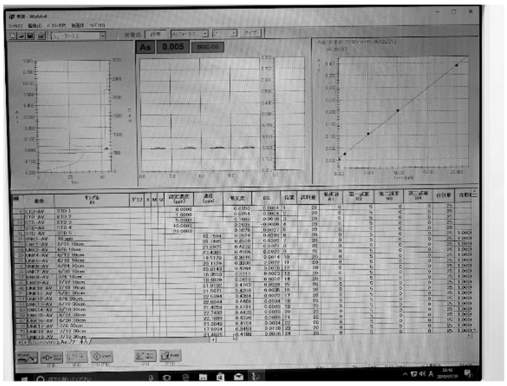
(d) 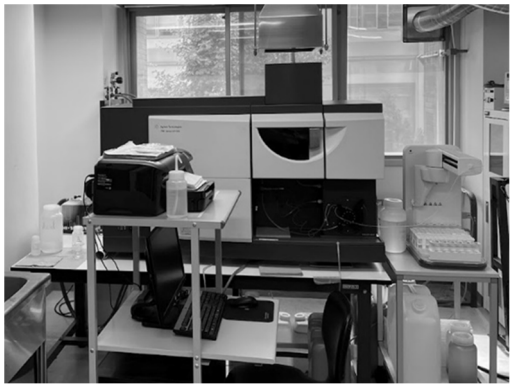

Figure 3.6 Machines for chemical analyses; (a) pH/EC meter (Horiba F-54), (b) Atomic absorption spectrophotometer (Shimadzu AA-6800), (c) an example of the standard line used in AA-6800, (d) Inductively coupled plasma optical emission spectrometer (Agilent Technologies ICP-OES 710).

3.2.3 Modeling the leaching behavior

3.2.3.1 Theory

The changes in the leaching kinetics of As and B, due to an increase in temperature, were evaluated. A first-order model was fitted to the experimental results to obtain the parameters of the leaching kinetics, according to the method used in a previous study (Igarashi et al., 2002). The following equation was used:

$$\frac{\partial Q_s}{\partial t} = -kQ_s \tag{3.1}$$

Eq. (3.2) was obtained by integrating Eq. (3.1).

$$Q_s = Q_{so} \exp(-kt) \tag{3.2}$$

The leached mass during the batch leaching tests was conserved as

$$Q_{so} = Q_s + CV \tag{3.3}$$

The leaching model was obtained by combining Eqs. (3.2) and (3.3) as

$$C = Q_{so}\left[1 - \exp\left(-kt\right)\right] / V \tag{3.4}$$

where t (h) is the solid–liquid interaction time, Q_s (mg/kg) is the concentration of toxic elements in the solid phase at time t, k (1/h) is the rate constant for leaching, Q_{so} (mg/kg) is the initial concentration of toxic elements in the solid phase with the potential to leach out, C (mg/L) is the concentration of toxic elements in the liquid phase at time t, and V (L/kg) is the volume of water per kilogram of sample.

3.2.3.2 Estimation of leaching kinetics

To model the experimental results of the batch leaching tests, the experimental data were fitted using Eq. (3.4). The values for k and Q_{so} were obtained by minimizing the residual sum of the squared estimate of errors (SSE) between the model and the experimental data as

$$\mathrm{SSE} = \sum_{i=1}^{n} (C_i - C_i')^2 \tag{3.5}$$

where C_i represents the experiment data and C'_i represents the predicted data.

3.3 Results

3.3.1 Batch leaching tests under shaking conditions

Figure 3.7(a) shows the chemistry of the leachate from the shale rock sample. Arsenic was leached in greater amounts at temperatures of 30 and 40°C than at a temperature of 20°C. These results suggest that the leaching concentrations might increase when the rocks are exposed to elevated temperatures. Furthermore, the concentrations at temperatures of 30 and 40°C were higher than the regulatory limit of As in Japan (0.01 mg/L). The leaching of Ca increased with the increasing temperature. This result suggests that the dissolution of Ca minerals in the rock sample increased because of the increase in temperature. The shale rock sample did not leach B or Fe. The pH values decreased as the temperature increased, although the leachates were still alkaline. The alkaline conditions are attributed to the dissolution of the carbonate minerals in the rock sample. The pH values at 20°C were one pH unit higher than those at 40°C. The sulfide minerals in the rock (refer to Table 3.1) may dissolve under high temperatures and reduce the pH values (Sasaki, 1998; Tabelin and Igarashi, 2009).

Arsenic is leached because of the dissolution of minerals or because of the desorption from soil

particles (Tabelin et al., 2018). The clay minerals in the rock sample are generally negatively charged, which will promote the desorption of As (Masscheleyn et al., 1991; Carrilo and Drever, 1998). Moreover, the surface charge of the soil particles became more negatively charged as the pH decreased, as shown in Fig. 3.4. Given these points, As should have desorbed during the tests because of the high pH values. However, the As concentrations were lower under the high pH conditions. Therefore, the leaching of As might be mainly attributable to the dissolution of the minerals in the rock, suggesting that the leaching mechanism due to dissolution is affected by temperature.

Figure 3.7(b) shows the chemistry of the leachate from the mudstone sample. The leaching concentrations of As were generally lower at higher temperatures, and the concentrations generally exceeded the regulatory limit in Japan (0.01 mg/L). In contrast, the leaching concentrations of B were similar at both 20 and 40°C. More importantly, the concentrations were acceptable values in Japan (<1.0 mg/L). The Ca concentrations increased as the temperature was raised. The dissolution of the Ca minerals in the rock may have increased under the higher temperatures. Leaching greater amounts of Ca can improve the sorption of As by rendering the surface of the Fe-oxyhydroxides/oxides more positive (Wilkie and Hering, 1996). Therefore, the decrease in the As concentration observed in the present study might be attributed to coexisting Ca. Increasing the shaking time reduced the amount of released Fe. It is possible that Fe was released and precipitated, but this process could not be verified with the available data. Additional studies will be necessary to fully understand the effects of the shaking time. The pH values decreased because of the elevated temperatures; however, the leachates were still alkaline. The alkaline conditions are attributed to the dissolution of the carbonate minerals in the rock sample. The pH values at 20°C were one pH unit higher than those at 60°C, similar to the case of the shale rock sample.

Boron is leached because of the dissolution of the carbonate minerals, such as calcite or aragonite (Tabelin et al., 2018), and the desorption from soil particles. As the chemical form of B in the solutions is a negatively charged oxyanion [i.e., $B(OH)_4^{2-}$] or charge-neutral H_3BO_3 (Magara et al., 1998), B is easily desorbed from the soil particles as the pH level increases. When only desorption is considered, differences in the leaching amount should be observed because the pH values differ between the temperatures of 20 and 40°C. However, the leaching amounts are similar, which suggests that desorption mechanisms are not critical to the leaching of B under these pH conditions. Thus, the dissolution of B, which is strongly temperature-dependent, might be the primary mechanism.

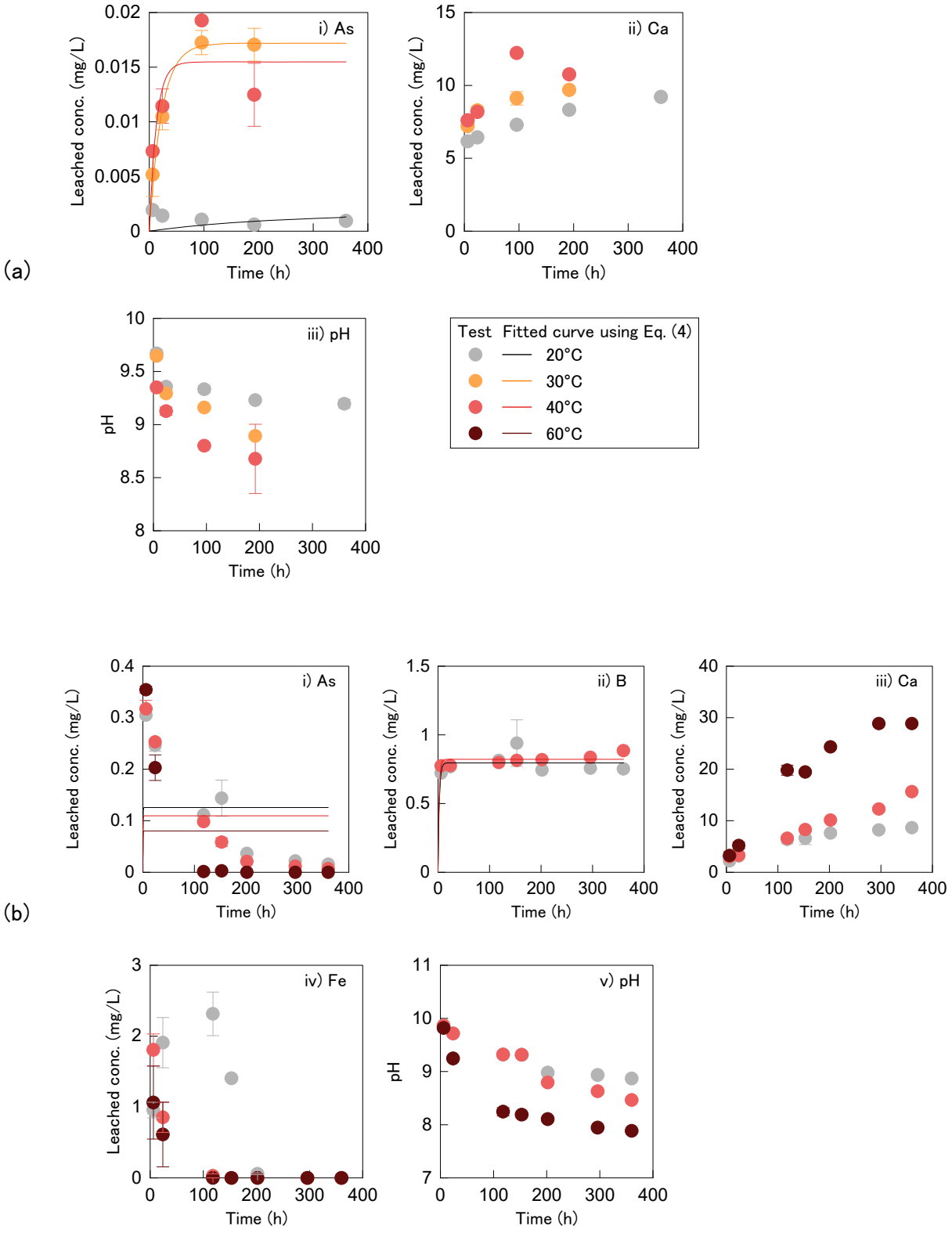

Figure 3.7 Leachate chemistry after the shaking tests for the (a) shale rock sample and (b) mudstone sample. These data are the average values. The error bars are the standard deviations.

3.3.2 Nonshaking conditions

Figure 3.8(a) shows the chemistry of the leachate from the shale rock sample. Arsenic was leached in greater amounts at 40°C than at temperatures less than 30°C. The results also suggest that leaching concentrations can increase when the temperatures are greater than room temperature. The concentrations at 40°C were higher than the regulatory limit in Japan. The leaching concentrations of Ca increased with the increasing temperature, and a similar trend was observed in the shaking tests. An increase in the Ca concentration with an increase in temperature suggests that the dissolution of the Ca minerals in the shale rock was promoted under elevated temperatures. The shale rock sample did not leach B or Fe even under nonshaking conditions. Due to the elevated temperatures, the pH values decreased, but the leachates remained alkaline.

Figure 3.8(b) shows the chemistry of the leachate from the mudstone sample. As and B were leached in greater amounts when the temperature was increased from 20 to 40 and 60°C. Notably, the nonshaking tests resulted in higher concentrations of As than the shaking tests when the tests were run for more than 24 h. The leaching concentrations of Ca and Fe did not seem to change in response to an increase in temperature. The nonshaking tests resulted in smaller amounts of Ca and Fe than the shaking tests, suggesting that the dissolution of these minerals was less promoted under the nonshaking conditions. Due to the elevated temperatures, the pH values decreased; however, the leachates were still alkaline.

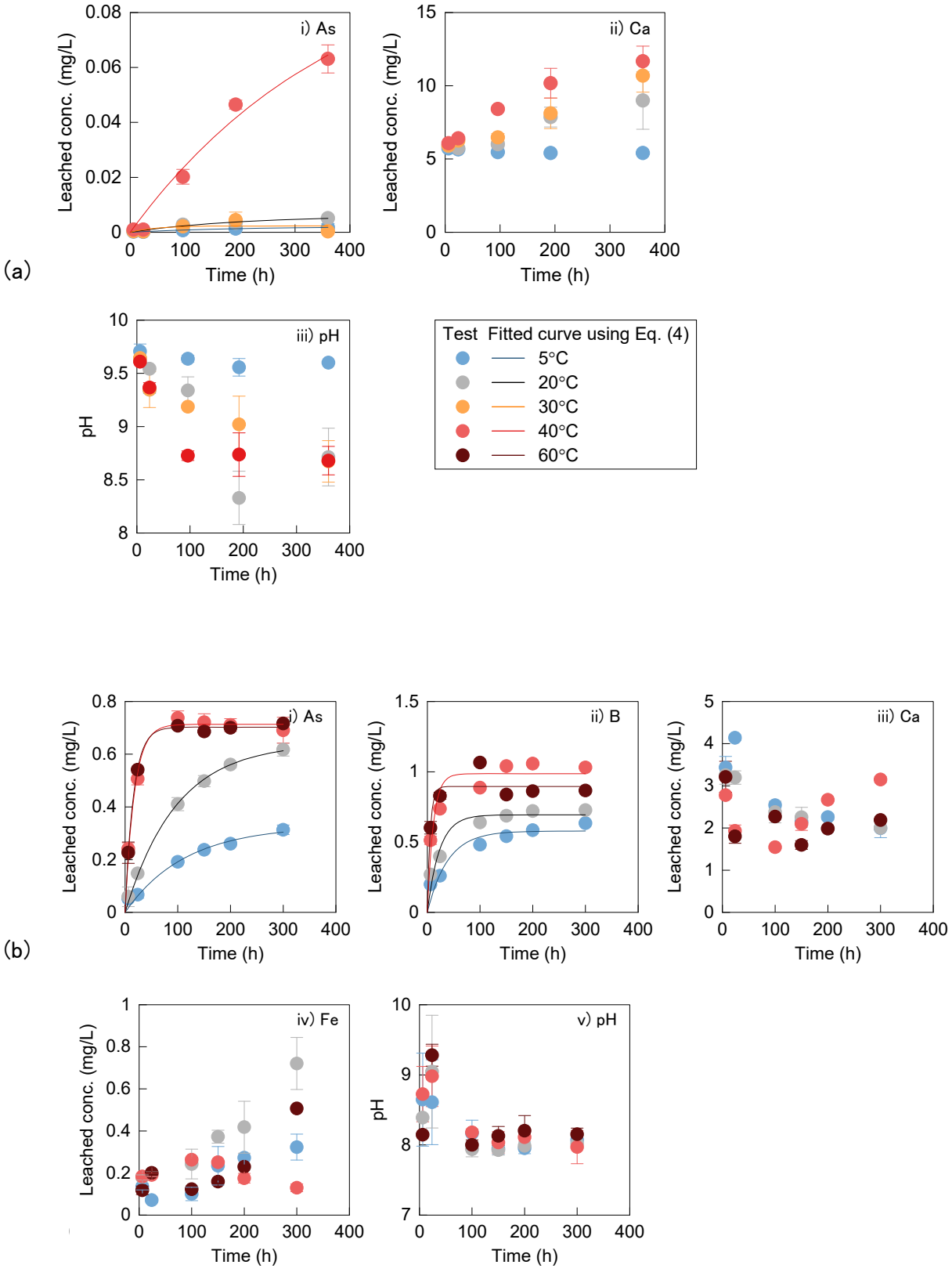

Figure 3.8 Leachate chemistry after the nonshaking tests for the (a) shale rock sample and (b) mudstone sample. These data are the average values. The error bars are the standard deviations.

3.3.3 Changes in leaching kinetics of As and B

The rate constant k was used as an index to characterize the changes in the leaching kinetics of As and B. Tables 3.3 to 3.6 summarize the k values obtained using the steps described in Section 3.2.3. For the shale rock sample, the k value increased as the temperature was raised in the shaking test, as shown in Table 3.3. At 40°C, the k value was 7.7×10^{-2}/h, which is approximately 2.5 times greater than the k value at 30°C. Thus, the leaching kinetics of As increased with the increasing temperature. The shaking test results were well fitted using the first-order kinetics model, except for the case of 20°C. The reason for the disagreement in the results obtained at 20°C is unclear. When the sample was subjected to nonshaking tests, no noticeable change in k in response to an increase in temperature was observed, as shown in Table 3.5.

For the mudstone sample, the shaking test results for As could not be fitted using the aforementioned model, as shown in Fig. 3.7(b). Thus, the trends in the leaching kinetics of As could not be evaluated. Further study will be required to evaluate the leaching kinetics for the cases in which the leaching concentrations decrease with time. For the nonshaking tests, the k values increased with the increasing temperature as shown in Table 3.6. At 40°C, the k value was 5.7×10^{-2}/h, which is approximately six times greater than that at 20°C.

The results for B from the shaking and nonshaking tests on the mudstone sample were well fitted using the model, as shown in Figs. 3.7(b) and 3.8(b). Tables 3.4 and 3.6 show that the leaching kinetics of B increased with the increasing temperature in both the shaking and nonshaking tests. Table 3.4 shows that, during the shaking tests at 40°C, the k value was 4.7×10^{-1}/h, which is approximately 1.2 times greater than that at 20°C. Table 6 shows that, during the nonshaking tests at 40°C, the k value was 8.8×10^{-2}/h, which is approximately two times greater than that at 20°C.

Table 3.3 Fitting parameters for the results of the shaking tests on the shale rock sample.

	Temperature (°C)	Q_{so} (mg/kg)	k (1/h)
Arsenic	20	1.6×10^{-2}	4.6×10^{-3}
	30	1.7×10^{-1}	4.6×10^{-2}
	40	1.6×10^{-1}	7.7×10^{-2}

Table 3.4 Fitting parameters for the results of the shaking tests on the mudstone sample.

	Temperature (°C)	Q_{so} (mg/kg)	k (1/h)
Arsenic	20	1.3	3.0
	40	1.1	2.8
	60	8.0×10^{-1}	3.2
Boron	20	8.0	4.0×10^{-1}
	40	8.2	4.7×10^{-1}

Table 3.5 Fitting parameters for the results of the nonshaking tests on the shale rock sample.

	Temperature (°C)	Q_{so} (mg/kg)	k (1/h)
Arsenic	5	2.1×10^{-2}	5.1×10^{-3}
	20	6.0×10^{-2}	5.1×10^{-3}
	30	2.3×10^{-1}	2.1×10^{-2}
	40	1.1	2.6×10^{-3}

Table 3.6 Fitting parameters for the results of the nonshaking tests on the mudstone sample.

	Temperature (°C)	Q_{so} (mg/kg)	k (1/h)
Arsenic	5	3.3	8.8×10^{-3}
	20	6.4	1.0×10^{-2}
	40	7.1	5.7×10^{-2}
	60	7.0	6.3×10^{-2}
Boron	5	5.8	2.6×10^{-2}
	20	6.9	4.4×10^{-2}
	40	9.9	8.8×10^{-2}
	60	9.0	1.8×10^{-1}

3.4 Discussion

3.4.1 Temperature effects on leaching behavior

The leaching concentrations of toxic metals and metalloids might increase as a result of the increasing ground temperature. In some cases, the concentrations can exceed the regulatory limits, necessitating an evaluation of the effects of temperature. The leaching of toxic metals and metalloids occurs mainly via the dissolution of the minerals in the rocks or the desorption from the soil particles (Tabelin et al., 2018). The results herein indicate that the leaching concentrations due to dissolution changed drastically as the temperature increased. Since the rock samples contained certain amounts of sulfide minerals, it is reasonable to assume that the dissolution of sulfide minerals is one of the leaching mechanisms of As. Moreover, at high temperatures, the As derived from sulfide minerals is more likely to leach. However, not only sulfide minerals, but also other minerals (e.g., calcite) are present in the rock samples. Thus, the amount of As leaching cannot be attributed to sulfide mineral dissolution alone. It has been shown that calcite will have a significant impact on As adsorption (Tabelin et al., 2012). However, these processes could not be verified with the available data. The fact that the results of the nonshaking tests fit the first-order rate law well suggests that surface reactions may be driving the dissolution process, as noted by Igarashi et al. (2002). When leaching concentrations decrease with time, it is difficult to understand the leaching behavior based on the first-order rate law.

Implications of this research are discussed herein. When excavated materials containing geogenic contaminants are utilized in embankments, a solute transport analysis is usually conducted to predict the risks of geogenic contamination to the surrounding ground and to design appropriate countermeasures against these risks (e.g., Tabelin et al., 2014). Since the initial concentrations of leachates applied in the analysis drastically affect the predictions, the appropriate leachate concentrations expected in practice must be carefully determined. This study indicates that leaching concentrations of As could be up to five times higher than the regulatory limit under elevated temperatures. For this reason, leachate concentrations several times the regulatory limit should be accounted for in the analysis.

3.4.2 Soil–water interaction time for evaluation of geogenic contamination

Leaching concentrations were found to change because of increases in the soil–water interaction time. These results indicate that the dissolution of minerals is an important factor that should be further evaluated. Generally, the dissolution process requires a longer time to complete (Tabelin et al., 2017). Therefore, to obtain equilibrium concentrations from the batch tests, the tests need to be conducted for a relatively long period of time. Short test times (e.g., 6 h, as specified in the standard leaching test in Japan) may not be suitable because they might lead to underestimations of the leaching concentrations. When rocks are used in an embankment, the materials will make contact with water for a relatively long time during the infiltration of water into the embankment. The leaching concentrations are expected to increase before chemical equilibrium is achieved. The leaching of geogenic contaminants may continue for a long time because of dissolution.

The attenuation layer method is a recently proposed countermeasure for the excavated soils and rocks with geogenic contamination (Tatsuhara et al., 2012; Gathuka et al., 2021; Kato et al., 2021). The attenuation layer is a soil layer with attenuation capacity, underlying the excavated soils and rocks with geogenic contamination. Typically, the attenuation layer is constructed of soils mixed with a stabilizing agent (Gathuka et al., 2021; Kato et al., 2021). The stabilizing agent for the attenuation layer method should be carefully selected because the dissolution of minerals might occur slowly, as shown in this study. Stabilizing agents that quickly hydrate and lose their attenuation capacity after a short period should be avoided because leaching is expected to continue for a relatively long time.

3.4.3 Shaking versus nonshaking conditions

Batch tests were conducted under shaking and nonshaking conditions. Although shaking conditions are commonly used in standard leaching tests in Japan, nonshaking conditions might better represent the in situ conditions. Differences in the shaking and nonshaking conditions were noticeable for the mudstone sample. For example, the shaking tests resulted in higher leaching concentrations of As than the nonshaking tests during the first hours of the tests. In contrast, the concentrations increased with the increasing test duration in the nonshaking tests.

Such differences in the leaching behavior might be attributable to the mudstone being friable.

Crushing during the shaking tests might have promoted the release of Ca. A higher Ca concentration is known to promote the sorption of As onto soil particles (e.g., Tabelin et al., 2012). Crushing could also have contributed to the release and precipitation of Fe during the shaking tests. Accordingly, the dissolved As can be immobilized via precipitation reactions to form less-soluble compounds (e.g., Tabelin et al., 2018). Furthermore, the surface area increases as a result of the soil particles being crushed during the shaking tests; the greater surface area might promote the sorption of As. Further study will be required to elucidate the effects of shaking tests on such friable rocks. When the leaching behavior of excavated rocks is investigated, nonshaking tests might be more suitable, especially for friable samples. Nonshaking conditions might be closer to the in-situ conditions. Water flowing through the rocks might prevent the substantial crushing of the rocks that would induce greater amounts of released As.

3.5 Summary and Conclusions

Batch leaching tests were performed under shaking and nonshaking conditions at temperatures of 5 to 60°C to investigate the leaching behavior of As and B from two crushed excavated rock samples with geogenic contamination. In addition, a first-order kinetic model was used to fit the experimental results to investigate the leaching kinetics. The results support the following conclusions:

1. Elevated temperatures often led to the release of greater amounts of As and B. After conducting the nonshaking tests for 15 days at 40°C, the mudstone sample leached arsenic and boron at concentrations of ~0.7 mg/L and ~1.0 mg/L, respectively. The arsenic and boron concentrations were approximately 20% and 40% higher than those of the sample leached at a temperature of 20°C.
2. The first-order kinetic model fitted the experimental data when the leaching concentrations increased or remained stable over time, but it was not applicable when the concentrations decreased. The rate constant k obtained from the fitting line was used as an index to characterize the changes in the leaching kinetics of As and B. Elevated temperatures increased the leaching kinetics of the toxic elements. For the shale rock sample, the k value for As was 7.7×10^{-2}/h at 40°C, which was about 2.5 times greater than the value at 30°C.
3. Leaching concentrations of As and B did not reach equilibrium within 6 h. To better assess the risk of geogenic contamination, it is important to run batch tests for a relatively longer period of time than the 6 h indicated in the Japanese standard leaching test.
4. Nonshaking tests are recommended for friable rocks because possible crushing may lead to unrealistic estimations of the leaching amounts.

References for Chapter 3

Alam, M.R., Zain, M.F.M., Kaish, A.B.M.A., and Jamil, M., 2015. Underground soil and thermal conductivity materials based heat reduction for energy-efficient building in tropical environment. *Indoor and Built Environment* 24(2), 185–200. https://doi.org/10.1177/1420326X13507591.

Barton, P. and Vatanatham, T., 1976. Kinetics of limestone neutralization of acid waters, *Environmental Science & Technology* 10, 262–266. https://doi.org/10.1007/s002540050311.

Başer, T., Dong, Y., Moradi, A.M., Lu, N., Smits, K., Ge., S., Tartakovsky, D., and McCartney, J.S., 2018. Role of nonequilibrium water vapor diffusion in thermal energy storage systems in the vadose zone. *Journal of Geotechnical and Geoenvironmental Engineering* 144(7), 04018038. https://doi.org/10.1061/(ASCE)GT.1943-5606.0001910.

Carrilo, A. and Drever, J.I., 1998. Adsorption of arsenic by natural aquifer material in the San Antonio EI Triufo mining area, Baja, California, Mexico. J. *Environmental Geology* 35, 251–257. https://doi.org/10.1007/s002540050311.

Gathuka, L.W., Kato, T., Takai, A., Flores, G., Inui, T., and Katsumi, T., 2021. Effect of acidity on the attenuation performance of sandy soil amended with granular calcium-magnesium composite. *Soils Foundations* 61(4), 1099–1111, https://doi.org/10.1016/j.sandf.2021.05.007.

Igarashi, T., Izutsu, T., and Oka, Y., 2002. Evaluation of pyrite dissolution rates by two-step leaching model. *Journal of the Japan Society of Engineering Geology* 43(4), 208–215 (in Japanese). https://doi.org/10.5110/jjseg.43.208.

Ito, H. and Katsumi, T., 2020. Leaching characteristics of naturally derived toxic elements from soils in the western Osaka area: Considerations from the analytical results under the Soil Contamination Countermeasures Act. *Japanese Geotech. Journal* 15(1), 119–130 (in Japanese). https://doi.org/10.3208/jgs.15.119.

JIS A 1202, 2009. Test Method for Density of Soil Particles. Japanese Standards Association.

JIS A 1204, 2009. Test Method for Particle Size Distribution of Soils. Japanese Standards Association.

Kamata, A. and Katoh, M., 2019. Arsenic release from marine sedimentary rock after excavation from urbanized coastal areas: Oxidation of framboidal pyrite and subsequent natural suppression of arsenic release. *Science of the Total Environment* 670, 752–759. https://doi.org/10.1016/j.scitotenv.2019.03.217.

Kato, T., Gathuka, L.W., Okada, T., Takai, A., Katsumi, T., Imoto, Y., Morimoto, K., Nishikata, M., and Yasutaka, T., 2021. Sorption-desorption column tests to evaluate the attenuation layer using soil amended with a stabilizing agent. *Soils Foundations* 61(4), 1112–1122. https://doi.org/10.1016/j.sandf.2021.05.004.

Katsumi, T., 2015. Soil excavation and reclamation in civil engineering: environmental aspects. *Journal of Soil Science and Plant Nutrition* 61, 22–29. https://doi.org/10.1080/00380768.2015.1020506.

Li, J., Kosugi, T., Riya, S., Hashimoto, Y., Hou, H., Terada, A., and Hosomi, M., 2018. Investigations of water-extractability of As in excavated urban soils using sequential leaching tests: Effect of testing parameters. *Journal of Environmental Management* 217, 297–304.

https://doi.org/10.1016/j.jenvman.2018.03.105.

Magara, Y., Tabata, A., Kohki, M., Kawasaki, M., and Hirose, M., 1998. Development of boron reduction system for sea water desalination. *Desalination* 118, 642–645. https://doi.org/10.1016/S0011-9164(98)00076-9.

Masscheleyn, P.H., Delaune, R.D., and Patrick, W.H., 1991. Effect of redox potential and pH on arsenic speciation and solubility in a contaminated soil. *Environmental Science & Technology* 25(8), 1414–1419. https://doi.org/10.1021/es00020a008.

Menberg, K., Bayer, P., Zosseder, K., Rumohr, S., and Blum, P., 2013. Subsurface urban heat islands in German cities. *Science of the Total Environment* 442, 123–133. https://doi.org/10.1016/j.scitotenv.2012.10.043.

Ministry of Environment (1995) Environmental Agency Notification No.46: Leaching Test Method for Soils. http://www.env.go.jp/kijun/dojou.html (in Japanese) (accessed 27 October 2021).

Niu, A. and Lin, C., 2021. Managing soils of environmental significance: A critical review. *Journal of Hazardous Materials* 417, 125990. https://doi.org/10.1016/j.jhazmat.2021.125990.

Saito, T., Hamamoto, S., Ueki, T., Ohkubo, S., Moldrup, P., Kawamoto, K., and Komatsu, T., 2016. Temperature change affected groundwater quality in a confined marine aquifer during long-term heating and cooling. *Water Research* 94, 120–127. https://doi.org/10.1016/j.watres.2016.01.043.

Sasaki, K., 1998. Experimental geochemical studies on oxidation of pyrite at ambient temperatures. *Journal of the Mineralogical Society of Japan* 27(2), 200–209 (in Japanese). https://doi.org/10.2465/gkk1952.27.93.

Tabelin, C.B., and Igarashi, T., 2009. Mechanisms of arsenic and lead release from hydrothermally altered rock. *Journal of Hazardous Materials* 169(1–3), 980–990. https://doi.org/10.1016/j.jhazmat.2009.04.049.

Tabelin, C.B., Igarashi, T., Tamoto, S., and Takahashi, R., 2012. The roles of pyrite and calcite in the mobilization of arsenic and lead from hydrothermally altered rocks excavated in Hokkaido, Japan. *Journal of Geochemical Exploration* 119, 17–31. https://doi.org/10.1016/j.gexplo.2012.06.003.

Tabelin, C.B., Igarashi, T., Arima, T., Sato, D., Tatsuhara, T., and Tamoto, S., 2014. Characterization and evaluation of arsenic and boron adsorption onto natural geologic materials, and their application in the disposal of excavated altered rock, Japan. *Geoderma* 213, 163–172. https://doi.org/10.1016/j.geoderma.2013.07.037.

Tabelin, C.B., Sasaki, R., Igarashi, T., Park, I., Villacorte-Tabelin, M., Park, I., Tamoto, S., Arima, T., Ito, M., and Hiroyoshi, N., 2017. Simultaneous leaching of arsenite, arsenate, selenite and selenate, and their migration in tunnel-excavated sedimentary rocks: I. Column experiments under intermittent and unsaturated flow. *Chemosphere* 186, 558–569. https://doi.org/10.1016/j.chemosphere.2017.07.145.

Tabelin, C.B., Igarashi, T., Villacorte-Tabelin, M., Park, I., Opiso, E.M., Ito, M., and Hiroyoshi, N., 2018. Arsenic, selenium, boron, lead, cadmium, copper, and zinc in naturally contaminated rocks: a review of their sources, modes of enrichment, mechanisms of release, and mitigation strategies. *Science of the Total Environment* 645, 1522–1553. https://doi.org/10.1016/j.scitotenv.2018.07.103.

Tabelin, C.B., Silwamba, M., Paglinawan, F.C., Mondejar, A.J.S., Duc, H.G., Resabal, V.J., Opiso, E.M., Igarashi, T., Tomiyama, S., Ito, M., Hiroyoshi, N., and Villacorte-Tabelin, M., 2020. Solid-phase partitioning and release-retention mechanisms of copper, lead, zinc and arsenic in soils impacted by artisanal and small-scale gold mining (ASGM) activities. *Chemosphere* 260, 127574. https://doi.org/10.1016/j.chemosphere.2020.127574.

Tamoto, S., Tabelin, C.B., Igarashi, T., Ito, M., and Hiroyoshi, N., 2015. Short and long term release mechanisms of arsenic, selenium and boron from a tunnel-excavated sedimentary rock under in situ conditions. *Journal of Contaminant Hydrology* 175–176, 60–71. https://doi.org/10.1016/j.jconhyd.2015.01.003.

Tatsuhara, T., Arima, T., Igarashi, T., and Tabelin, C.B., 2012. Combined neutralization–adsorption system for the disposal of hydrothermally altered excavated rock producing acidic leachate with hazardous elements. *Engineering Geology* 139–140, 76–84. https://doi.org/10.1016/j.enggeo.2012.04.006.

Wang, B., Bouazza, A., Singh., R.M., Haberfield, C., Barry-Macaulay, D., and Baycan, S., 2015. Posttemperature effects on shaft capacity of a full-scale geothermal energy pile. *Journal of Geotechnical and Geoenvironmental Engineering* 141(4), 04014125. https://doi.org/10.1061/(ASCE)GT.1943-5606.0001266.

Wilkie, J.A. and Hering, J.G., 1996. Adsorption of arsenic onto hydrous ferric oxide: Effects of adsorbate/adsorbent ratios and co-occurring solutes. *Colloids and Surfaces A: Physicochemical and Engineering Aspects* 107, 97–110. https://doi.org/10.1016/0927-7757(95)03368-8.

Chapter 4

Monotonous Decreasing Leaching Behavior of Geogenic Contamination from Marine Sediments by Up-Flow Column Percolation Tests

4.1 General remarks

Geogenic contaminants such as lead or arsenic, etc. are widely contained in the ground of Japan (e.g., Ito and Katsumi, 2020). Therefore, it is typical for excavated soils and rocks generated from construction work to contain naturally occurring heavy metals or metalloids (e.g., Katsumi, 2018). Then, proper countermeasures must be taken to prevent soil groundwater contamination (Tatsuhara et al., 2015; Ministry of Environment, 2019; Ministry of Land Infrastructure, 2023). However, since the leached geogenic contaminants are often at a low concentration that slightly exceeds the environmental standard values, if the concentration levels of the geogenic contamination are lower than the artificial contamination, the countermeasures, such as the containment, might be too conservative. It might be desirable to consider the utilization of the excavated soils and rocks with geogenic contamination as geo-material for road embankments or river levees. Therefore, evaluating leaching characteristics is essential for soil and rock utilization.

The leaching behavior of geogenic contaminants from the soil is affected by various factors, such as the type of contaminants, the chemical species in which they exist in the soil, pH values, and the effects of coexisting substances (e.g., Cappuyns and Swennen, 2008; Shimada 2013; Tabelin et al., 2018). Therefore, evaluating the leaching behavior at each construction site is desirable because the geology and environment differ. Batch leaching tests or column leaching tests are often conducted. For example, the column tests can obtain the maximum concentration or cumulative leaching amount of the target chemicals. Although column tests with various conditions (e.g., height, flow rate, saturation time) have been conducted, the standardization of column tests is established to compare test results (International Standardization Organization, 2019).

When analyzing the risk of soil or groundwater contamination, boundary conditions of the advection-dispersion analysis are often decided based on the leaching test results. A batch leaching test, such as the Environment Agency Notification No. 46 test, is usually conducted in Japan. Then, advection-dispersion analysis is performed to evaluate solute transport in the ground, using the obtained leaching concentration as the boundary condition with a constant concentration. On the other hand, in Germany, for recycling material regulations, contaminants leaching from waste and incineration ash are classified into i) easily soluble chemicals, ii) metals, and iii) organic compounds (Susset and Grathwohl, 2012). Then,

advection-dispersion analysis is performed. Specifically, the boundary condition for metals and organic compounds is a concentration with a constant cumulative leaching concentration up to a liquid-solid ratio (*L*/*S*) of 2. However, for readily soluble chemicals, the boundary condition is defined as the breakthrough curve obtained in a column test as a function of time. The leaching behavior of easily soluble chemicals is such that leaching is terminated relatively quickly. Therefore, the leaching behavior in the field environment can be predicted from the column test results.

As mentioned above, column testing can provide much information regarding the shape of the breakthrough curves. For example, the breakthrough curves for sulfuric acid (SO_4) had a monotonically decreasing shape, and many cases have been reported in which leaching terminated quickly (e.g., Kalbe et al., 2007, 2008; Naka et al., 2016). On the other hand, the breakthrough curves for arsenic (As) did not show a monotonous decrease, and leaching continued for an extended period in many cases (e.g., Naka et al., 2016; Yasutaka et al, 2017).

Table 1 shows the previous research on column leaching tests. Most studies have been conducted to shorten the test period and evaluate the reproducibility toward standardization. For example, the effects of differences in column volume filled with waste (Meza et al, 2010), differences in initial saturation time and flow rate, sample preparation methods (Naka et al, 2016), and dry density of the specimen on the leaching test results have been evaluated (Nakamura et al, 2014). On the other hand, interpreting the column test results combined with geological knowledge was conducted in a few studies (e.g., Tamaoto et al, 2015). Further, the leaching behavior of geogenic arsenic at different depths was investigated using a column test with a rainfall simulator (Inui et al, 2020).

Table 4.1 Examples of the previous researches on leaching tests using column devices.

Authors	Purpose	Materials	Focused parameters
Kalbe et al, 2007	Reproducibility	Incineration ash	Flow rate, column volume
Kalbe et al, 2008	Reproducibility	Incineration ash	Comparing to batch tests
Wehrer et al, 2008	Modeling breakthrough curves	Incineration ash	pH of the influent
Kadoki et al., 2009	Establishing test protocols	Waste glasses	Comparing to batch tests
Meza et al, 2010	Shortening test duration	Incineration ash	Column volume
Nakamura et al., 2014	Reproducibility	Geogenic soils	Sample preparation
Tamoto et al, 2015	Modeling breakthrough curves	Geogenic rocks	Geological knowledge
Naka et al., 2016	Reproducibility Shortening test duration	Geogenic and artificial soils	Saturation time Flow rate
Yasutaka et al, 2017	Reproducibility	Geogenic soils	13 organizations joined.
Finckel et al, 2017	Modeling breakthrough curves	Recycled materials	Saturation time
Bandow et al, 2019	Evaluating equilibriums	Waste bricks	Flow rate, particle size
Ishimori et al., 2020	Modeling breakthrough curves	Tsunami deposits	Comparing to batch tests
Inui et al., 2020	Evaluating at different depths	Geogenic soils	Simulating rainfall

However, most previous studies in Table 1 focused on establishing the test protocols and evaluated the reproducibility of standardizing column tests. Limited research focuses on interpreting breakthrough curves and their application in the field.

If the concentration of the contaminant monotonically decreases and terminates quickly, countermeasures must be designed considering the risks in the early stages of leaching. Therefore, the criteria for determining whether a contaminant is readily soluble should be discussed. Although the leaching behavior of geogenic contaminants changes due to various factors, as mentioned before, if the leaching behavior of easily soluble chemicals considered to be relatively easy to predict, can be evaluated from column test results, the boundary conditions during advection-dispersion analysis can be more closely to the on-site conditions. As a result, this will promote the utilization of the excavated soils and rocks with geogenic contamination.

In this study, based on the above background, an up-flow column test was conducted to evaluate the leaching behavior of readily soluble chemicals based on the shape of the breakthrough curve. Chemicals with monotonically decreasing breakthrough curves showing maximum concentration when PVF≒0 and whose concentration becomes half of the maximum concentration when PVF= 1 or less are judged as easily soluble chemicals in this study. In addition, in previous studies, most column tests were conducted using a height of 30 cm and a flow rate of 12 mL/h, as specified by ISO standards. In particular, few tests were conducted on the height of the column as a parameter. This study applied two types of marine sediments and two different specimen heights and flow rates to discuss the robust application of the column leaching tests.

4.2 Methodologies for monotonous decreasing leaching behavior of geogenic contaminants using column leaching tests

4.2.1 Materials

Boring surveys were conducted in two coastal areas in western and eastern Japan, respectively. Each sample containing geogenic contaminants was collected. In this study, they are called sandy soil one and two, respectively. Considering the history of land use at the collection point and the samples collected from a sufficiently deep depth, there is no anthropological contamination. Soil particle density, natural water content, particle size distribution, and ignition loss were measured for each sample.

Table 4.2 Fundamental physical properties of the samples

	Sandy soil 1	Sandy soil 2
Soil particle density, ρ_s (g/cm^3)	2.669	2.708
Natural water content, w （%）	21.3	27.7
Sandy fraction （%）	90.8	84.0
Silty fraction （%）	4.9	9.6
Clay fraction （%）	4.3	6.4
Ignition loss （%）	2.0	3.7

(a) 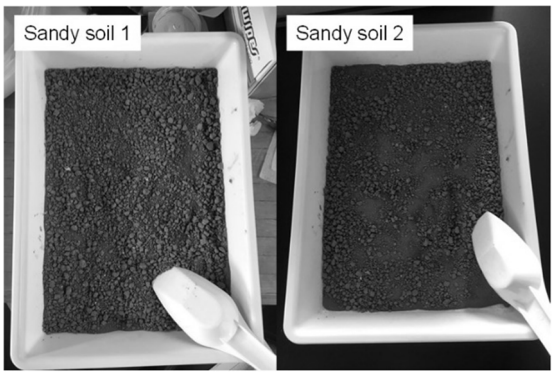

(b) 

Figure 4.1 Samples used in this study: (a) Appearance of the sandy soils, and (b) Sieving process.

Table 4.2 shows the fundamental physical properties of the samples used. The sample was sieved while still wet, and the sample that passed through the 2 mm sieve was used for the column leaching tests, as shown in Fig. 4.1.

4.2.2 Column leaching tests

This study performed an up-flow column test following ISO 21268-3. The reason for upward permeating water is to prevent selective flow generation as much as possible. The test condition is shown in Table 4.3. An acrylic column with a diameter of 5 cm and a height of 30 cm was used for the column test. The sample was poured into five layers with a height of 2 cm each, and after filling each layer, the sample was compacted by dropping a 125 g rammer from a height of 20 cm three times. A 0.001 mol/L calcium chloride ($CaCl_2$) solution was permeated as the influent. Before starting the column test, water was permeated through the specimen to make it into a pseudo-saturated state. Precisely, the influent was permeated through the column using a peristaltic pump at a flow rate of 12±2 mL/h until the influent reached the top of the column. Then, the column was stood for 48 hours. After that, the flow rate was set to 12 mL/h and continued until a liquid-solid ratio (L/S) 20, as shown in Fig. 4.2. The leachate from the column should be sampled at L/S of 0.1, 0.2, 0.5, 1, 2, 5, 10. If L/S is ten or more, collect it once at L/S 2.5 to 5.

Table 4.3 Cases of the column leaching tests.

Testing No.	1	2	3	4	5	6	7
Sandy soil No.	1	1	1	1	2	2	2
Diameter of the column, D (cm)	5	5	5	5	5	5	5
Height of the column, H (cm)	30	30	10	10	30	30	10
Flow rate, r (mL/h)	12	36	12	36	12	36	12
Darcy velocity, v_s (cm/day)	15	44	15	44	15	44	15
Dry density, ρ_d (g/cm^3)	1.33	1.36	1.35	1.36	1.41	1.40	1.40
Porosity, n (-)	0.50	0.49	0.49	0.49	0.48	0.48	0.48
Soil-water contact tome, T (h)	24.3	7.9	8.1	2.7	24.3	7.9	8.1

(a)  (b) 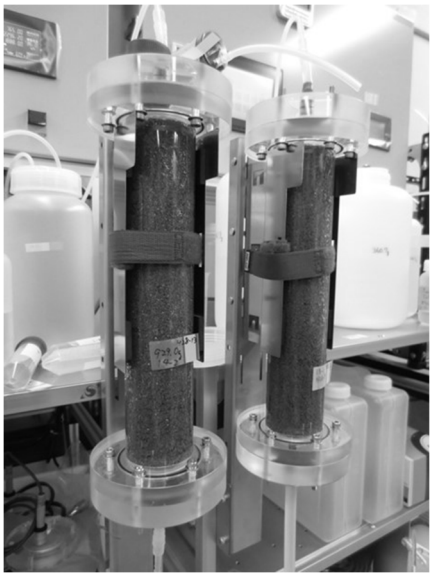

Figure 4.2 Setting up the column leaching tests: (a) After compaction, and (b) During permeation.

After that, the frequency of leachate sampling was reduced. The amount of leachate sampled was approximately 40 mL at *L*/*S* 0.1. After that, 100 to 150 mL of the total amount of liquid sampled was transferred to a centrifuge tube, and the sample was subjected to suction filtration using a membrane filter with a pore size of 0.45 μm.

In this study, concentrations of lead (Pb), arsenic (As), fluorine (F), boron (B), and selenium (Se) in filtrate were measured. They are frequently reported among geogenic contaminants. Concentrations of sodium (Na), sulfate ions (SO_4), magnesium (Mg), iron (Fe), and aluminum (Al) were measured as soil constituents. Since a $CaCl_2$ solution was used as the influent, the calcium (Ca) concentration was not measured. Chemicals such as F, SO4, Na, and Mg in the filtrates were measured using ion chromatography, while As, B, Se, Pb, Fe, and Al were measured by Inductively coupled plasma (ICP) mass spectrometry (JIS K 0102). In addition, the pH and electrical conductivity (EC) of the filtrates were measured.

The column height of 30 cm and flow rate of 12 mL/h are the test conditions specified by ISO 21268-3, while comparative experiments were conducted in this study, as shown in Table 3. In a column with a height of 10 cm, the soil sample was poured in five layers of 2 cm each, and other test conditions were the same as those specified by ISO 21268-3. Furthermore, tests were conducted at a flow rate of 36 mL/h, three times faster than the ISO 21268-3. Note that for sandy soil 2, since the sample amount was limited, the case of flow rate of 36 mL/h at a height of 10 cm was not conducted. Also, chemical analysis of the filtrate for tests No. 6 and 7 was conducted up to *L*/*S* 13 and 5, respectively.

When the height of the specimen or the flow rate differs, the time required for the influent to pass through the column changes. As a result, the solid-liquid contact time, *T*, differs. The contact time, *T*, was determined as when pore water contacted the soil particles using the following equation (4.1). Herein, V_v is the pore volume (cm^3), and *r* is the flow rate (mL/h). Longer T means a longer leaching reaction time.

$$T = \frac{V_v}{r} \tag{4.1}$$

In this study, the horizontal axis of the breakthrough curve obtained in the column test was organized in terms of the permeated volumes of solution dividing pore volume (pore volumes of flow, PVF), as shown in equation (4.22).

$$\mathrm{PVF}=\frac{V_{\mathrm{w}}}{V_{\mathrm{v}}} \tag{4.2}$$

Herein, V_{w} (cm^3) is the flow rate. Under the conditions of this study, 1 PVF = approximately 0.8 L/S.

In the column tests, leachate is sampled at arbitrary time intervals. Therefore, the concentration in the leachate does not represent the concentration at the time of water sampling but the average concentration during the sampling period (Finkel and Grathwohl, 2017). In other words, the actual breakthrough curve is represented by the red line in Fig. 4.3. Therefore, the intersection of the red and black lines in Fig. 4.3 must be determined to obtain the breakthrough curve. However, it is difficult to determine the intersection of the red and black lines accurately. Therefore, in this study, the midpoint between the sampling times is assumed to represent approximately the red line in Fig. 4.3. Then, breakthrough curves were obtained by calculating the PVF.

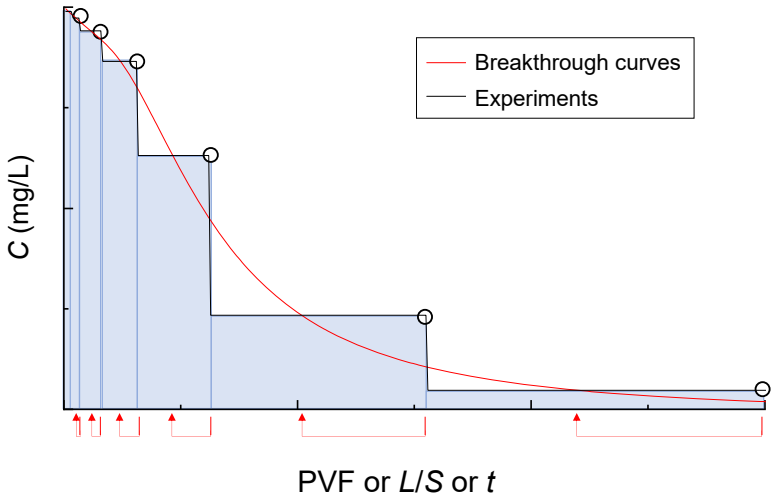

Figure 4.3 Relation between concentrations obtained from a column test and breakthrough curve.

4.2.3 Evaluating readily soluble chemicals using breakthrough curves

This study focuses on the following two points as indicators that the leaching reaction diminishes early. Chemicals with a monotonically decreasing breakthrough curve, showing a maximum concentration at approximately 0 PVF and having a concentration half of the maximum concentration at PVF $\leqq$ 1, were defined as easily soluble.

i) Shape of the breakthrough curves and maximum leaching concentration, $C_{\max}$

Whether the concentration decreased monotonically was investigated. Then, the maximum

concentration C_{max} and the PVF at that concentration were determined. As mentioned in Chapter 4.1, most easily soluble chemicals are considered as the leaching at the beginning of the permeation (while the PVF or L/S is small), and then leaching concentrations decrease rapidly (Susset and Grathwohl, 2011). Therefore, if the shape of the breakthrough curve is monotonically decreasing, the on-site leaching behavior can be predicted as a readily soluble substance (Susset and Grathwohl, 2011). On the other hand, if the breakthrough curve increased once and then decreased, it cannot be confirmed that leaching is completed quickly. Therefore, leaching behavior in the field cannot be predicted based on the breakthrough curve obtained from the column leaching tests.

ii) PVF at the relative concertation $C/C_{max} = 0.5$

This study defined chemicals with a monotonically decreasing breakthrough curve and a relative concentration (C/C_{max}) of 0.5 at 1 PVF or less as readily soluble. C is the concentration of the chemicals in the filtrates. Regardless of the reaction between the solid and liquid phases, readily soluble chemicals are rapidly leaching from the soil. Then, the chemicals migrate within the pores by dispersion. Therefore, the breakthrough curve obtained from the column leaching test should have a similar shape to the analytical solution of the advection-dispersion equation shown in Fig. 4.4, such as a point symmetry. At 1 PVF, when the pore water is replaced once, C/C_{max} becomes 0.5. At 2 PVF, the discharging of readily soluble chemicals from the pores is almost terminated. Therefore, in this study, the value of C/C_{max} at 1 PVF was focused, and readily soluble chemicals are determined as $C/C_{max} = 0.5$ in PVF $\leqq 1$.

As a result of the procedure i), ii) was performed for the column test results in which the breakthrough curve was monotonically decreasing. The concentration of the first filtrate was used for the value of C_{max}, C at 0.1 PVF. Furthermore, the value of PVF at $C/C_{max} = 0.5$ was determined by linear approximation of two points before and after $C/C_{max} = 0.5$. As shown in Figure 4.4, for the relative concentration (C/C_{max}) to be 0.5 at 1 PVF, the effective porosity, n_e, of the specimen should be equal to the porosity n. In this study, since the soil used for the column test was sandy soil, n_e might be a manageable size compared to n. For reference, n_e was calculated as (PVF where $C/C_{max} = 0.5$) × n to investigate whether ne was too smaller than n.

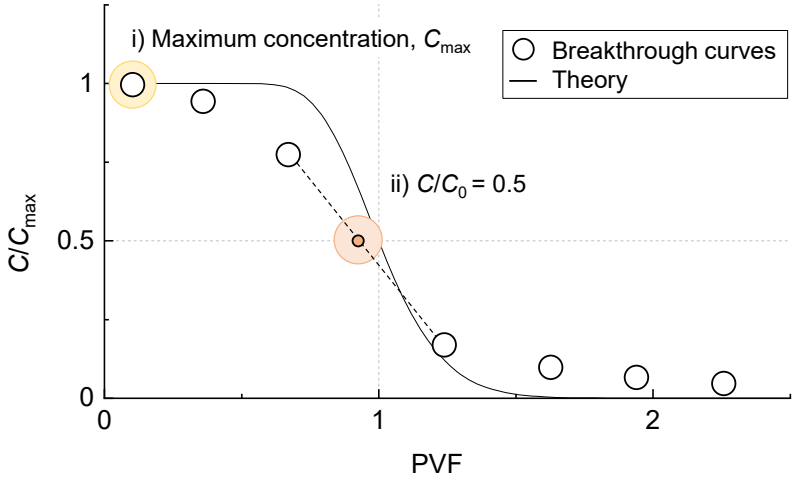

Figure 4.4 Determination of readily soluble chemicals using a breakthrough curve.

4.3 Results

4.3.1 Breakthrough curves of monotonous decreasing

For chemicals whose breakthrough curves monotonically decreased, C_{max} was determined. Table 4.4 shows the C_{max} values of B, Se, Na, Mg, and SO_4, whose leaching concentrations decreased monotonically. When the leaching reaction in the column is not in equilibrium, the longer the solid-liquid contact time T, the greater the leaching concentration C. Among test Nos. 1-4, the C_{max} of B increased in the order of Nos. 3, 2, 4, and 1. The leaching concentration did not necessarily increase or decrease proportionally to the solid-liquid contact time. Similarly, for Na, Mg, and SO_4, C_{max} did not increase or decrease in proportion to T. In other words, the difference in T due to the difference in h = 10, 30 cm and the difference in r = 12, 36 mL/h might have a negligible effect on the value of C_{max}.

The effect of the difference in specimen height h on the difference in C_{max} was investigated. As shown in Table 4.4, comparing Nos. 2 and 4, the B concentration at h = 30 cm was lower than that at h = 10 cm. Although h was increased, and solid-liquid contact was prolonged, the leaching amount did not necessarily increase. A similar trend was confirmed by comparing Na and SO_4 in Nos. 1 and 3, and no apparent tendency was confirmed in the C_{max} for the specimen height of 10 or 30 cm. Even when h increased from 10 to 30 cm, C_{max} varied between increasing and decreasing, and the difference in C_{max} was within a range of approximately 1.5 times. Although only two conditions (10 and 30 cm) were compared, a clear relationship between h and C_{max} could not be confirmed. Therefore, the effect of the difference in h on C_{max} is likely small. Considering the range of variation in evaluating the reproducibility of column test results for geogenic contamination, the difference in leaching concentration was up to 1.8 times (e.g., Naka et al., 2016; Yasutaka et al., 2017; Inui et al., 2020). Several types of research imply the heterogeneity of the geogenic contaminants in soil. Therefore, a difference of approximately 1.5 times in C_{max}, as shown in Table 4.4, was insignificant. The results suggest only a slight difference in specimen height of 10 and 30 cm on the C_{max} of B, Se, Na, Mg, and SO_4 obtained in this study.

Table 4.4 The C_{max} values obtained from column leaching tests.

Testing No.		1	2	3	4	5	6	7
Types of sandy soil		1	1	1	1	2	2	2
h (cm)		30	30	10	10	30	30	10
r (mL/h)		12	36	12	36	12	36	12
T (h)		24.3	7.9	8.1	2.7	24.3	7.9	8.1
C_{max} (mg/L)	B	4.25	3.71	3.07	3.84	0.038	0.024	0.034
	Se	0.006	0.004	0.004	0.004	-	-	-
	Na	1900	1860	2010	1790	22.8	22.7	15.3
	Mg	304	310	277	280	47.9	48.2	30.4
	SO_4	2440	3290	3010	2410	120	127	73.5

The effect of the difference in flow rate r on the difference in C_{max} was investigated. Comparing the B concentrations in No. 3 and 4, the C_{max} at 12 mL/h, where r was smaller and solid-liquid contact was more prolonged, was lower than the C_{max} at 36 mL/h. A similar trend can be confirmed from the breakthrough curves of Mg and SO_4 for Nos. 1 and 2. No apparent regularity was observed in the obtained C_{max} under the different conditions of r = 12, 36 cm in this study. Even when r increased from 12 to 36 mL/h, the difference in C_{max} was still approximately 1.5 times. The leaching amount did not necessarily decrease as the r value increased, and no clear relationship was observed. The effect of the difference in r on C_{max} is small compared to the above.

Herein, readily soluble chemicals are determined. Figure 4.5 shows the monotonous decreasing breakthrough curves for sandy soil 1. In sandy soil 1, Se, Na, Mg, and SO_4 were all determined to be readily soluble chemicals because C/C_{max} = 0.5 at 0.5-0.6 PVF, which is smaller than 1 PVF. Then, the effective porosity, n_e, of the specimen was estimated at approximately 50-60% of the porosity, n. On the other hand, as shown in Fig. 4.5(b), (d), B has PVF≦1 and C/C_{max} = 0.5, but in Figure 4.5(a), (c), PVF > 1 and C/C_{max} = 0.5. Since several breakthrough curves did not show the behavior of the readily soluble chemicals, B was not judged as readily soluble. Regarding B, although the PVF at which C/C_{max} =0.5 did not meet the criterion of PVF≦1 proposed in this study, it was in the range of PVF≦1.5. Since the shape of the breakthrough curve for B is closer to that of other readily soluble chemicals, there is room for further discussion about the criteria of the readily soluble chemicals. For example, providing a permissible range of readily soluble is conceivable.

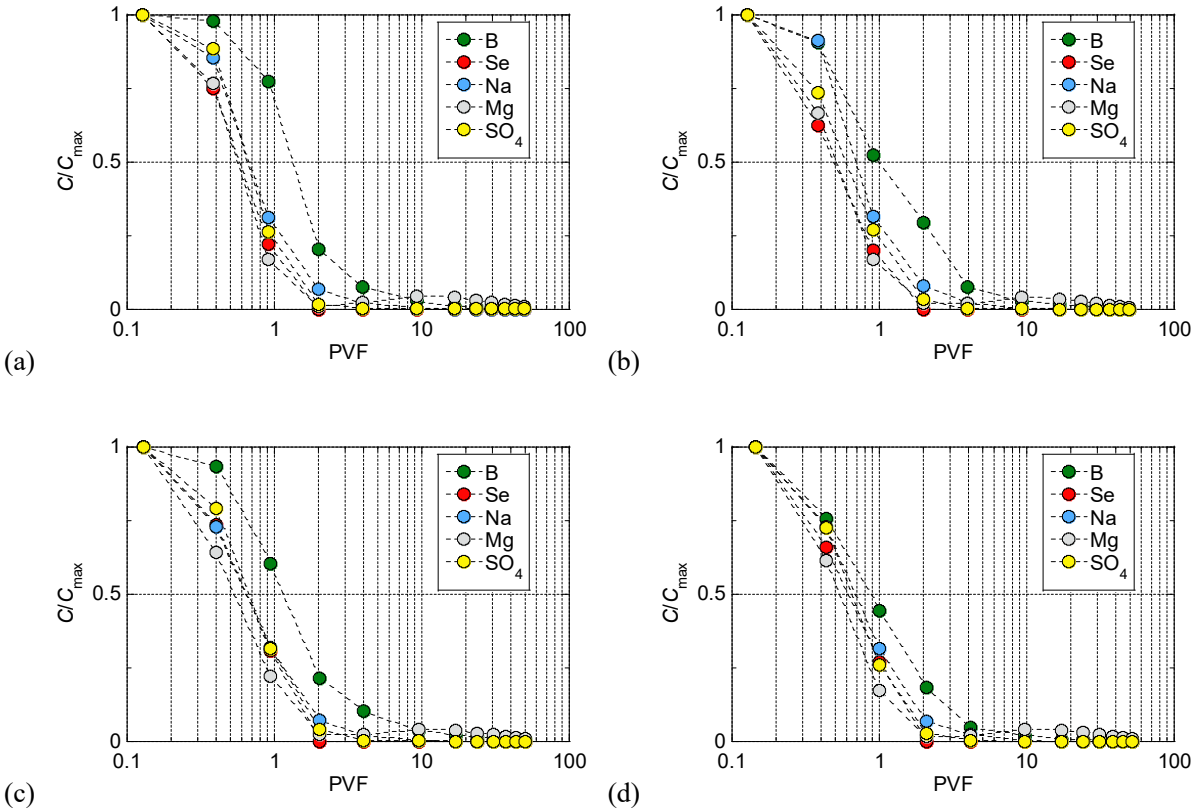

Figure 4.5 Monotonous decreasing breakthrough curves for sandy soil 1: (a) h = 30 cm, r = 12 mL/h (No.1), (b) h = 30 cm, r = 36 mL/h (No.2), (c) h = 10 cm, r = 12 mL/h (No.3), and (d) h = 10 cm, r = 36 mL/h (No.4).

The breakthrough curve for sandy soil 2 is shown in Fig. 4.6. In sandy soil 2, Se was not leached. In sandy soil 2, since SO_4 had C/C_{max} = 0.5 between 0.4 and 0.7 PVF, it was judged to be a readily soluble chemical. From this result, n_e of the sandy soil 2 specimens was supposed to be approximately 40-70% of n. For B, as shown in Fig. 4.6(b) and (c), C/C_{max} = 0.5 was achieved in PVF≦1, while in Fig. 4.6(a), C/C_{max} = 0.5 was achieved in PVF > 1. Boron was determined not to be readily soluble since it could not be determined in all breakthrough curves. Similarly, as shown in Fig. 4.6(a) and (b), Na and Mg were determined to be not readily soluble since C/C_{max} = 0.5 at PVF > 1. While the B leaching terminated relatively quickly, Na and Mg continued even at 10 PVF. Further, judging from the breakthrough curves, Na and Mg leaching are assumed to continue for a relatively long period, albeit at low concentrations.

In sandy soil 2, a tailing in which the decrease in concentration over time was smaller than that in sandy soil 1 was confirmed to be more significant (Vries et al., 2017; Ishimori et al., 2020). One of the reasons why tailing was clearly observed is that the C_{max} of sandy soil 2 is approximately 1-2 orders of magnitude smaller than sandy soil 1. This result suggests that the effect was in a lower concentration area than sandy soil 1 (Ishimori et al., 2020). A study states that Na leaching from molten slag was readily soluble (Kida et al., 2003). However, this study found that whether leaching Na or Mg was judged to be readily soluble depends on the concentration. The definition of readily soluble should be discussed in the future, considering the concentration levels. In particular, since the tailing phenomenon is noticeable, breakthrough curves obtaining C_{max} should be carefully examined. However, in practical terms, the leaching amount in the low concentration area can be negligible since the small C_{max} value.

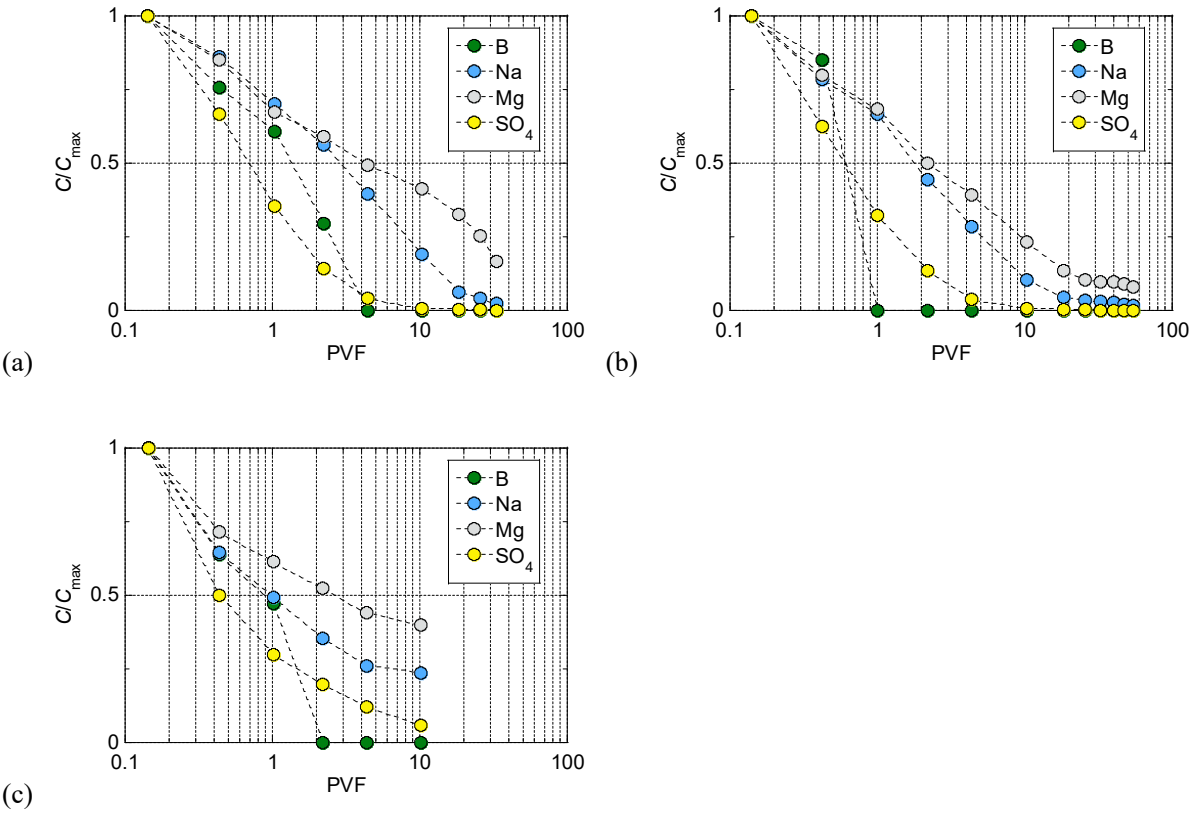

Figure 4.6 Monotonous decreasing breakthrough curves for sandy soil 2: (a) h = 30 cm, r = 12 mL/h (No.5), (b) h = 30 cm, r = 36 mL/h (No.6), and (c) h = 10 cm, r = 12 mL/h (No.7).

Investigate the effect of differences in h or r on the breakthrough curve of readily soluble. First, as shown in Fig. 4.5, all Se, Na, Mg, and SO_4 showed a monotonous decrease. Also, the PVF with $C/C_{max} = 0.5$ was similar, and the leaching terminated quickly. The shape of the breakthrough curve did not change significantly under h or r considered in this study, even if the solid-liquid contact time was affected by h or r. Also, a similar breakthrough curve shape was obtained when compared with the column test results of previous studies (Naka et al., 2016; Yasutaka et al., 2017). Similarly, in sandy soil 2, the breakthrough curves for SO_4, which was determined to be readily soluble, showed a monotonous decrease and a similar PVF for $C/C_{max} = 0.5$ in three cases, as shown in Fig. 4.6. From the above, almost the same breakthrough curve shape was obtained for readily soluble substances regardless of h or r.

Almost the same shape breakthrough curve was obtained under different specimen heights. Therefore, even if the column's scale becomes large, the leaching behavior of readily soluble chemicals is likely to quickly terminate and be discharged from the column as pore water is exchanged. Furthermore, the breakthrough curves were almost the same despite different flow rates. Therefore, the leaching kinetics of the readily soluble chemical is presumed to reach equilibrium quickly. In the range examined in this study, the leaching behavior of readily soluble chemicals could be considered generally the same even if h and r were different. Although this assumption is based on one-dimensional, small-scale column test results, if a chemical is readily soluble, it may be possible to predict the leaching behavior from the column test result in a field where the solid-liquid contact time is longer than the column leaching test.

The reason why the breakthrough curves of B and Se were monotonically decreasing and the leaching was terminated quickly was discussed. Generally, B exists as boric acid $B(OH)_3$ in the solution and is known to have no electrical charge (e.g., Shimada, 2013). Since the chemical species of B changes depending on the pH, B becomes borate ion $B(OH)_4^-$ at pH > 12. As shown in Fig. 4.7, pH values were 6.5-8.5 in sandy soils 1 and 2, suggesting that most B existed in $B(OH)_3$ (Igarashi and Shimogaki, 1998). Since $B(OH)_3$ existed in a non-charged state, B was challenging to adsorb to minerals in the soil. Therefore, the breakthrough curves of B monotonically decreased, and the leaching terminated quickly. Also, the possibility that $B(OH)_3$ is loosely adsorbed on the surface of clay minerals has been mentioned (Ito and Katsumi, 2020). As shown in Figs. 4.5 and 4.6, why B breakthrough curves were delayed by approximately 1 PVF compared to SO_4 might be explained by the adsorption.

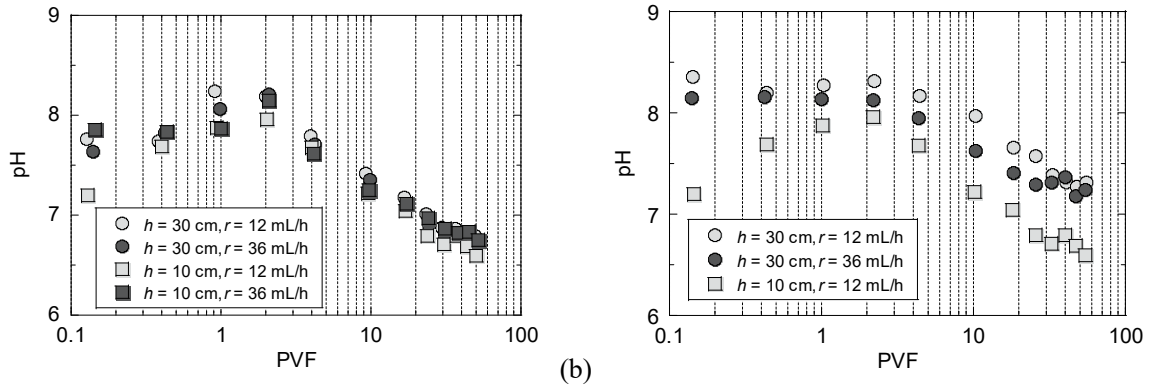

Figure 4.7 Profiles of pH values of column leaching tests: (a) sandy soil 1, and (b) sandy soil 2.

In this study, Se was determined to be readily soluble. Similarly, in a previous study of field tests, the breakthrough curve for Se was C/C_{max} = 0.5 below 1 PVF (Tamoto et al., 2015). Since Se exists in +6, +4, +1, 0, and -2 valent chemical species, Se state is known to be affected by pH and redox potential (E_h) (Shimada, 2014). Since E_h value was not measured in this study, the chemical species of Se cannot be completely identified. However, considering that the column test was conducted in an open atmosphere and the pH values were 6.5-8.5, Se was supposed to be a hexavalent(+6) or tetravalent(+4) oxyanion. In particular, hexavalent Se is difficult to adsorb due to its low reactivity (Shimada, 2014). Therefore, Se is a readily soluble chemical due to its high migration properties.

4.3.2 Breakthrough curves of arsenic, fluorine, and aluminum

Figure 4.8 shows the breakthrough curve for sandy soil 1, which did not show a monotonous decrease. Concentrations of Fe and Pb were not detected. Figure 4.8(a) shows the result of As. The As concentration increased to 2 PVF and then decreased regardless of the test conditions. Furthermore, arsenic leaching continued at approximately 0.005 mg/L even after 10 PVF.

Figure 4.8(b) shows the breakthrough curve of F. Similar to As, the leaching concentration of F increased to 2 PVF and then decreased. One of the reasons why the concentration decreased after once increasing is thought to be i) diffusion-controlled leaching from the solid phase or ii) dissolution of minerals as the influent permeating, but it is difficult to determine the cause definitively.

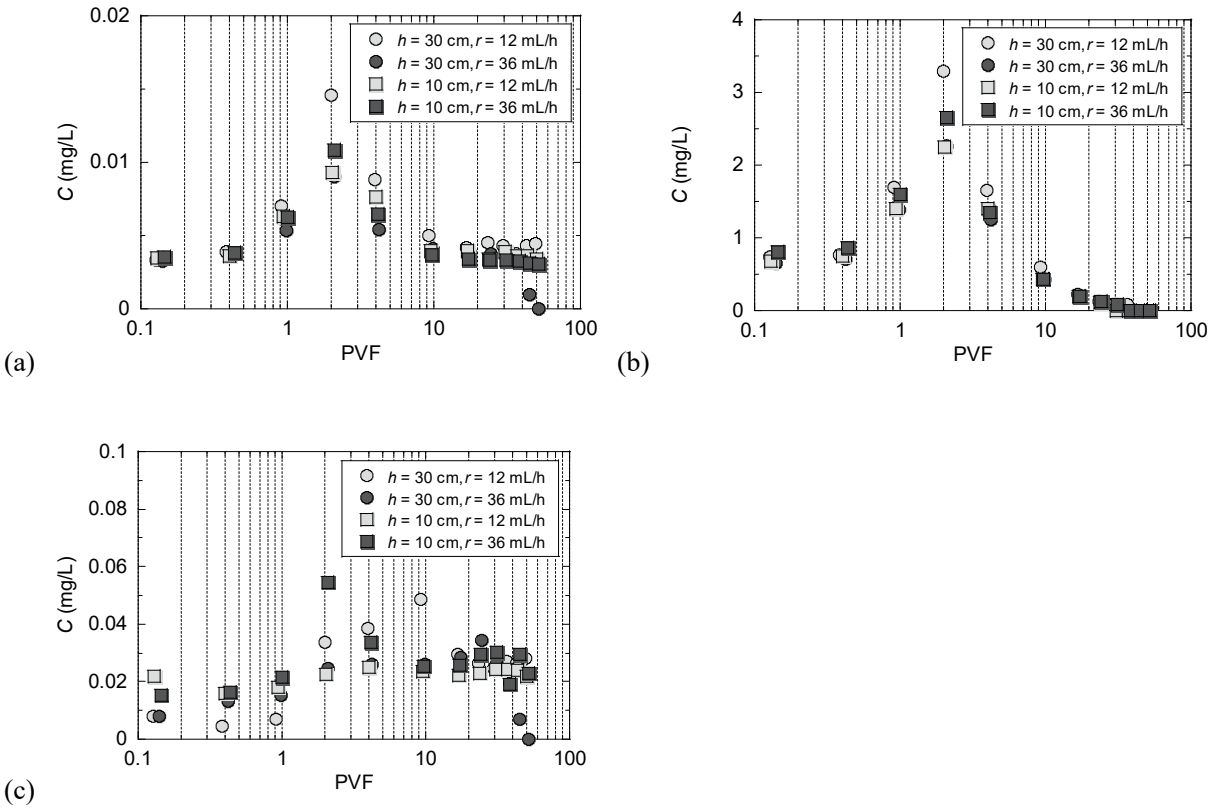

Figure 4.8 Breakthrough curves whose concentration were not monotonous decreasing in sandy soil 1: (a) arsenic (As), (b) fluorine (F), and (c) aluminum.

The leaching of F from clay minerals such as illite in sediments occurs through ion exchange with hydroxide ions (OH^-) when the pH is slightly alkaline (Shimada, 2011). As shown in Figs. 4.7(a) and 4.8(b), the pH reached its maximum value (pH = 8.3) at approximately 2 PVF, while the leaching concentration of F also reached its maximum value. In other words, there was a correlation between pH and the F leaching. As shown in Table 4.2, sandy soil 1 contains approximately 10% silt and clay, and F might leach by an ion exchange reaction with OH^- during the column test. However, since this study used sandy soil with a smaller specific surface area than clay minerals, the F leaching mechanism should be further investigated.

Previous studies have also obtained similar breakthrough curves for geogenic As and F increased once and then decreased as PVF increased (Nakamura et al., 2014; Naka et al., 2016). As shown in Fig. 4.8(a) and (b), the maximum concentration around 2 PVF for both As and F differed approximately 1.5 times in each case. Compared to the fluctuation of leaching concentration in previous studies, the influence of the specimen height and flow rate on the difference in the shape of As and F breakthrough curves should be minimal (Naka et al., 2016; Yasutaka et al., 2017). From the above, although the influence of h and r on the shape of the breakthrough curve might also be undersized for not readily soluble chemicals, such as As and F, the leaching behavior of onsite is complex to predict from the column test results because whether the discharge terminates quickly or the leaching kinetics is high is not unclear. In such cases, inflow boundary concentration conditions must be determined based on the cumulative leaching concentration up to L/S 2 (Susset and Grathwohl, 2011). A relatively large concentration should be assumed for chemicals expected to leach over a long period, such as As and F, and safe side inflow concentration conditions should be set for advective-dispersion analysis (Susset and Grathwohl, 2011).

Figure 4.8(c) shows the Al breakthrough curve. The Al concentration was low after the permeation started. Also, the concentrations were still approximately 0.02 mg/L even when the PVF increased. Arsenic contained in marine sediments is known to be adsorbed by oxides and hydroxides in soil, such as Fe and Al (Shimada, 2011; Katayama et al., 2020). The pH values should influence the amount of As adsorbed by oxides and hydroxides. As shown in Fig. 4.8(a), focusing on the behavior of As after 10 PVF, arsenic showed a constant concentration of around 0.005 mg/L, while Al after 10 PVF was around 0.02 mg/L. The correlation between As and Al concentrations was also confirmed in this study. Furthermore, as shown in Figs. 4.7(a) and 4.8(a), pH and As concentrations reached their maximum values around 2 PVF and then decreased similarly. A correlation between pH and As concentration was also confirmed. Inui conducted a rainfall-simulating column test using marine sediments collected from a similar area of sandy soil 1. The result showed that pH was not the only dominant factor for the As leaching; depth and saturation degree also influenced it. (Inui et al., 2020). This study conducted column tests with a similar saturation degree. However, the depths were different. The results showed that the effect of the difference in depth was small, as shown in Fig. 4.8(a). In the future, column tests under different saturation conditions should be conducted to elucidate the mechanism of As leaching.

Figure 4.9 shows the breakthrough curves for sandy soil 2. The concentrations of F, Pb, and Fe were not detected. The As concentration was about 1/10 lower than that in sandy soil 1, as shown in Fig. 4.9(a). The As leaching concentration showed differences in each test case. Due to a low concentration of As, the difference in the shape of breakthrough curves is likely due to the heterogeneity of the soil or the

limitations of chemical analysis. Therefore, the impact of *h* or *r* cannot be concluded. As shown in Fig. 4.9(a), the leaching of arsenic continued at around 0.001 mg/L after 30 PVF. This result indicates that arsenic leaching might continue for a longer duration.

Figure 4.9(b) shows the breakthrough curve of Al. Aluminum continued to show values of approximately 0.01-0.07 mg/L. As with sandy soil 1, no apparent differences were observed due to differences in *h* and *r*. Also, the correlation between As and Al leaching concentrations observed in sandy soil 1 could not be confirmed in sandy soil 2 (Shimada, 2011; Katayama et al., 2020). This result suggests that other mechanisms besides adsorption/desorption reactions from Al oxides or hydroxides are possible as the leaching mechanism of As.

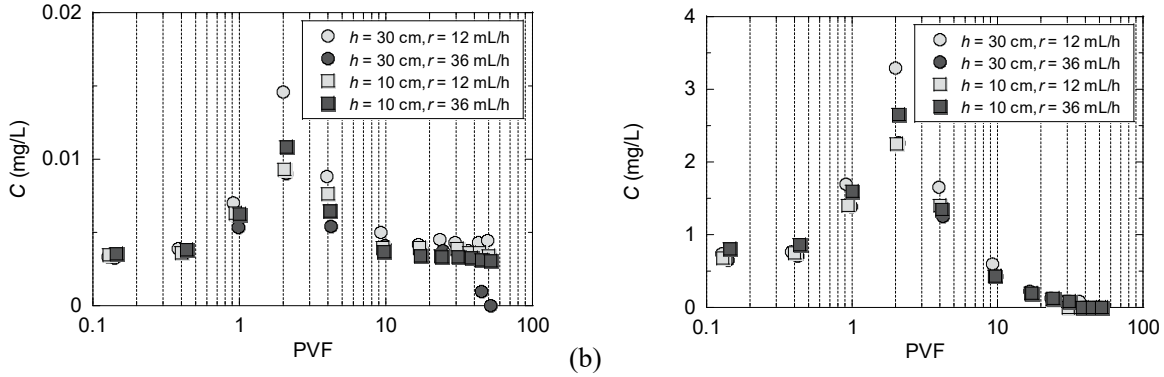

(a) (b)

Figure 4.9 Breakthrough curves whose concentration were not monotonous decreasing in sandy soil 2: (a) arsenic (As), and (b) aluminum.

4.4 Interpretation and application of the column leaching tests

4.4.1 Risk assessment for a readily soluble chemical

How to utilize the results of determining the readily soluble substances in column tests is discussed. Herin, the boundary condition of the inflow concentration for contaminant during advection-dispersion analysis is considered to be determined based on the results of column tests. In this study, the impacts of the difference in *h* or *r* on the leaching behavior of the readily soluble chemicals on C_{max} or breakthrough curves shape. In both sandy soils 1 and 2, since differences in *h* or *r* are not significant, the breakthrough curves of the readily soluble chemicals are assumed to be similar regardless of the h and r. Therefore, assuming the construction of an embankment, when conducting an advection-dispersion analysis, as shown in Fig. 4.10(a), it is highly possible to focus on the number of exchanges of pore water. Then, breakthrough curves can be utilized for the design of the embankment. In other words, the risk assessment closer to the onsite condition can be conducted by setting the inflow concentration conditions, as shown in Figure 4.10(b). Figure 4.10(b) is the boundary condition that gives C_{max} up to 2 PVF, where the leaching concentration of a readily soluble chemical can be considered to approach 0, with the maximum concentration C_{max} obtained in the column test as the inflow concentration. Figure 4.10(b) is closer to reality because it gives the maximum C_{max} concentration obtained in the column test. Moreover, since the leaching of readily soluble chemicals is *C*/

C_{max} = 0.5 at 1 PVF and terminates at approximately 2 PVF, such behavior is included in Fig. 4.10 b).

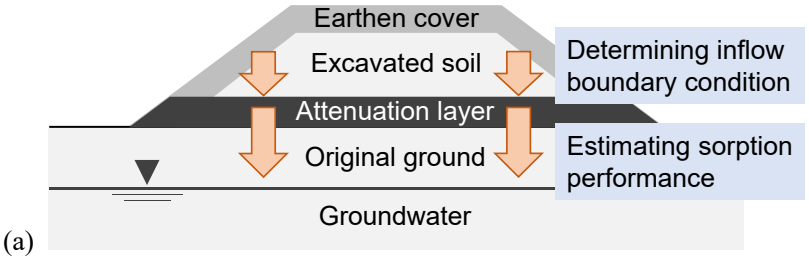

(a)

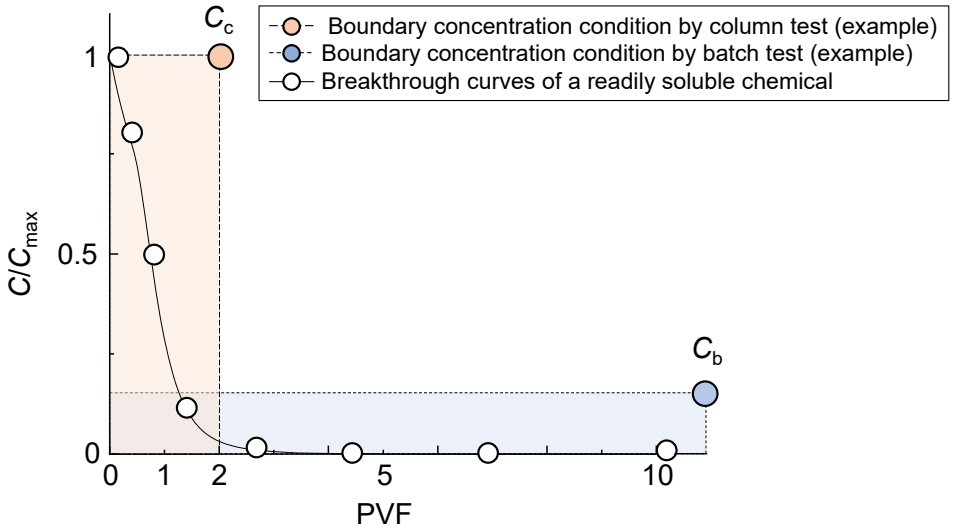

(b)

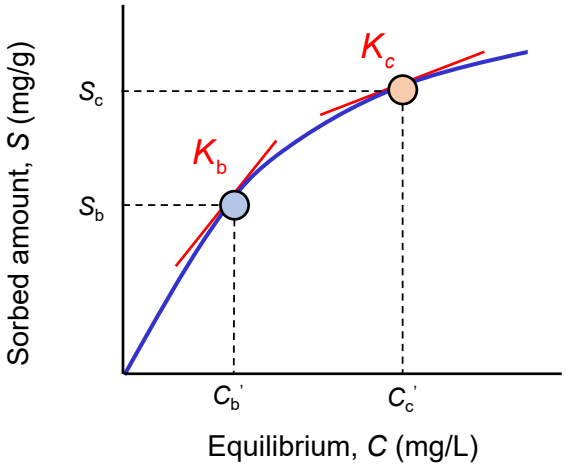

(c)

Figure 4.10 Application of the result after determining a readily soluble chemical: (a) an image of the utilization of the excavated soils and rocks with geogenic contamination, (b) breakthrough curve of a readily soluble chemical and determination of the inflow boundary concentration, and (c) relation between an equilibrium concentration and a sorbed amount of the contaminant.

However, some challenges should be clarified. For example, column tests' dry density, redox state, material heterogeneity, and permeability heterogeneity are not entirely equivalent to the in-situ conditions. Since the column test is just a laboratory test and cannot wholly represent reality, the boundary concentration should be determined on the safe side. Therefore, the leaching concentration was continuously given C_{max} up to 2 PVF, as shown in Fig. 4.10(b). By performing a column test to determine readily soluble chemicals, appropriate countermeasures can be taken against readily soluble chemicals that leach at relatively high concentrations during the initial permeation period. In this study, although B is not determined to be readily soluble, its breakthrough curve shape is close to readily soluble. Therefore, when the countermeasure is designed against B, the period of giving C_{max} can be lengthened. The criteria for the readily soluble chemicals a future issue. In addition, due to the regulations of the column leaching test method specified by ISO, C_{max} was the concentration sampled in this study when L/S was 0.1. Therefore, how to obtain the C_{max} value should be discussed.

As shown in Chapter 4.1, the leaching behavior of readily soluble chemicals is expressed using the analytical solution of the advection-dispersion equation, and it is used for the inflow concentration condition in Germany (Susset and Grathwohl, 2011). In other words, numerical analysis is performed using numerical solutions of the advection-dispersion equation. In contrast, a constant concentration of C_{max} is proposed in this study, mainly for two reasons. First, since it is a boundary condition that gives a constant concentration, a simple analysis using the advection-dispersion equation's analytical solution can be conducted while considering the readily soluble behavior. Furthermore, a breakthrough curve model for column leaching tests has yet to be established. Also, the analytical solution of the advection-dispersion equation might not describe the breakthrough curve obtained in the leaching test, mainly when the tailing mentioned in 4.3.1 is observed (Ishimori et al., 2020). Since it is challenging to express breakthrough curves as a function completely, the expressed function might not represent reality. Therefore, the constant concentration C_{max} was given for a certain period as the inflow concentration conditions for the readily soluble chemicals in this study.

Herein, explain the significance of identifying the readily soluble chemical using a column leaching test. The readily soluble chemical shows maximum concentration at the beginning of the permeation. Therefore, the highest concentration is obtained at the initial stage of the test. As mentioned in Chapter 4.1, the concentration C_b is often determined in a batch leaching test using L/S 10 in Japan. Then, the inflow boundary concentration is determined, and advection-dispersion analysis is performed. Batch testing provides the total leaching amount under a specific L/S condition. However, a profile of the leaching concentration, especially at the initial stage of the test, cannot be examined compared to a column test. Also, the concentration C_b is the average leaching concentration under relatively large L/S. Therefore, C_b is expected to be smaller than the maximum concentration C_c (same as C_{max}) obtained in the column leaching test. When using excavated soil as a geomaterial, after determining the inflow concentration based on leaching tests, estimate the sorption capacity required of the attenuation layer or the original ground. As shown in Fig. 4.10(c), when the sorption performance of the attenuation layer or the original ground is expressed in the Freundlich isotherm, the partition coefficient K_c calculated by C_c should be smaller than K_b calculated by C_b. In order to perform a safer risk assessment for the readily soluble chemicals, column leaching tests should be conducted to obtain C_c.

When determining the readily soluble chemicals, the general trend of the breakthrough curve can be obtained by performing a column test up to at least 2 PVF (approximately equivalent to *L*/*S* 1.5). Although the length of the test duration has been pointed out as an issue with column tests (Nakamura et al., 2014; Naka et al., 2016), safer risk assessment can be carried out using the short-term column tests up to about *L*/*S* 2. In this study, Na and Mg were not judged to be readily soluble in all soils. Whether a chemical is readily soluble depends on the soil type. Therefore, conducting a column test for each soil is desirable to evaluate its leaching behavior precisely. For example, B was monotonically decreasing (e.g., Naka et al., 2016), but the concentration of B was once increasing and then decreasing (e.g., Arima et al., 2011). As mentioned in Section 4.3.1, pH influences boron's fate and transport. Therefore, the breakthrough curve of B, which was a monotonically decreasing curve in this study, might not be a monotonically decreasing curve in alkaline soils. These results suggest column tests for each soil type and construction site.

4.4.2 Column leaching test results organization using PVF as index

Organizing column test results using PVF is recommended in this study. Unlike the conventional arrangement using *L*/*S*, the soil particle density measurement for calculating the pore volume is required. Therefore, the accumulating information is not only on the amount of leaching fraction but also on the fundamental physical properties of the soil. Furthermore, as shown in Table 4.1, conventional column tests are often applied in environmental chemistry, such as treating incinerated ash or waste using *L*/*S*. On the other hand, the excavated soils and rocks with geogenic contamination are used in earth structures such as embankments. Therefore, the leaching behavior should be evaluated considering the soil conditions, such as dry density, compaction degree, and degree of saturation. As shown in 4.3.1, since the effective porosity, ne, might be smaller than the porosity, if n_e, is not considered, the leaching amount might be underestimated. Therefore, organizing the breakthrough curve using PVF and evaluating the effective porosity is essential to get closer to reality.

4.4.3 Influences of column length

This study conducted column tests at different heights of 10 and 30 cm. There was no significant difference in the shape of the breakthrough curve for readily soluble chemicals, even if the height of the specimen was different. From this result, the leaching behavior of readily soluble chemicals in the practical condition can be predicted by focusing on the number of exchanging pore water, as in column tests. This fact also indicates the possibility of applying a column test with a smaller specimen height to shorten the test period. However, it is still being determined whether the results of this study can be applied to all excavated soils and rocks with geogenic contamination. In particular, there needs to be more knowledge to apply test results on the scale of several centimeters in the laboratory to the scale of several meters in reality. It is desirable to accumulate knowledge in the future by carrying out larger-scale column tests and model experiments extended to two or three dimensions. Conducting on-site monitoring and clarifying the relationship between experiments and reality is also essential.

4.5 Summary and Conclusions

In this study, an up-flow column test was conducted on marine sediments. The breakthrough curves were obtained by organizing the horizontal axis of the concentration profile with PVF. A chemical whose concentration profile monotonically decreases and shows the maximum concentration when PVF≒0, and whose concentration is half of the maximum concentration when PVF≦1, was defined as a "readily soluble chemical" whose leaching was terminated quickly. The results support the following conclusions:

1. In sandy soil 1, since Se, Na, Mg, and SO_4 concentrations decreased monotonically and reached C/C_{max} = 0.5 below 1 PVF, they were determined to be readily soluble. On the other hand, the concentration profiles of B showed a monotonous decrease, but C/C_{max} = 0.5 was not achieved at PVF≦1. Boron was not determined to be a readily soluble chemical.
2. In sandy soil 2, the concentration profiles of B, Na, Mg, and SO_4 were monotonically decreasing, but only SO_4 was determined to be readily soluble. The leaching of Na and Mg continued even after 10 PVF, indicating the possibility that the leaching may continue for a long time, albeit at a low concentration.
3. The concentrations of As and F decreased after increasing once. Therefore, they were not determined to be readily soluble. The leaching of As and F continued after 10 PVF.
4. When readily soluble chemicals are determined, the concentration profiles can be determined by performing a column test up to approximately 2 PVF. Since readily soluble chemicals show the maximum leaching concentration at the beginning of permeation, a more realistic risk assessment can likely be performed by determining the inflow concentration conditions through a short-term column test.

References for Chapter 4

Arima, T., Sato, D., Igarashi, T., Tamoto, S, and Tatsuhara, T., 2011. Reduction and retardation of arsenic and boron leached from excavated rocks by volcanic ash adsorption layer. *Journal of the Japan Society of Engineering Geology* 52(3), 88–96 (in Japanese). https://doi.org/10.5110/jjseg.52.88.

Bandow, N., Finkel, M., Grathwohl, P., and Kalbe, U., 2019. Influence of flow rate and particle size on local equilibrium in column percolation tests using crushed masonry, *Journal of Material Cycles and Waste Management* 21, 642–651. https://doi.org/10.1007/s10163-019-00827-3.

Cappuyns, V. and Swennen, R., 2008. The application of pHstat leaching tests to assess the pH-dependent release of trace metals from soils, *Journal of Hazardous materials* 158, 185–195. https://doi.org/10.1016/j.jhazmat.2008.01.058.

Carrilo, A., and Drever, J.I., 1998. Adsorption of arsenic by natural aquifer material in the San Antonio EI Triufo mining area, Baja, California, Mexico, *Environmental Geology* 35, 251–257. https://doi.org/10.1007/s002540050311.

de Vries, E. T., Raoof, A., and van Genuchten, M. T., 2017. Multiscale Modelling of Dual-porosity Porous Media; A Computational Pore-scale Study for Flow and Solute Transport, *Advances in Water Resources* 105, 82–95. https://doi.org/10.1016/j.advwatres.2017.04.013.

Finkel, M. and Grathwohl, P., 2017. Impact of pre-equilibration and diffusion limited release kinetics on effluent concentration in column leaching tests: Insights from numerical simulations, *Waste Management* 63, 58–73. https://doi.org/10.1016/j.wasman.2016.11.031.

Igarashi, T., and Shimogaki, H., 1998. Migration characteristics of boron by batch and column methods, *Journal of Groundwater Hydrology* 40(2), 121–132 (in Japanese). https://doi.org/10.5917/jagh1987.40.121.

Inui, T., Hori, M., Katsumi, T., and Takai, A., 2020. Long-term leaching behavior of marine sediment by a large column percolation test. *Journal of the Society of Materials Science, Japan* 69(4), 53–56 (in Japanese). https://doi.org/10.2472/jsms.69.53.

Ishimori, H., Tang, J., Nakagawa, M., and Sakanakura, H., 2020. Effects of nonlinear adsorption/desorption mathematical models on chemical concentration profiles of leachate from tsunami deposits: simplified calculation method for advection-dispersion analysis. *Japanese Geotechnical. Journal* 15(3), 497–508 (in Japanese). https://doi.org/10.3208/jgs.15.497.

ISO 21268-3, 2019. Soil Quality—Leaching Procedures for Subsequent Chemical and Ecotoxicological Testing of Soil and Soil Materials—Part 3: Up-Flow Percolation Test. International Standardization Organization.

Ito, H. and Katsumi, T., 2020. Leaching characteristics of naturally derived toxic elements from soils in the western Osaka area: Considerations from the analytical results under the Soil Contamination Countermeasures Act. *Japanese Geotechnical. Journal* 15(1), 119–130 (in Japanese). https://doi.org/10.3208/jgs.15.119.

JIS K 0102, 2016. Testing Methods for Industrial Wastewater. Japanese Standards Association.

JIS A 1202, 2009. Testing Methods for Density of Soil Particles. Japanese Standards Association.

JIS A 1204, 2009. Testing Methods for Particle Size Distribution of Soils. Japanese Standards Association.

Kalbe, U., Berger, W., Simon, F., Eckardt, J., and Christoph, G., 2007. Results of interlaboratory comparisons of column percolation tests, *Journal of Hazardous Materials* 148, 714–720, https://doi.org/10.1016/j.jhazmat.2007.03.039.

Kalbe, U., Berger, W., Eckardt, J., and Simon, F., 2008. Evaluation of leaching and extraction procedures for soil and waste, *Waste Management* 28, 1027–1038. https://doi.org/10.1016/j.wasman.2007.03.008.

Katayama, J., Inui, T., Katsumi, T., and Takai, A., 2020. Leaching behavior of naturally-contained arsenic in marine sediment by the long-term column percolation test. *Japanese Geotechnical. Journal* 15(4), 675–682 (in Japanese). https://doi.org/10.3208/jgs.15.675.

Katsumi, T., 2017. Use of excavated soils with natural contamination. *Japanese Geotechnical Society Magazine*. 65 (11/12), 1–3 (in Japanese).

Kida, A., Osako, M., and Sakai, S., 2003. Evaluation of soil and groundwater contamination from molten slag generated from solid waste by column test. *Environmental Science* 16(6), 497–516 (in Japanese). https://doi.org/10.11353/sesj1988.16.497.

Meza, S.L. Kalbe, U., Berger, W., and Simon, F.G., 2010. Effect of contact time on the release of contaminants from granular waste materials during column leaching experiments, *Waste Management* 30, 565–571. https://doi.org/10.1016/j.wasman.2009.11.022.

Ministry of Land, Infrastructure, and Transport, Japan, 2023. Technical Manual on the Countermeasure Against Soils and Rocks Containing Naturally Occurring Heavy Metals in Construction Works. https://www.mlit.go.jp/sogoseisaku/region/recycle/d11pdf/recyclehou/manual/shizenyurai2023.pdf (accessed 29 November 2023) (in Japanese).

Ministry of Environment, 1995. Environmental Agency Notification No.46: Leaching Test Method for Soils. http://www.env.go.jp/kijun/dojou.html (in Japanese) (accessed 27 October 2021).

Mongi, H., Kida, A., and Hosoi, Y., 2009. Leaching characteristics of heavy metals from recycled glass materials and evaluation of effect on groundwater. *Journal of the Japan Society of Material Cycles and Waste Management* 20(1), 24–38 (in Japanese). https://doi.org/10.3985/jjsmcwm.20.24.

Naka, A., Yasutaka, T., Sakanakura, H., Kalbe, U., Watanabe, Y., Inoba, S., Takeo, M., Inui, T., Katsumi, T., Fujikawa, T., Sato, K., Higashino, K., and Someya, M., 2016. Column percolation test for contaminated soils: key factors for standardization, *Journal of Hazardous Materials* 320, 326–340. https://doi.org/10.1016/j.jhazmat.2016.08.046.

Nakamura, K., Ysutaka, T., Fujikawa, T., Takeo, M., Sato, K., Watanabe, Y., Inoba, S., Tamoto, S., and Sakanakura, H., 2014. Up-flow column tests to evaluate heavy metal leaching for standardization. *Japanese Geotechnical. Journal* 9(4), 697–706 (in Japanese). https://doi.org/10.3208/jgs.9.697.

Shimada, N., 2011. The essence of problems on groundwater and soil pollutions caused by naturally occurring heavy metals and harmful elements: Fluorine, *Oyo Corporation Annual Report* 30. (in Japanese) https://www.oyo.co.jp/pdf/technology_annual/2010_01.pdf (accessed 26 November 2023).

Shimada, N., 2013. The essence of problems on groundwater and soil pollutions caused by naturally

occurring heavy metals and harmful elements: Boron, *Oyo Corporation Annual Report* 32. (in Japanese) https://www.oyo.co.jp/pdf/technology_annual/2013_02.pdf (accessed 26 November 2023).

Shimada, N., 2014. Naturally derived heavy metals and environmental pollution - Applied geological and geochemical data bank, ISBN 978-4-87256-423-5, 152–171 (in Japanese).

Susset, B. and Grathwohl, P., 2011. Leaching standards for mineral recycling materials – A harmonized regulatory concept for the upcoming German Recycling Decree, *Waste Management* 31, 201–214. https://doi.org/10.1016/j.wasman.2010.08.017.

Tabelin, C.B., Igarashi, T., Villacorte-Tabelin, M., Park, I., Opiso, E.M., Ito, M., and Hiroyoshi, N., 2018. Arsenic, selenium, boron, lead, cadmium, copper, and zinc in naturally contaminated rocks: a review of their sources, modes of enrichment, mechanisms of release, and mitigation strategies. *Science of the Total Environment* 645, 1522–1553. https://doi.org/10.1016/j.scitotenv.2018.07.103.

Tamoto, S., Tabelin, C.B., Igarashi, T., Ito, M., and Hiroyoshi, N., 2015. Short and long term release mechanisms of arsenic, selenium and boron from a tunnel-excavated sedimentary rock under in situ conditions. *Journal of Contaminant. Hydrology* 175–176, 60–71. https://doi.org/10.1016/j.jconhyd.2015.01.003.

Tatsuhara, T., Jikihara, S., Tastumi, T., and Igarashi, T., 2015. Effects of the layout of adsorption layer on immobilizing arsenic leached from excavated rocks. *Japanese Geotechnical. Journal* 10(4), 635–640 (in Japanese). https://doi.org/10.3208/jgs.10.635.

Wehrer, M. and Totsche, K.U., 2008. Effective rates of heavy metal release from alkaline wastes – Quantified by column outflow experiments and inverse simulations, *Journal of Contaminant Hydrology* 101, 53–66. https://doi.org/10.1016/j.jconhyd.2008.07.005.

Yasutaka, T., Naka, A., Sakanakura, H., Kurosawa, A., Inui, T., Takeo, M., Inoba, S., Watanabe, Y., Fujiwara, T., Miura, T., Miyaguchi, S., Tatsuhara, T., Chida, T., Hirata, K., Ohori, K., Someya, M., Katoh, M., Umino, M., Negishi, M., Ito, K., Kojima, J., and Ogawa, S., 2017. Reproducibility of up-flow column percolation tests for contaminated soils, *PLoS ONE* 12(6), 1–17. https://doi.org/10.1371/journal.pone.0178979.

Chapter 5

Sorption-Desorption Column Tests to Evaluate the Attenuation Layer Using Soil Amended with a Stabilizing Agent

5.1 General remarks

To reduce the disposal of soils, the excavation of new materials, the carbon footprint, etc., the utilization of soils and rocks excavated at construction sites is highly encouraged (e.g., Magnusson et al., 2019). However, the utilization of these materials in Japan remains a challenge for several reasons. One large concern is that a certain percentage of these excavated materials contain toxic geogenic chemicals, such as arsenic (As), fluorine (F), and lead (Pb) (e.g., Naka et al., 2016; Tabelin et al., 2018; Tamoto et al., 2015). If contaminated materials fail to meet the environmental standards and/or the Soil Contamination Countermeasures Law (SCCL), actions for contaminant control must be implemented (e.g., Katsumi et al., 2019; Ministry of Land, Infrastructure, and Transport, 2010). Considering the leaching load and the nature of the materials, measures such as containment and chemical treatment are inappropriate for two main reasons. First of all, in many cases, toxic chemicals are leached in concentrations that slightly exceed the mandated limits under the SCCL (e.g., Ito and Katsumi, 2020). Second of all, although significantly large volumes of excavated soils and rocks are generated at construction sites, only a certain percentage contains toxic chemicals (e.g., Ministry of Land, Infrastructure, and Transport, 2010). Therefore, the implementation of cost-effective countermeasures for the proper utilization of these contaminated materials is desirable (Katsumi, 2015).

One possible countermeasure for preventing the contamination of the adjacent ground, where such contaminated soils are utilized, is the attenuation layer method. The benefits of this method are its low material costs and reduced management efforts (e.g., Tatsuhara et al., 2012, 2015; Nozaki et al., 2013a). To prevent (or reduce to acceptable levels) the infiltration of toxic chemicals from these contaminated materials into the adjacent ground, an attenuation layer is installed on the embankment foundation, as shown in Fig. 5.1 (Mo et al., 2020; Nozaki et al., 2013b; Tabelin et al., 2013). A typical attenuation layer material is clean sandy soil mixed with a stabilizing agent.

The sorption performance should be evaluated for the attenuation layer to prevent the infiltration of contaminants. The partition coefficient, K_d (cm^3/g), is a common index for evaluating the sorption performance of geomaterials. This parameter can be determined through various laboratory experiments, including batch tests, column tests, and other experimental methods. The advantage of the batch test is that

it has a simple experimental protocol with a short testing time. In this test, K_d is obtained from at least one of the empirical sorption isotherms. However, the applicability of this test is limited for three reasons. Firstly, it usually employs a liquid-to-solid (L/S) ratio of 10–50 L/kg, which is much higher than the in-field infiltration. Secondly, the temporal changes in concentrations are difficult to be distinguished (Martínez-Lladó et al., 2011). Thirdly, the test does not consider solute kinetics or the in-field flow conditions (Plassard et al., 2000).

Recently, the column test has become more prevalent for evaluating the sorption performance. In this test, the concentrations in the effluents can be monitored for several L/S ratios, including much smaller ratios than in the batch test. The smaller L/S ratios can better represent the in-field conditions. By modelling the breakthrough curves from this test, K_d can be determined (Igarashi and Shimogaki, 1998; Martínez-Lladó et al., 2011; Wang and Liu, 2005).

The sorption performance of the stabilizing agent against geogenic contaminants is more commonly investigated by batch experiments (e.g., Morishita and Wada., 2013; Nishikata et al., 2020; Nozaki et al., 2013b) than by column experiments (Mo et al., 2020; Tatsuhara et al., 2012). Furthermore, the sorption performance of the agent has been individually evaluated (Nishikata et al., 2020; Nozaki et al., 2013b; Tabelin et al., 2013), while the soil-agent mixture has not been fully evaluated. As an evaluation of the sorption performance has shown that it is much closer to the in-field conditions, it should be performed by column tests using a soil-agent mixture.

Contaminants sorbed by a soil-agent mixture should be immobilized in the attenuation layer. The concentrations of geogenic contaminants leached from excavated soils often decrease and approach zero over time (Inui et al., 2014; Naka et al., 2016). In this situation, contaminants sorbed by relatively weak chemical interactions may be desorbed by seepage water. The desorption behavior should be considered in order to evaluate the sorption performance of the attenuation layer.

Sorption-desorption column tests have the potential for use in evaluating the attenuation layer. This test has been conducted to assess 1) the migration characteristics of chemicals in the ground (Igarashi and Shimogaki, 1998; Wang and Liu, 2005), 2) the recovery percentage of metals in soils (Martínez-Lladó et al., 2011), and 3) the regeneration of the sorption performance (Ye et al., 2018). The sorption-desorption column test can indicate whether contaminants immobilized by soil amended with a stabilizing agent are leached during the desorption phase because weakly attracted contaminants can be leached.

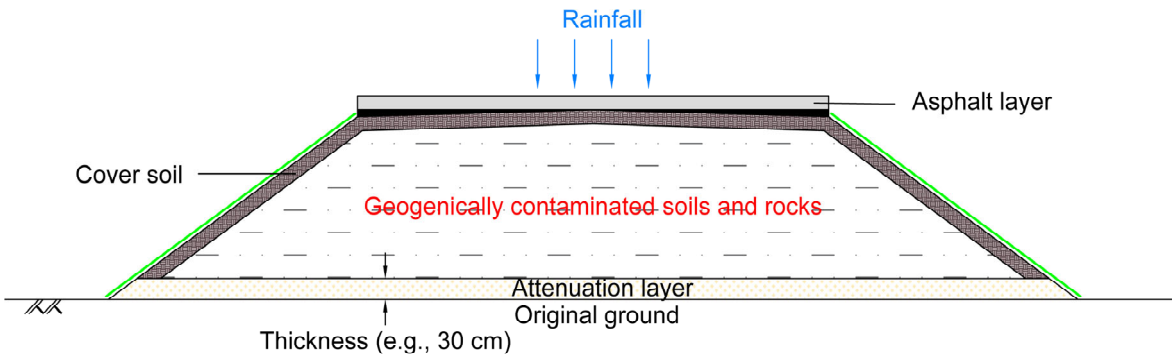

Figure 5.1 Schematic of conventional design of attenuation layer method.

In this study, sorption-desorption column tests were conducted to discuss the sorption performance of soil amended with a stabilizing agent. Fluoride (F^-) was selected as the target contaminant because it is a geogenic contaminant whose concentration exceeds the acceptable limit regulated under the SCCL (e.g., Ito and Katsumi, 2020; Naka et al., 2016). Magnesium oxide (MgO) was used as the stabilizing agent because it is a promising agent for the attenuation layer (Nozaki et al., 2013b). To estimate the sorption and desorption parameters, the analytical solution for the one-dimensional advection-dispersion equation (ADE) was fitted to the breakthrough curves obtained from column experiments.

5.2 Methodologies for sorption-desorption column tests

5.2.1 Materials

Silica sand was used as the clean parent material. Table 5.1 summarizes its physical properties. Figure 5.2 shows its X-ray diffraction (XRD) profile with CuKα, 40 kV, 100 mA (RINT-2500, Rigaku in GSJ-Lab, AIST), as shown in Fig. 5.3(a).

The stabilizing agent was manufactured by Taiheiyo Cement. The chemical composition of the agent was evaluated by X-ray fluorescence (XRF) (EDX-720, Shimadzu), as shown in Fig. 5.3(b), and it was determined that the agent mainly constituted MgO and its content was ~91%. It also contained a certain amount of CaO (~6.7%). It had a Blaine specific surface area of 5970 cm^2/g, which was determined as per JIS R 5201 (2015). The residue on a 90-μm sieve was 21.2 wt.%. It had a particle density of 3.21 g/cm^3, which was determined as per JIS R 5201 (2015).

The test specimens had three agent contents (1, 5, or 10%). These agent contents of 1, 5, and 10% corresponded to stabilizing agent contents of 10 g-, 50 g-, and 100 g per kg of dry soil, respectively. In the experiment, silica sand was poured into a steel bowl, and then the appropriate amount of stabilizing agent was added. Finally, the sand and the stabilizing agent were manually mixed with care to prepare the homogenous mixtures.

Table 5.1 Physical properties of silica sand.

Parameter	Standard	Value
Particle density	JIS A 1202 (2009)	2.62 g/cm^3
Particle size distribution	JIS A 1204 (2009)	
Sand [0.075–2 mm]		98%
Fines [< 0.075 mm]		2%
Maximum particle size		0.425 mm
Coefficient of uniformity		1.04
Coefficient of curvature		2.17

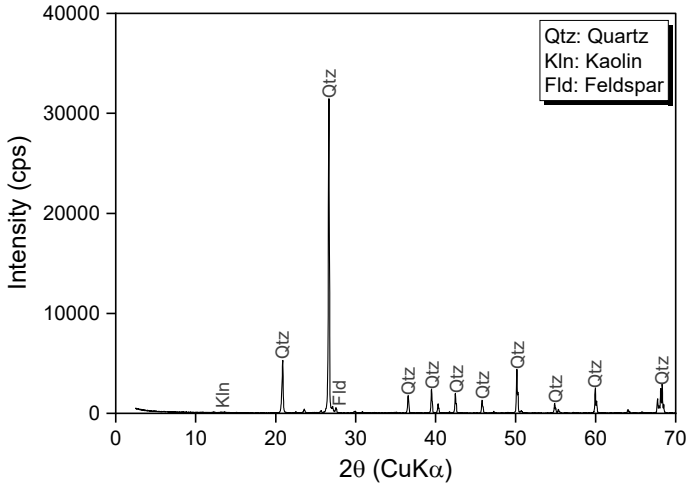

Figure 5.2 XRD profile of the silica sand.

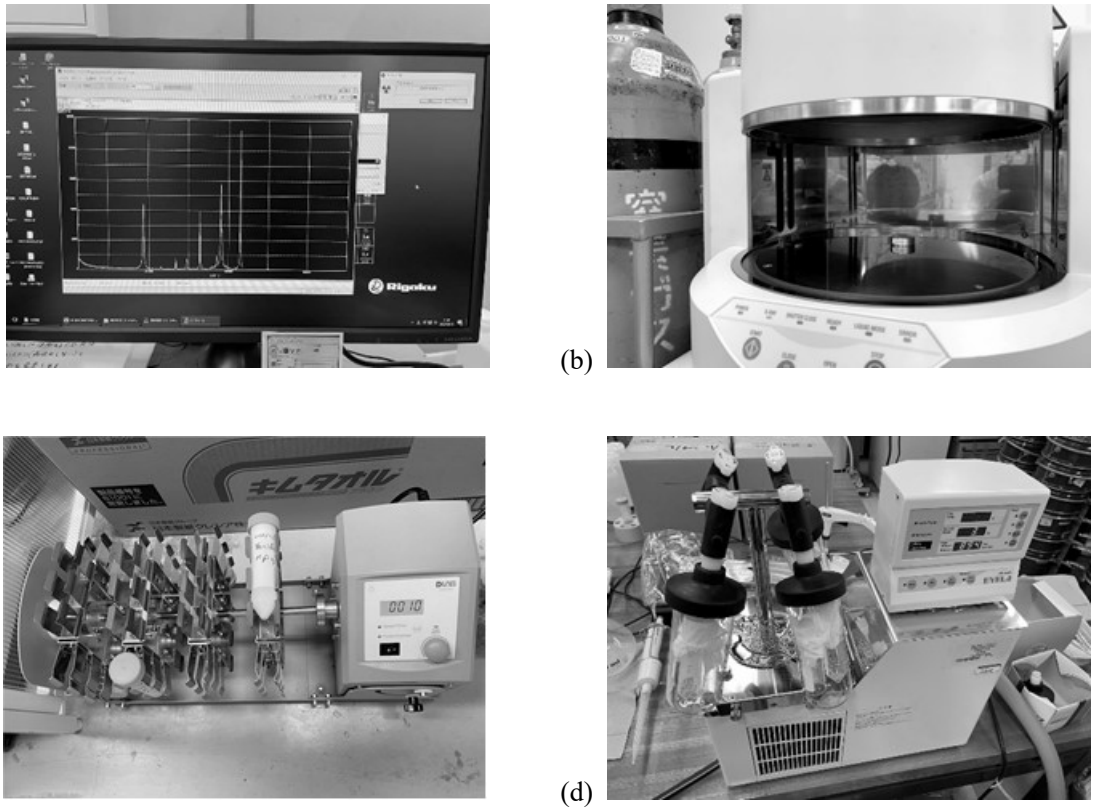

Figure 5.3 Experiments evaluating hydration kinetics: (a) XRD (RINT-2500, Rigaku in GSJ-Lab, AIST), (b) XRF (EDX-720, Shimadzu), (c) Rotator, and (d) Freeze dryer (FDS-1000, EYELA).

5.2.2 X-ray diffraction analysis

5.2.2.1 Hydration tests

Understanding hydration kinetics is important for evaluating the sorption performance of MgO. Here, hydration tests were used to investigate whether hydration was complete within 24 hours. In these tests, 0.6-

g samples of the agent were put in contact with 30 mL of distilled water using plastic tubes, as shown in Fig. 5.3(c). To investigate the kinetics of hydration as fundamental information, the samples were left for a given length of time (1, 4, or 27 days). After the hydration tests, the solid and the liquid were separated using centrifugation. The pH values of the liquid were measured using a pH/EC meter (F-54, Horiba). The XRD profiles with CuKα, 40 kV, 100 mA were measured after 1, 4, and 27 days.

5.2.2.2 XRD pattern for sample after column tests

An XRD analysis was conducted after completing the sorption-desorption column test for a 10% agent content. It took 110 days to complete the column test for a 10% agent content. The agent particles were manually separated from the particles of silica sand after freeze-drying with a freeze dryer (FDS-1000, EYELA), as shown in Fig. 5.3(d). The freeze-dried specimen was sieved by passing it through a 106-μm opening screen. Afterwards, the sieved material was examined by XRD analysis. Only the 10% case was evaluated because it was difficult to distinguish the agent particles from the silica sand. Even at this relatively high agent content, the sieving step could not remove all the quartz particles. However, the passing fraction was mainly considered to show the components of the agent particles after the column test.

5.2.3 Sorption-desorption column tests

Sorption-desorption column tests were used to evaluate the sorption and desorption behaviors of the specimens. Two-stage column tests were conducted using acrylic columns (ϕ 5 cm × h 10 cm) at room temperature (~20ºC), as shown in Fig. 5.4(a). A dried soil-agent mixture was placed in the column, as shown in Fig. 5.4(b). Each specimen was compacted in the acrylic column in five layers of equal heights, as shown in Fig. 5.4(c). During compaction, a 125-g rammer was dropped freely from a height of 20 cm. This method was based on the corresponding ISO 21268-3 (2019). The specimen was placed between filter papers to prevent channel clogging due to the fine soil particles. Then distilled water was percolated in an up-flow direction using a peristaltic pump at a flow rate of approximately 36 mL/h until the specimen reached saturation. Finally, percolation was interrupted for 24 hours to achieve a saturated condition. Table 5.2 summarizes the test conditions. Side wall leakage should not occur in this test considering two aspects. The first aspect is that the hydraulic conductivity of this silica sand is approximately 10-4 m/s ~ 10-5 m/s. The second aspect is that the ratio of the maximum particle size to the column diameter is less than 1/40.

In the first stage (sorption phase), the influent was a fluoride solution prepared using sodium fluoride (NaF) with a concentration of C_0 = 80 mg/L F^-. The solution was continuously percolated in an up-flow direction via a peristaltic pump at 36 mL/h, which is equivalent to a Darcian velocity of 44 cm/d. The first stage was terminated when the concentration in the effluent, C, exceeded 76 mg/L F^-, where C/C_0 = 0.95. In the second stage (desorption phase), distilled water was percolated under the same flow conditions until the concentration in the effluent was less than 4 mg/L F^-, where C/C_0 = 0.05.

Effluents were collected periodically in plastic bottles and filtered using a 0.45-μm membrane filter. The filtrate pH was measured using a pH/EC meter (F-54, Horiba). The fluoride concentration was measured using a fluoride selective electrode (6561S-10C, Horiba).

(a)  (b)  (c) 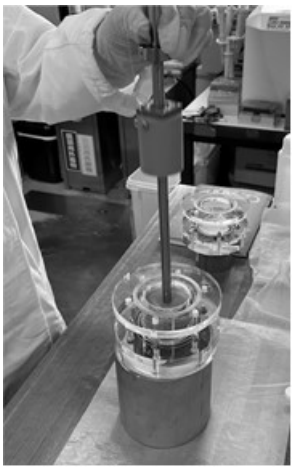

Figure 5.4 Preparation of the specimens for column tests; (a) Assembling the column, (b) Pouring the soil amended with the stabilizing agent, and (c) Compacting the soil.

Table 5.2 Specimen properties used in this study.

Agent content (%)	ρ_d (g/cm^3)	n
1	1.40	0.47
5	1.38	0.48
10	1.43	0.47

5.2.4 Solute transport analysis

5.2.4.1 Theory

Breakthrough curves from the column tests can be modelled using a one-dimensional ADE as

$$R\frac{\partial C}{\partial t} = D\frac{\partial^2 C}{\partial x^2} - v\frac{\partial C}{\partial x} \tag{5.1}$$

Assuming that the initial and "constant-flux" boundary conditions are given as

$$C\big|_{x\geq 0,t=0} = 0, -D\frac{\partial C}{\partial x} + vC\bigg|_{x=0,t\geq 0} = vC_0, \frac{\partial C}{\partial x}\bigg|_{x=\infty,t\geq 0} = 0 \tag{5.2}$$

the solution to Eq. (5.1) for these conditions is given by van Genuchten and Parker (1984) as

$$\frac{C}{C_0}=\frac{1}{2}\operatorname{erfc}\left[\frac{RL-vt}{\left(4RDt\right)^{1/2}}\right]+\left(\frac{v^2t}{\pi RD}\right)^{1/2}\exp\left[-\frac{\left(RL-vt\right)^2}{4RDt}\right]$$
$$-\frac{1}{2}\left(1+\frac{vL}{D}+\frac{v^2t}{RD}\right)\exp\left(\frac{vL}{D}\right)\operatorname{erfc}\left[\frac{RL+vt}{\left(4RDt\right)^{1/2}}\right] \tag{5.3}$$

where R (= 1 + $\rho_d K_d/n$, in which ρ_d (g/cm^3) and n are the dry density and porosity of the specimen, respectively) is the retardation factor, D (cm^2/s) is the longitudinal dispersion coefficient, v (cm/s) is the average pore water velocity, C (mg/L) is the solute concentration at distance x from the source at time t, C_0 (mg/L) is the initial solute concentration, and L (cm) is the column length.

To model the breakthrough curves from the tests, it is assumed that the solute transport parameters, R, D, v, and C_0, are constant. For the sorption phase, the experimental data were directly fitted using Eq. (5.3). For the desorption phase, the experimental data were fitted using Eq. (5.3), but C/C_0 was subtracted from 1 [i.e. (1 - C/C_0)], as recommended by Grathwohl and Susset (2009). This is because the initial and boundary conditions for the desorption phase differ from those of the sorption phase, as shown in Fig. 5.5.

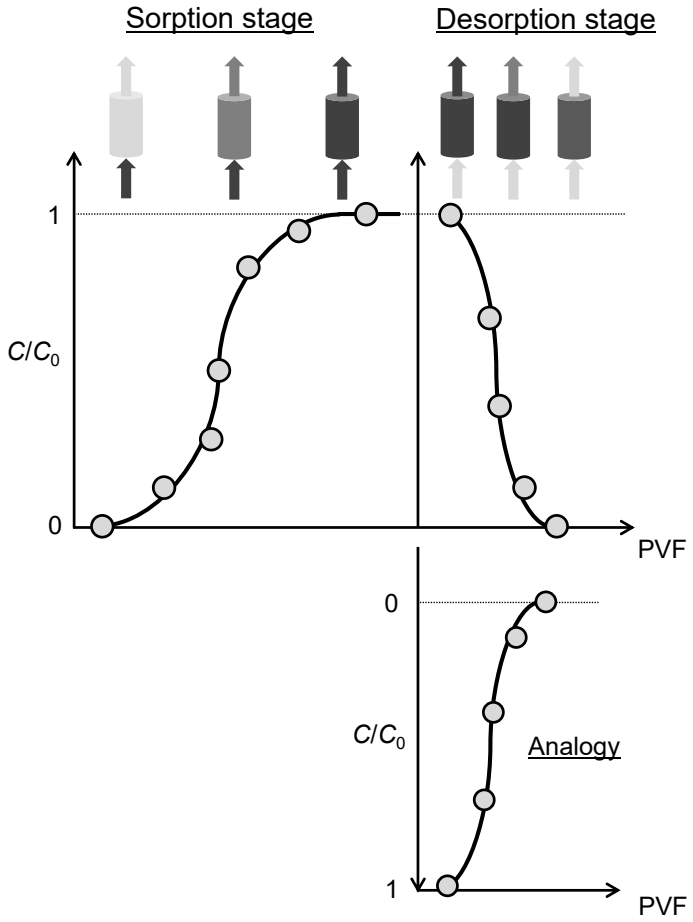

Figure 5.5 Parameter determination in an analytical solution, where the sorption and desorption phases are determined using the results of the column test and analogical concept, respectively.

5.2.4.2 Estimation of dispersion coefficients using chloride tracer tests

Tracer tests were conducted to determine the values for D during the sorption and desorption phases after the sorption-desorption column tests. This test followed the two-stage column test using the same specimen (Table 5.2). Chloride (Cl^-) was used as the non-sorbed chemical. A chloride solution with a concentration of 1000 mg/L Cl^- was prepared using sodium chloride (NaCl). The specimens were percolated using the Cl^- solution until the concentrations in the effluents were 1000 mg/L Cl^-, where $C/C_0 = 1.0$. After that, percolation was continued using distilled water until the concentrations in the effluents were 50 mg/L Cl^-, where $C/C_0 = 0.05$. The flow rate was similar to that in the two-stage column tests (refer to Section 5.2.3). The chloride concentration was measured using a chloride selective electrode (6560S-10C, Horiba).

To estimate the values for D, the breakthrough curves were modelled from the tracer test using Eq. (5.3). As Cl^- is a non-sorbed chemical, it was assumed that $R = 1$. The values for D were obtained by minimizing the residual sum of the squares (SSE) between the predicted data and the experimental data as

$$\mathrm{SSE} = \sum_{i=1}^{n} (C_i - C_i')^2 \tag{5.4}$$

where $(C/C_0)_i$ is the experiment data series and $(C/C_0)_i$' is the predicted data series. When the experimental value and the analytical solution at $C/C_0 = 0.5$ disagreed, the v value in the analytical solution was manually adjusted. This calculation was conducted using the following data sheet, as show in Fig. 5.6.

Figure 5.7 and Table 5.3 summarize the results of the tracer tests. The obtained prediction curves are analogous to the experimental data.

解析パラメータ							解析値の計算					
名称	値	単位					実験値 C/Co	t(h)	解析値 C/Co	r2	error	RMSE
	R	-	79.23539				0	0	0	0.89922		
	z	cm	10				0.0030875	11.44007	2.27E-65		-3.09E-03	0.162299
	v	cm/h	3.10E+00				0.02575	34.8801	3.93E-19		-2.58E-02	
	Kd	L/kg	27.07327				0.068125	59.42999	7.25E-10		-6.81E-02	
	D	cm^2/h	1.10E+00	3.06E-04			0.1375	82.47987	2.82E-06		-1.37E-01	
	θ	-	0.479112				0.20875	105.0798	2.32E-04		-2.09E-01	
	ρd	g/cm^3	1.384521				0.2675	130.1797	4.36E-03		-2.63E-01	
							0.34125	165.1796	4.64E-02		-2.95E-01	
解析結果				実験結果			0.4125	199.6794	1.72E-01		-2.41E-01	
PVF	t	C/Co	t	C/Co	PVF	0.380484	0.47625	224.8793	3.11E-01		-1.65E-01	
vl/Vv	(h)		(h)		vl/Vv		0.50875	250.3293	4.67E-01		-4.21E-02	
0	0	0	0	0	0		0.5525	287.0793	6.70E-01		1.17E-01	
3.804839	10	2.94E-75	11.44007	0.003088	4.35276		0.6	335.5791	8.50E-01		2.50E-01	
7.609677	20	6.18E-36	34.8801	0.02575	13.2713		0.63375	383.4206	9.40E-01		3.06E-01	
11.41452	30	8.37E-23	59.42999	0.068125	22.6122		0.66	430.7621	9.78E-01		3.18E-01	
15.21935	40	3.01E-16	82.47987	0.1375	31.3823		0.68875	467.5122	9.90E-01		3.01E-01	SSE 1.161518
19.02419	50	2.48E-12	105.0798	0.20875	39.9812		0.72	503.7623	9.96E-01		2.76E-01	
22.82903	60	9.64E-10	130.1797	0.2675	49.5313		0.74	551.5124	9.99E-01		2.59E-01	
26.63387	70	6.52E-08	165.1796	0.34125	62.8482		0.7725	588.0141	9.99E-01		2.27E-01	
30.43871	80	1.48E-06	199.6794	0.4125	75.9748		0.7975	623.7647	1.00E+00		2.02E-01	
34.24355	90	1.60E-05	224.8793	0.47625	85.563		0.81125	671.7637	1.00E+00		1.89E-01	
38.04839	100	1.04E-04	250.3293	0.50875	95.2463		0.82	719.9637	1.00E+00		1.80E-01	
41.85323	110	4.66E-04	287.0793	0.5525	109.229		0.835	767.9137	1.00E+00		1.65E-01	
45.65806	120	1.57E-03	335.5791	0.6	127.682		0.85125	815.4137	1.00E+00		1.49E-01	
49.4629	130	4.28E-03	383.4206	0.63375	145.885		0.86625	863.1636	1.00E+00		1.34E-01	
53.26774	140	9.84E-03	430.7621	0.66	163.898		0.8775	911.6136	1.00E+00		1.22E-01	
57.07258	150	1.97E-02	467.5122	0.68875	177.881		0.8925	958.8136	1.00E+00		1.07E-01	
60.87742	160	3.55E-02	503.7623	0.72	191.673		0.9025	1006.964	1.00E+00		9.75E-02	
64.68226	170	5.83E-02	551.5124	0.74	209.842		0.91375	1055.963	1.00E+00		8.62E-02	
68.4871	180	8.89E-02	588.0141	0.7725	223.73		0.925	1102.813	1.00E+00		7.50E-02	

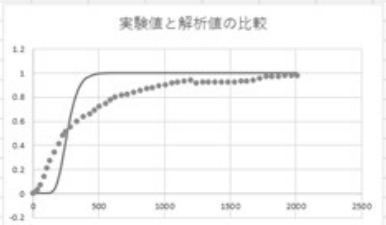

Figure 5.6 Data sheet minimizing the residual sum of the squares (SSE) between the predicted data and the experimental data.

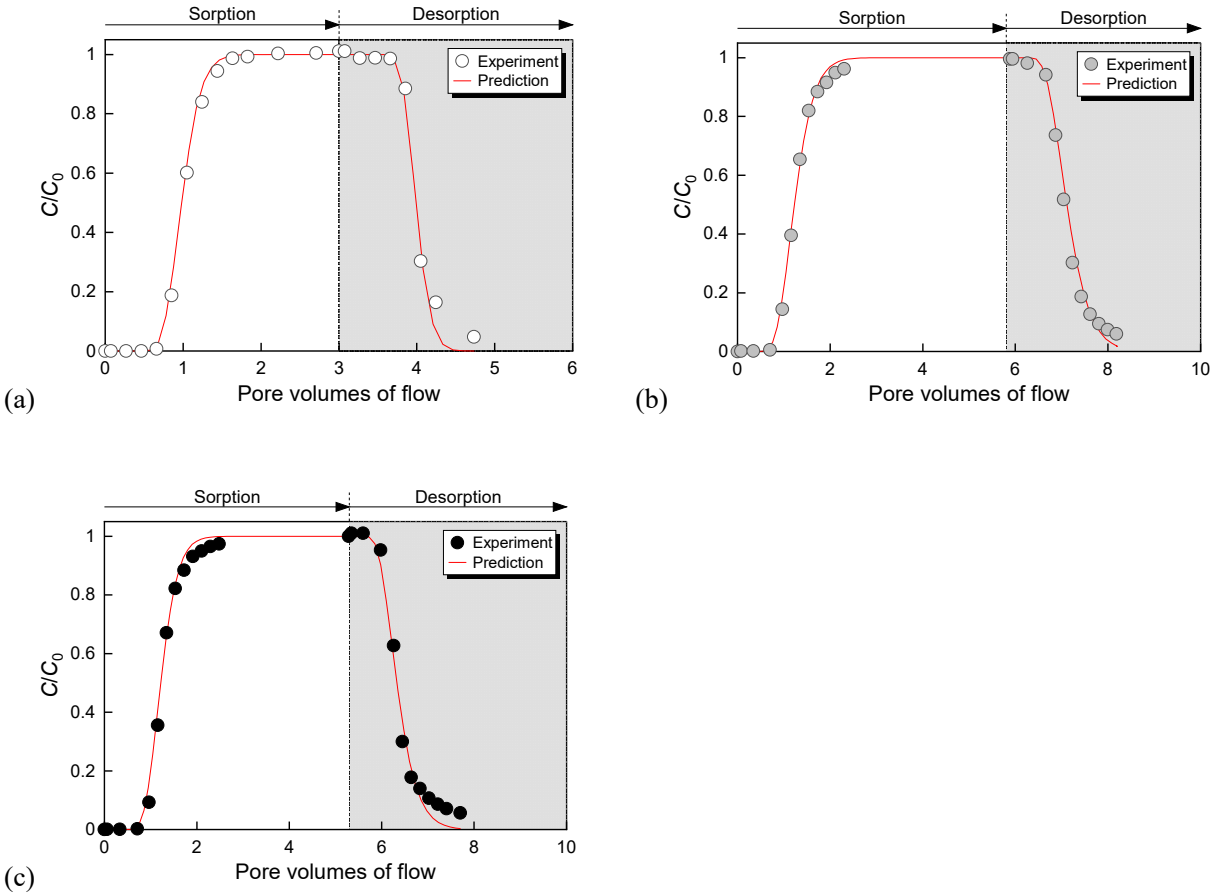

Figure 5.7 Results of the chloride tracer tests for agent contents of (a) 1%, (b) 5%, and (c) 10%.

Table 5.3 Estimated solute transport parameters.

Agent content	Sorption		Desorption	
(%)	K_d (cm^3/g)	D (cm^2/s)	K_d (cm^3/g)	D (cm^2/s)
1	0.54	2.3×10^{-4}	0.081	1.3×10^{-4}
5	27	3.1×10^{-4}	0.13	4.3×10^{-4}
10	50	2.5×10^{-4}	0.11	5.4×10^{-4}

5.3 Results

5.3.1 Hydration kinetics

The hydration kinetics of the stabilizing agent was investigated based on Section 5.2.2. Figure 5.8(a) shows the XRD patterns. Prior to hydration, the MgO peaks were significant, but during hydration, the magnesium hydroxide [$Mg(OH)_2$] peaks were predominant. However, the MgO peak was clearly observed after 27 days. These results show that the hydration kinetics of this agent is relatively slow, and that not all of the MgO was immediately hydrated after the 24-hour saturation step. Although this test did not consider or clarify the individual chemical reactions occurring in the column test, it did reveal the general trend of hydration kinetics. The pH values after 1, 4, and 27 days were 11.1, 11.7, and 9.89, respectively.

Figure 5.8(b) shows the XRD pattern of the stabilizing agent after the sorption-desorption column test. This XRD pattern was investigated based on the method described in Section 5.2.2. Peaks for both $Mg(OH)_2$ and MgO were detected. These results imply that the MgO contained in this agent is not consumed immediately. Quartz, kaolin, and feldspar peaks, derived from the silica sand component (refer to Fig. 5.2), were observed.

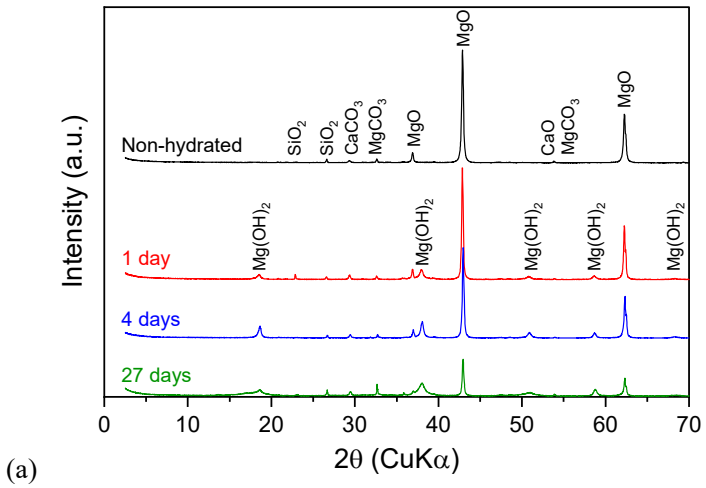

(a)

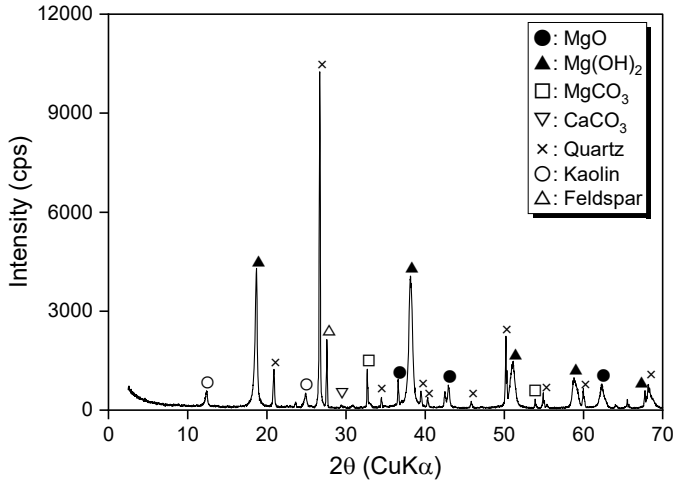

(b)

Figure 5.8 XRD patterns of the stabilizing agent after (a) hydration tests, and (b) the column test.

5.3.2 Sorption-desorption column tests

5.3.2.1 Transport parameters

Figure 5.9 shows breakthrough curves obtained from the column tests. The changes in C/C_0 were evaluated with respect to the pore volumes of flow (PVF) during the sorption and desorption phases. The PVF was calculated by dividing the cumulative volume of the effluent collected during the test by the volume of the voids in the specimen. Previous research defined the breakthrough point as the concentration in the effluents where C exceeds 5% of C0. That is, $C/C_0 = 0.05$ (Chen et al., 2011; Tor et al., 2009). Breakthroughs occurred after approximately 1, 20, and 50 PVF when using agent contents of 1, 5, and 10%, respectively. These results suggest that increasing the agent content can delay the breakthrough.

Table 5.3 summarizes the values for K_d and D obtained during the sorption and desorption phases using the method described in Section 5.2.4. For the sorption phase, the prediction curve and the experimental data agreed relatively well, as shown in Fig. 5.9. However, the predictions gave different estimates for the breakthrough point ($C/C_0 = 0.05$). The predictions indicated that the breakthroughs occurred much later, namely, after approximately 2, 70, and 130 PVF for agent contents of 1, 5, and 10%, respectively. This means that the predicted retardation was not observed experimentally. Thus, the obtained K_d may not be a suitable index for evaluating the sorption performance. For the desorption phase, the predictions and the experimental data for $1 > C/C_0 > 0.4$ agreed well, but further modifications will be necessary to improve the agreement.

In terms of pH, all effluents were alkaline, as shown in Fig. 5.10. For an agent content of 1, 5, or 10%, the initial effluents had pH ~11.5. In all cases, the effluent pH decreased as the number of PVFs increased. The pH > 11 values were higher than the expected values when $Mg(OH)_2$ was equilibrated with water. Although the reason is not completely clear, it is possible that this is because of the calcium. Figure 5.8(a) shows that this stabilizing agent contained some calcium oxide (CaO) and calcium carbonate ($CaCO_3$). Hence, it is possible that the Ca dissolved first, initially increasing the pH value to one higher than the Mg, and then the Mg dissolved slowly. In addition, the pH values during the hydration tests decreased after 27 days (refer to Section 5.3.1). The higher pH values might be attributed to the calcium contained in the stabilizing agent. However, additional studies will be necessary to validate this assertion. Considering that the effluent pH was less than 12, as shown in Fig. 5.10, which is below the isoelectric points of MgO (= pH 12.4) and $Mg(OH)_2$ (= pH 12) (Parks, 1965), the net potential of the agent's surface should be positive. It is assumed that electrostatic attraction attracts fluoride on the surface.

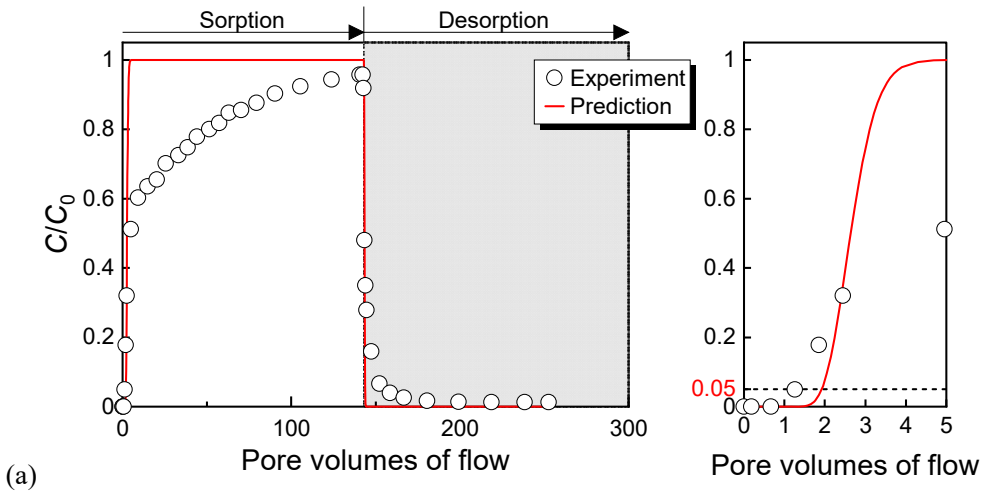

(a)

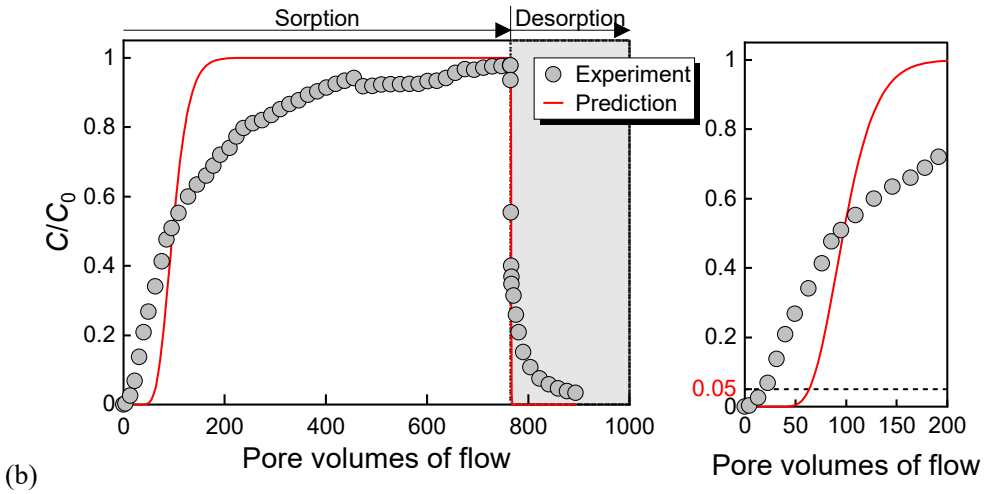

(b)

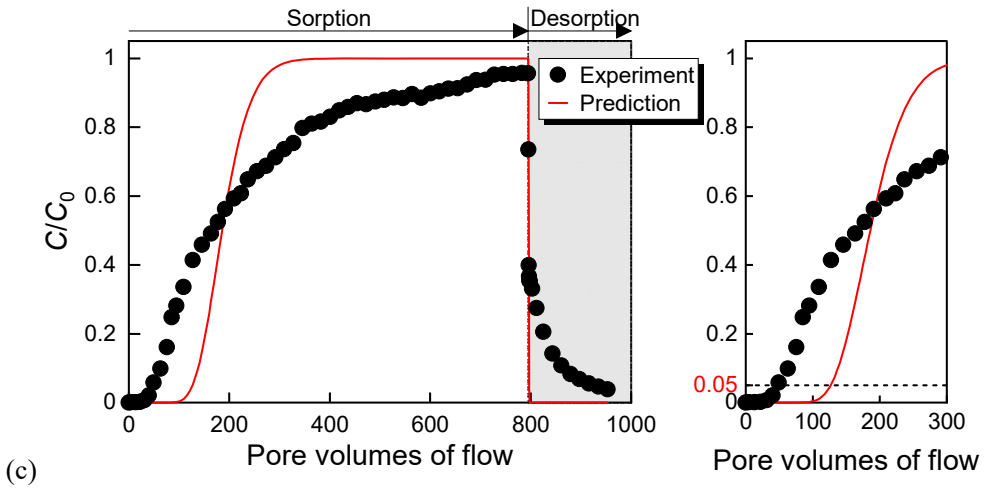

(c)

Figure 5.9 Results of sorption-desorption column tests for agent contents of (a) 1%, (b) 5%, and (c) 10%.

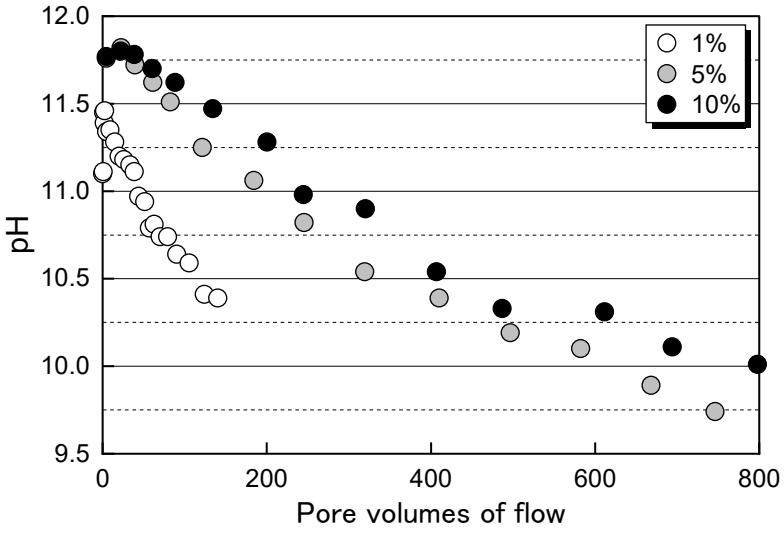

Figure 5.10 Profile of the effluent pH during sorption phase.

5.3.2.2 Immobilized fraction

The immobilized fraction was calculated from the difference in the cumulative sorbed mass, S_s (mg/g), and the desorbed mass, S_d (mg/g) (i.e., S_s - S_d), using the obtained breakthrough curves shown in Fig. 5.11. C/C_0 = 0.95 is considered to be the exhaustion point for sorption; it implies that the sorbed fraction is almost saturated. On the other hand, C/C_0 = 0.05 is considered to be the exhaustion point for desorption; it implies that the desorbed fraction is almost saturated.

The cumulative sorbed mass, S_s was calculated from the data on the sorption phase using Eq. (5.5), while S_d was determined from the data on the desorption phase using Eq. (5.6). For a better understanding and a clearer comparison, Fig. 5.11(b) plots S_s and S_d from 0 PVF. Cumulative fluoride sorbed mass S_s, per unit mass of soil-agent mixture, was calculated as follows:

$$S_s = \sum_{s=1}^{n} \frac{(C_0 - C_s)V_s}{m} \tag{5.5}$$

$$S_d = \sum_{d=1}^{n} \frac{C_d V_d}{m} \tag{5.6}$$

where C_s and C_d (mg/L) are the instantaneous effluent concentrations during the sorption and desorption phases, respectively, V_s and V_d (L) are the instantaneous volumes of the effluent collected during the sorption and desorption phases, respectively, and m (g) is the mass of the soil-agent mixture.

Figure 5.12 shows the profiles of S_s and S_d for agent contents of 1, 5, and 10%. For agent contents of 1, 5 and 10%, $S_s - S_d$ was estimated as 0.5, 4.0, and 6.0 mg/g, respectively. Considering the values for S_s and S_d, the desorbed amount was approximately 20% when using an agent content of 1%. A much smaller percentage of desorbed mass was estimated as the agent content increased.

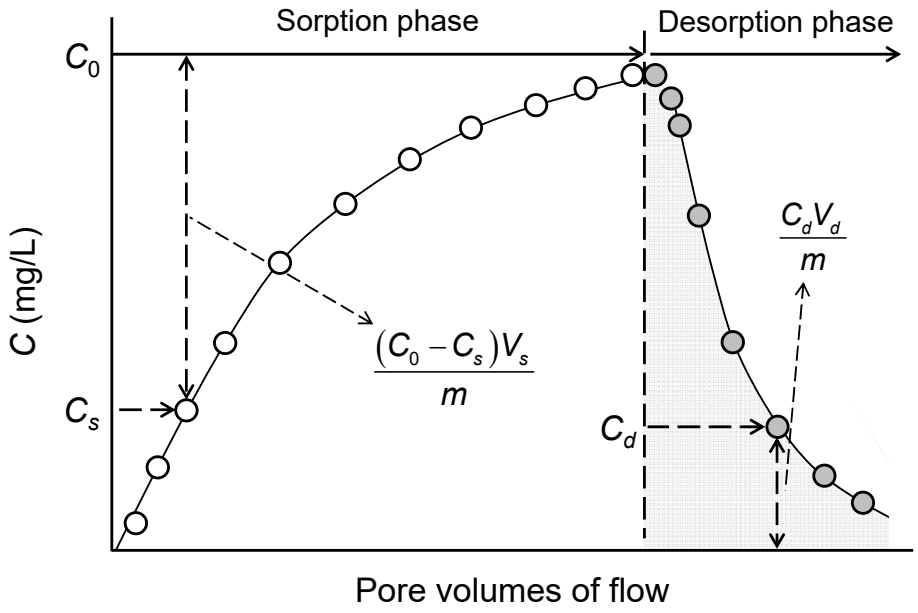

(a)

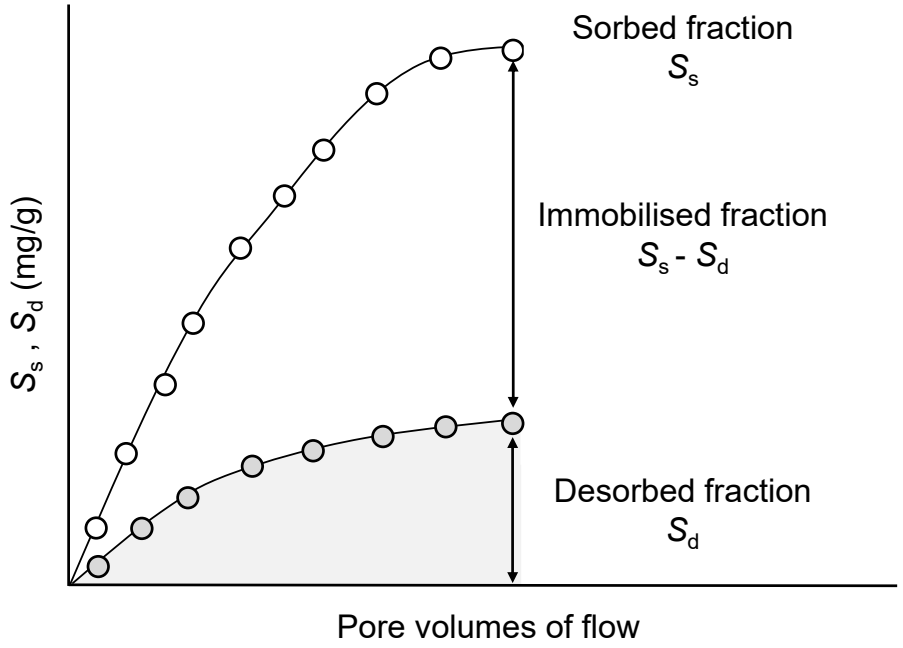

(b)

Figure 5.11 Conceptual method to estimate the immobilized fraction from the sorption-desorption column test: (a) An example of effluent concentrations in the sorption-desorption column test, (b) Concept to obtain immobilized fraction.

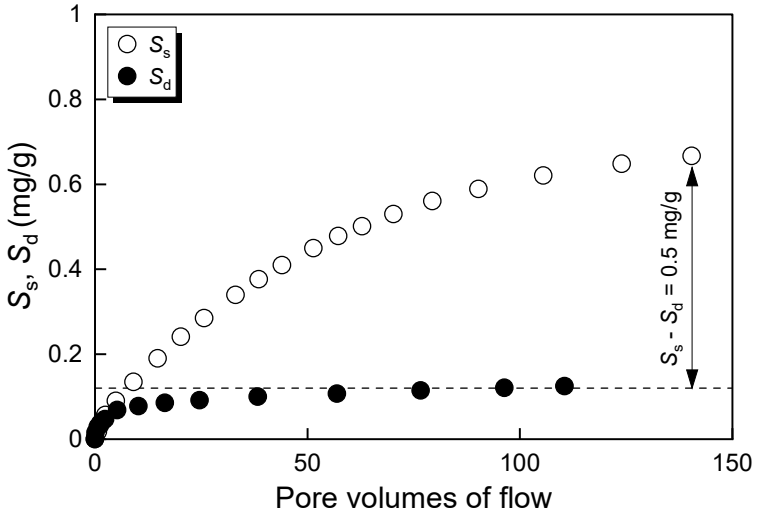

(a)

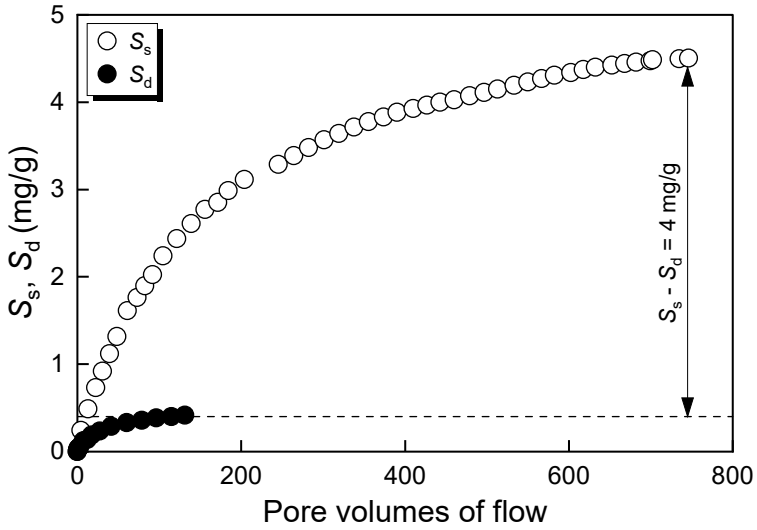

(b)

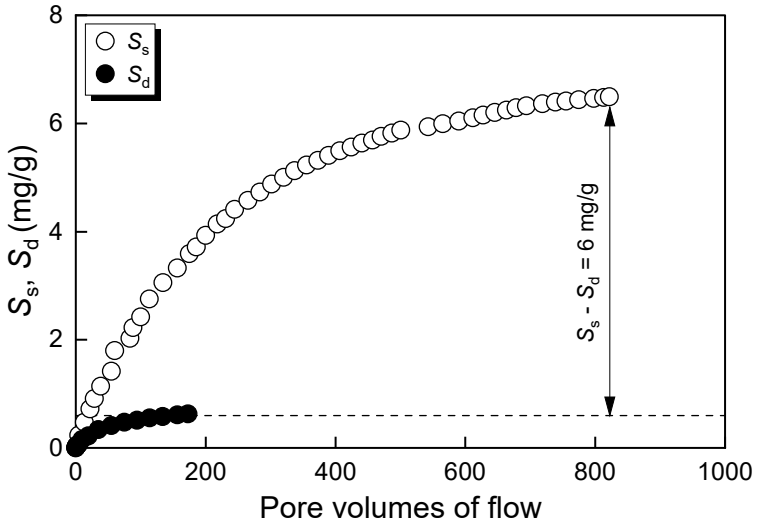

(c)

Figure 5.12 Profiles of S_s and S_d for (a) 1%, (b) 5%, and (c) 10% agent content.

5.4 Discussion

5.4.1 Applicability of one-dimensional advection-dispersion analytical solution

The applicability of a one-dimensional ADE is discussed. For the sorption phase, in terms of the breakthrough point (C/C_0 = 0.05), the predictions show much higher pore volumes than the experiment, as shown in Fig. 5.9. The breakthrough point may be difficult to predict using the one-dimensional ADE when silica sand amended with this MgO agent is used as the attenuation layer material because the relatively slow chemical reaction, namely, the fluoride incorporation into the MgO, is not considered in the ADE. Additionally, the hydration kinetics of this agent is relatively slow, as shown in Fig. 5.8(a). The MgO peaks are still detected after 110 days, as shown in Fig. 5.8(b), and the incorporation occurred throughout the entire column sorption-desorption test. The prediction agrees well with the experimental results (Igarashi and Shimogaki, 1998). The previous study attributed the main reaction mechanism to reactions such as the ion exchange. However, an improved analytical method is required for the solute transport on the MgO agent since limitations exist in the ADE when analyzing the sorption behavior using MgO, particularly in terms of the following two issues. First of all, the transformation of MgO to $Mg(OH)_2$ was not taken into account in the aforementioned analysis. Incorporating the sink-source terms and the time-dependent sorption behavior into the ADE may be considered, such as is shown in the work conducted by Wang and Liu (2005) on the migration of selenium on calcareous soils. Second of all, the pH-dependent behavior of K_d was not taken into account in the analysis presented here. The electrostatic attraction, dependent on the pH and other indices, may be included in the analysis to consider such pH-dependent behavior.

5.4.2 Evaluation of attenuation layer based on sorption-desorption column test

Figure 5.12 shows that the immobilized fraction can be determined using the sorption-desorption column tests. The mechanisms of the ion exchanges by $Mg(OH)_2$ are distinguished between 1) ligand exchange (inner sphere complexes) and 2) electrostatic interaction (outer-sphere complexes) (Morimoto et al., 2009). The chemical interaction of the ligand exchange is stronger than that of the electrostatic interaction. Although these sorption mechanisms are challenging to definitively distinguish, the general trend of the immobilized fraction or the desorbed fraction can be understood through sorption-desorption column tests. When silica sand amended with the stabilizing agent of MgO is applied as the attenuation layer material, the sorption and desorption parameters estimated using the analytical solution of the one-dimensional ADE may provide unrealistic values. In such a case, the concept using the immobilized fraction, S_s - S_d, may be a suitable index for evaluating the attenuation layer instead of a solute transport analysis.

A simple evaluation using S_s - S_d under the assumed conditions is discussed. Whether an agent content of 5% is sufficient for use as an attenuation layer material is considered. For an agent content of 5%, S_s - S_d = 4.0 mg/g should be observed in this sorption-desorption column test. If the attenuation layer has a thickness of 50 and is compacted to achieve ρ_d = 1.4 g/cm^3, and if the leachate concentration, C_0 = 8 mg/L F^-, enters the attenuation layer, the required sorbed mass, S (mg/g), for 100 years can be calculated as:

$$S = \frac{C_0 V_i}{m} \tag{5.7}$$

where V_i [= $A \cdot I \cdot t$, in which A = 1 cm^2 is a unit area of the attenuation layer, I = 500 mm/yr is the constant infiltration, and t = 100 years] is the volume of the leachate entering the attenuation layer per unit area, and m (= $\rho_d \cdot A \cdot h$, where h = 50 cm is the thickness of the attenuation layer) is the mass of the attenuation layer material.

The required S is assumed to be 0.57 mg/g. This is lower than the immobilized fraction S_s - S_d = 4.0 mg/g. The constant concentration of 8 mg/L F^- is applied in this calculation, but the concentration is 10 times higher than the commonly reported leached value, which is below the limit in Japan regulated under the SCCL of 0.8 mg/L F^-. Ito and Katsumi (2020) reported that the concentration of F^- from excavated materials in Japan rarely exceeds 2–3 mg/L. Judging from this simple assumption, silica sand amended with this stabilizing agent may be an effective attenuation layer material against fluoride, even if the smaller agent content of 5% is used.

However, this evaluation has a problem. The MgO agent can immobilize more than 80% of the fluoride, as shown in Fig. 5.12. However, this value should be examined further. It is well known that fluoride is removed via two molecular mechanisms: (1) the incorporation of fluoride in $Mg(OH)_2$, which grows upon contact with water (Morishita and Wada, 2013; Sasaki et al., 2011), and (2) the ion exchange, which occurs on the external surfaces of formed $Mg(OH)_2$ (Morimoto et al., 2009; Sasaki et al., 2011; Ye et al., 2018; Zhen et al., 2015). In-field, the soil, agent, and water are mixed and the mixture is then spread on the ground to construct the attenuation layer (Mo et al., 2020). Therefore, the attenuation layer materials should remain moist even after construction. This means that the MgO in the attenuation layer materials may be hydrated before it makes contact with the in-field permeated fluoride. In this situation, the sorption performance may be overestimated because the sorption mechanism will not occur by incorporation, but fluoride is considered to be taken up only by the ion exchange at the external surfaces of the agent.

Nishikata et al. (2020) placed this MgO agent in distilled water for a month and conducted batch tests. The sorption performance of this MgO agent was seen to be affected by hydration, while the diminution of the sorbed fluoride mass was suppressed within 40% of that before hydration. In this study, the MgO agent was not immediately hydrated, as seen in Figs. 5.8(a) and (b). The ion exchange as well as the fluoride incorporation are assumed to occur for at least 110 days, but they should be evaluated for longer periods when considering hydration kinetics. Previous research reported that the leaching of some geogenic contaminants from excavated soils was complete within a relatively short period. That is, $L/S < 1$ (Naka et al., 2016). An important function of the attenuation layer is to immobilize the contaminants at an early stage. Considering these issues, this MgO agent holds promise as an attenuation layer material, but further studies will be necessary to confirm it.

The immobilized fraction can be an index for evaluating the sorption performance of the attenuation layer, while the fraction due to incorporation by hydration should be carefully examined. To consider the on-site conditions, future studies should include an investigation of sorption-desorption column

tests cured for several different periods using specimens mixed with soils, agents, and water.

5.5 Summary and Conclusions

This study evaluated the sorption performance of clean sandy soil amended with a stabilizing agent for use as an attenuation layer material by means of sorption-desorption column tests. Fluoride was selected as one of the geogenic toxic chemicals, and MgO was used as the stabilizing agent. The results support the following conclusions:

1. In the column sorption tests, breakthroughs ($C/C_0 > 0.05$) occurred after approximately 1, 20, and 50 PVF when the agent contents were 1, 5, and 10%, respectively. Hence, increasing the agent content was seen to delay the breakthrough.
2. A one-dimensional ADE was employed to model the breakthrough curves from the tests. Using an agent content of 10% produced a partition coefficient, K_d = 50 L/kg, but the predictions produced unrealistic estimates for the breakthrough point ($C/C_0 = 0.05$). Giving consideration to the chemical reaction, which depends on time, should improve the solute transport model.
3. For an agent content of 1% MgO, the percentage of sorbed fluoride mass, S_s, which was desorbed was approximately 20%. The percentage of desorbed mass was much smaller for higher agent contents.
4. Sorption-desorption column tests were used to determine the immobilized fraction, S_s - S_d. When an 80-mg/L fluoride solution was used as the influent in the sorption phase and distilled water was used in the desorption phase, S_s - S_d = 4.0 mg/g with an agent content of 5% MgO.
5. According to the XRD patterns, the hydration kinetics of this stabilizing agent was relatively slow. Peaks of MgO were still observed after 110 days from the start of the column test. These results suggest that both ion exchange and fluoride incorporation, due to the hydration of MgO, occurred during the column experiments. Future work on the attenuation layer should include a sorption performance evaluation, considering the hydration of MgO.

References for Chapter 5

Chen, N., Zhang, Z., C. Feng, M. Li, R. Chen and N. Sugiura, 2011. Investigations on the batch and fixed-bed column performance of fluoride adsorption by Kanuma mud. *Desalination* 268, 76–82. https://doi.org/10.1016/j.desal.2010.09.053.

Grathwohl, P. and Susset, B., 2009. Comparison of percolation to batch and sequential leaching tests: theory and data. *Waste Management* 29, 2681–2688. https://doi.org/10.1016/j.wasman.2009.05.016.

Igarashi, T. and Shimogaki, H., 1998. Migration characteristics of boron by batch and column methods. *Journal of Groundwater Hydrology* 40, 121–132. https://doi.org/10.5917/jagh1987.40.121 (in Japanese).

ISO 21268-3, 2019. Soil Quality—Leaching Procedures for Subsequent Chemical and Ecotoxicological Testing of Soil and Soil Materials—Part 3: Up-Flow Percolation Test. *International Standardization Organization*.

Inui, T., Katayama, M., Katsumi, T., Takai, A. and Kamon, M., 2014. Evaluating the long-term leaching characteristics of heavy metals in excavated rocks. *Journal of the Society of Materials Science, Japan* 63, 73–78. https://doi.org/10.2472/jsms.63.73 (in Japanese).

Ito, H. and Katsumi, T., 2020. Leaching characteristics of naturally derived toxic elements from soils in the western Osaka area: considerations from the analytical results under the Soil Contamination Countermeasures Act. *Japanese Geotechnical Journal* 15(1), 119–130. https://doi.org/10.3208/jgs.15.119 (in Japanese).

JIS A 1204, 2009. Test Method for Particle Size Distribution of Soils. *Japanese Standards Association*.

JIS A 1202, 2009. Test Method for Density of Soil Particles. *Japanese Standards Association*.

JIS R 5201, 2015. Physical Testing Methods for Cement. *Japanese Standards Association*.

Katsumi, T., 2015. Soil excavation and reclamation in civil engineering: environmental aspects. *Soil Science and Plant Nutrition* 61, 22–29. https://doi.org/10.1080/00380768.2015.1020506.

Katsumi, T., Inui, T., Yasutaka, T., and Takai, A., 2019. Towards sustainable soil management—reuse of excavated soils with natural contamination—. In: Zhan, L. et al. (Eds.), *Proceedings of the 8th International Congress on Environmental Geotechnics*, Hangzhou, China, Vol. 1. Springer, 99–118. https://doi.org/10.1007/978-981-13-2221-1_5.

Magnusson, S., Johansson, M., Frosth, S., and Lundberg, K., 2019. Coordinating soil and rock material in urban construction—scenario analysis of material flows and greenhouse gas emissions. *Journal of Cleaner Production* 241, 118236. https://doi.org/10.1016/j.jclepro.2019.118236.

Martínez-Lladó, X., Valderrama, C. M. Rovira, Martí, V., Giménez, J., and De Pablo, J., 2011. Sorption and mobility of Sb(V) in calcareous soils of Catalonia (NE Spain): batch and column experiments. *Geoderma* 160, 468–476. https://doi.org/10.1016/j.geoderma.2010.10.017.

Ministry of Land, Infrastructure, and Transport, Japan, 2010. Technical Manual on the Countermeasure Against Soils and Rocks Containing Naturally Occurring Heavy Metals in Construction Works (Draft). http://www.mlit.go.jp/sogoseisaku/region/recycle/recyclehou/manual/index.htm (accessed 1 June 2020) (in Japanese).

Mo, J., Flores, G., Inui, T., and Katsumi, T., 2020. Hydraulic and sorption performances of soil amended with calcium-magnesium composite powder against natural contamination of arsenic. *Soils and Foundations* 60(5), 1084–1096. https://doi.org/10.1016/j.sandf.2020.05.007.

Morimoto, K., Sato, T. and Yoneda, T., 2009. Complexation reactions of oxyanions on brucite surfaces. *Journal of the Clay Science Society of Japan* 48, 9–17 (in Japanese). https://doi.org/10.11362/jcssjnendokagaku.48.1_9.

Morishita, T. and Wada, S., 2013. Hydration reaction of magnesium oxide in soil. In: *Proceedings of the 48th Symposium on Japanese Geotechnical Society*, Kyoto, Japan (in Japanese).

Naka, A., Yasutaka, T., Sakanakura, H., Kalbe, U., Watanabe, Y., Inoba, S., Takeo, M., Inui, T., Katsumi, T., Fujikawa, T., Sato, K., Higashino, K., and Someya, M., 2016. Column percolation test for contaminated soils: key factors for standardization. *Journal of Hazardous Materials* 320, 326–340. https://doi.org/10.1016/j.jhazmat.2016.08.046.

Nishikata, M., Yasutaka, T., Morimoto, K., Imoto, Y. and Tsukimura, K., 2020. Evaluation of the effect of contact with water on the adsorption characteristics of adsorption materials for an adsorption layer method of construction. In: *Proceedings of the 55th Symposium on Japanese Geotechnical Society*, Kyoto, Japan (in Japanese).

Nozaki, F., Shimizu, Y., and Ito, K., 2013a. Discussion on construction method of heavy metals adsorption layer. In: *Proceedings of the 19th Symposium on Groundwater and Soil Contamination and Countermeasures*, Kyoto, Japan (in Japanese).

Nozaki, T., Matsuyama, Y., Sugiyama, A., Moriya, M., Komukai, Y., and Nagase, T., 2013b. Fundamental study of soil materials for absorbent construction method using MgO material. In: *Proceedings of the 19th Symposium on Groundwater and Soil Contamination and Countermeasures*, Kyoto, Japan. (in Japanese).

Parks, G.A., 1965. The Isoelectric points of solid oxides, solid hydroxides, and aqueous hydroxo complex systems. *Chemical Reviews* 65, 177–198. https://doi.org/10.1021/cr60234a002.

Plassard. F., Winiarski. T., and Petit-Ramel. M., 2000. Retention and distribution of three heavy metals in a carbonated soil: comparison between batch and unsaturated column studies. *Journal of Hazardous Contaminant Hydrology* 42, 99–111. https://doi.org/10.1016/S0169-7722(99)00101-1.

Sasaki, K., Fukumoto, N., Moriyama, S., and Hirajima, T., 2011. Sorption characteristics of fluoride on to magnesium oxide-rich phases calcined at different temperatures. *Journal of Hazardous Materials* 191, 240–248. https://doi.org/10.1016/j.jhazmat.2011.04.071.

Tabelin, C.B., Igarashi, T., Villacorte-Tabelin, M., Park, I., Opiso, E.M., Ito, M., and Hiroyoshi, N., 2018. Arsenic, selenium, boron, lead, cadmium, copper, and zinc in naturally contaminated rocks: a review of their sources, modes of enrichment, mechanisms of release, and mitigation strategies. *Science of the Total Environment* 645, 1522–1553. https://doi.org/10.1016/j.scitotenv.2018.07.103.

Tabelin, C.B., Igarashi, T., Yoneda, T., and Tamamura, S., 2013. Utilization of natural and artificial adsorbents in the mitigation of arsenic leached from hydrothermally altered rock. *Engineering Geology* 156, 58–67. https://doi.org/10.1016/j.enggeo.2013.02.001.

Tamoto, S., Tabelin, C.B., Igarashi, T., Ito, M., and Hiroyoshi, N., 2015. Short and long term release

mechanisms of arsenic, selenium and boron from a tunnel-excavated sedimentary rock under in situ conditions. *Journal of Contaminant Hydrology* 175–176, 60-71. https://doi.org/10.1016/j.jconhyd.2015.01.003.

Tatsuhara, T., Arima, T., Igarashi, T., and Tabelin, C.B., 2012. Combined neutralization–adsorption system for the disposal of hydrothermally altered excavated rock producing acidic leachate with hazardous elements. *Engineering Geology* 139, 76–84. https://doi.org/10.1016/j.enggeo.2012.04.006.

Tatsuhara, T., Jikihara, S., Tatsumi, T., and Igarashi, T., 2015. Effects of the layout of adsorption layer on immobilizing arsenic leached from excavated rocks. *Japanese Geotechnical Journal* 10(4), 635–640. https://doi.org/10.3208/jgs.10.635 (in Japanese).

Tor, A., Danaoglua, N., Arslan, G. and Cengeloglu, Y., 2009. Removal of fluoride from water by using granular red mud: Batch and column studies. *Journal of Hazardous Materials* 164, 271–278. https://doi.org/10.1016/j.jhazmat.2008.08.011.

van Genuchten, M. Th. and Parker, J.C., 1984. Boundary conditions for displacement experiments through short laboratory columns. *Soil Science Society of America Journal* 48, 703–708. https://doi.org/10.2136/sssaj1984.03615995004800040002x.

Wang, X. and Liu, X., 2005. Sorption and desorption of radioselenium on calcareous soil and its solid components studied by batch and column experiments. *Applied Radiation and Isotopes* 62, 1–9. https://doi.org/10.1016/j.apradiso.2004.05.081.

Wada, S., and Morishita, T., 2013. Stabilization of heavy metals contaminated soils by magnesium oxide and related chemical and mineralogical reactions. *Journal of the Clay Science Society of Japan* 51, 107–117 (in Japanese). https://doi.org/10.11362/jcssjnendokagaku.48.1_9.

Ye, Y., Yang, J., Jiang, W., Kang, J., Hu, Y., Ngo, H.H., Guo, W. and Liu, Y., 2018. Fluoride removal from water using a magnesia-pullulan composite in a continuous fixed-bed column. J*ournal of Environmental Management* 206, 929–937. https://doi.org/10.1016/j.jenvman.2017.11.081.

Zhen, J., Jia, Y., Luo, T., Kong, L.T., Sun, B., Shen, W., M, F.L. and Liu, J.H., 2015. Efficient removal of fluoride by hierarchical MgO microspheres: Performance and mechanism study. *Applied Surface Science* 357, 1080–1088. https://doi.org/10.1016/j.apsusc.2015.09.127.

Chapter 6

Evaluating the Performance of Attenuation Layer Using the Partition Coefficients Determined from Column Sorption Test

6.1 General remarks

A large amount of excavated soil is generated due to construction work. Excavated soil often contains geogenic contaminants such as arsenic (As), fluorine(F), and lead (Pb) in a specific concentration exceeding the environmental standards specified by the Soil Contamination Countermeasures Law (Ministry of Environment, Japan, 1995; from now on, referred to as SCCL). When the surplus soils are utilized as a geomaterial for embankment, if a leaching concentration of geogenic contaminant does not meet the environmental standards, proper measures must be taken to prevent harmful impacts on the surrounding environment (e.g., Gathuka et al., 2022; Ministry of Land, Infrastructure, and Transport, Japan, 2023). Since many construction works are ongoing and a large amount of excavated soil is generated, landfill space is challenging to keep. Further, although the leaching concentration does not meet the environmental standard, the exceeding is at most several times higher than the SCCL environmental standards (Ito and Katsumi, 2020). Excavated soils and rocks with geogenic contamination should be considered geomaterials with caring risks according to the concentration level of geogenic contaminants (Katsumi, 2017).

The attenuation layer method is discussed as one of the countermeasures for excavated soil containing geogenic toxic chemicals (e.g., Arima et al., 2011; Tatsuhara et al., 2015). In the attenuation layer method, leachate from surplus soil containing geogenic contaminants permeates through an attenuation layer that can immobilize contaminants, reducing the environmental impact and draining the pore water with acceptable levels into groundwater (e.g., Mo et al., 2020; Gathuka et al., 2021). Stabilizing agents, such as magnesium oxide (MgO), iron oxide (Fe_2O_3), or layered double hydroxides (LDH), are often mixed with clean host soil as the attenuation layer. The attenuation layer method is expected to have an advantage in terms of excellent workability and economics because only the bottom of the embankment needs to be treated. In addition, a robust earthen structure can be achieved through compaction (Katsumi, 2017).

When designing the attenuation layer, the sorption performance of soil amended with the stabilizing agent against toxic chemicals that might flow into the layer should be evaluated. In order to quantitatively evaluate the sorption performance, the partition coefficient K_d (L/kg) is often obtained through a batch sorption test (e.g., Wang and Liu, 2005; Martínez-Lladó et al., 2011). Not only the stabilizing agent but also when evaluating the sorption performance of natural ground, K_d has been obtained, and advection-dispersion analysis has been performed to conduct risk assessments to discuss the arrival of contaminants to

drinking wells. When designing embankment structures, the guidelines for the Soil Countermeasures Act, revised in March 2019, clearly state that a method for evaluating the fate and transport of contaminants by conducting advection-dispersion analysis using K_d obtained from batch sorption tests. (Katsumi et al, 2019).

In practice and previous research, when determining K_d, batch sorption tests are mainly conducted from the viewpoint of simple test protocol and speed (e.g., Nishikata et al., 2022; Itaya and Kuninishi, 2022). However, the batch sorption test has the following issues. i) Tests are conducted at a liquid-solid ratio (L/S = five to several thousand) that is higher than the liquid-solid ratio (usually one or less) in the practical condition of the attenuation layer. ii) It is not possible to simulate the situation in which pore water permeates into the ground (e.g., Plassard et al., 2000). iii) Dynamic concentration changes of chemicals (concentration profile) cannot be observed.

A column sorption test is conducted to overcome these challenges, allowing for more realistic performance evaluations. In the column sorption test, an inlet is continuously permeated through the soil specimen. Then, the sorption performance of the material is evaluated based on the concentration profiles of the toxic chemicals.

Various methods have been proposed to obtain K_d from the breakthrough curve obtained in the column sorption test. However, there needs to be a clear conclusion or regulation regarding the determining method. The influence of different calculation methods on the determined K_d value has been evaluated by column sorption tests using natural soils (Nkedi-Kizza et al., 1987; Igarashi and Shimogaki, 1998). It has been reported that when the shape of the breakthrough curve was symmetrical, there was no difference in the determined K_d value, while when it was asymmetrical, there was a difference in the determined K_d value (Bouchard et al., 1988).

Column sorption tests often obtain asymmetric breakthrough curves. For asymmetric breakthrough curves, many cases have been reported in which models that fit the numerical solution of the Freundlich-type advection-dispersion equation were obtained (Nkedi-Kizza et al., 1987; Bouchard et al., 1988; Maraqa et al., 1998). However, previous studies have only examined specific breakthrough curves obtained through experiments, and there are only a limited number of cases in which various breakthrough curve shapes have been comprehensively examined. Also, there are no examples of parametric comparisons of differences in K_d values determined from breakthrough curves. The determined value of K_d is expected to vary depending on the degree of asymmetry of the breakthrough curve. Since, in column experiments, the number of tests that can be investigated and the range of tests are limited, by using numerical experiments to create parametric asymmetric breakthrough curves and examining the relationship of the obtained K_d values for each K_d determination method, the characteristics and applicability of each method can be clarified.

As mentioned before, considering that risk assessment using advection-dispersion analysis has been introduced in the SCCL guidelines and manuals to utilize the excavated soils and rocks with geogenic contamination, determining the partition coefficient of natural ground or attenuation layer has been substantial. In particular, the importance of column sorption tests, which enable a more realistic evaluation of sorption performance, is expected to increase. In the advection-dispersion analysis noted by SCCL, a simplified Henry model using K_d is used instead of the Freundlich model because the Freundlich model is complicated. Therefore, it is essential to standardize the method for determining K_d from the breakthrough

curve obtained from column tests. Furthermore, since K_d can be determined using various methods, it is imperative to understand the characteristics of each determination method (the magnitude of the obtained K_d) to ensure the safety of risk assessment and predict the fate and transport of contaminants.

This study obtained asymmetrical breakthrough curves, especially Freundlich-type ones, from the simulating column sorption tests. Specifically, numerical simulation parametrically created breakthrough curves, and the partition coefficients were determined. After that, the effects of different K_d-determining methods on the sorption performance evaluation were investigated. Finally, advection-dispersion analysis was performed to evaluate the influence of the determined difference in K_d on predicting fate and transporting contaminants that permeate the attenuation layer.

6.2 Review of previous studies evaluating sorption parameters

6.2.1 Methods obtaining partition coefficients from breakthrough curves

Several methods have been applied for calculating the partition coefficient K_d using breakthrough curves obtained from column sorption tests. The first method is to fit the analytical or numerical solution of the advection-dispersion equation to the breakthrough curve (e.g., Igarashi and Shimogaki, 1998; Wang and Liu, 2005; Martínez-Lladó et al., 2011). The second is the area method, which integrates the area of the breakthrough curve (e.g., Bouchard et al., 1988; Maraqa et al., 1998, 2001; Chotpantarat et al., 2011). Calculate the amount of sorption and divide by the equilibrium concentration to find K_d. The third method is to calculate K_d by making the horizontal axis of the breakthrough curve dimensionless with pore volumes of flow (PVF) and the vertical axis with relative concentration, C/C_0 and calculating the retardation factor, R from the point of $C/C_0 = 0.5$ has also been proposed (Nkedi-Kizza et al., 1987; Bouchard et al., 1988; Maraqa et al., 1998). The third method is simple compared to the first and second methods.

6.2.2 Henry and Freundlich-type sorption models

Herein, Figure 6.1 presents the two different sorption isotherms. The sorption model includes the Henry type, which assumes linear sorption, as shown in equation (6.1). A Freundlich-type nonlinear adsorption model is also shown in equation (6.2). The Henry model has been used to express boron adsorption and desorption in sandy and loamy soils (Igarashi and Shimogaki, 1998) and has been applied to express boron adsorption and desorption in low concentration ranges (Gathuka et al. et al., 2021). On the other hand, the Freundlich model expresses the adsorption and desorption of lead, cadmium, and fluorine in black soil and clayey soil (Nakamura et al., 2017) and the adsorption and desorption of phthalate in loamy soil (Maraqa et al., 2001). The different concentration ranges of the contaminants determine the applicability of the model. At higher concentrations, the Freundlich model tends to be well-fitted. Moreover, it has been shown that the Freundlich model fits well when the surface of soil particles is heterogeneous (Nkedi-Kizza et al., 1987).

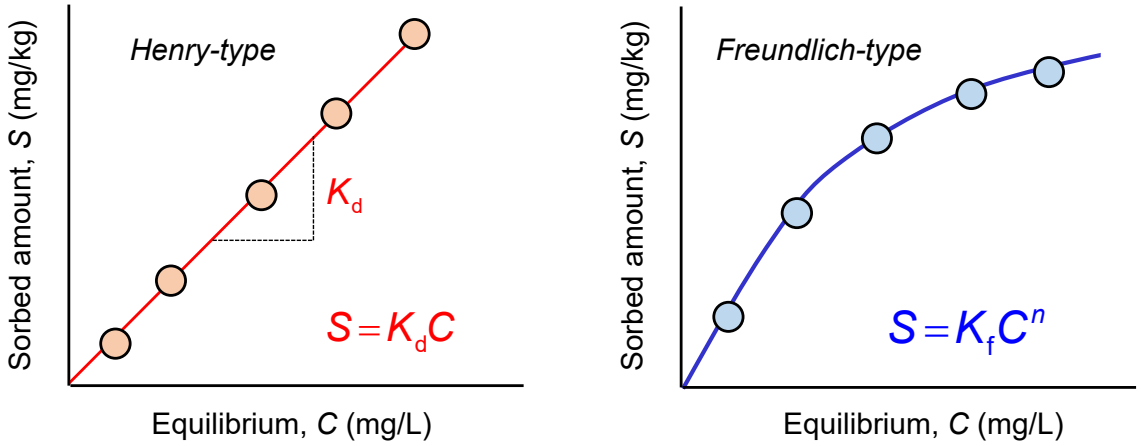

Figure 6.1 Images of the difference between Henry and Freundlich-type sorption isotherms.

$$S = K_d C \tag{6.1}$$

$$S = K_f C^n \tag{4.2}$$

Here, S is the amount of contaminants taken into the solid phase from the liquid phase (mg/kg), C is the concentration of contaminants in the solution (equilibrium concentration) (mg/L), and K_f (mg/kg)/(mg /L)^n, and n are the coefficients of the Freundlich-type sorption model. K_d and K_f are indicators of the affinity between contaminants and soil, and higher values indicate higher sorption capacity.

6.2.3 Estimated partition coefficients from asymmetrical breakthrough curves

Many studies show asymmetric breakthrough curves obtained from column sorption tests. When the breakthrough curve was nearly symmetrical, the area method and the method of calculating the retardation factor, R, from the point $C/C_0 = 0.5$ obtained approximately the exact value of K_d (Bouchard et al., 1988), while R was calculated from the point $C/C_0 = 0.5$, the value differed by about 30% from K_d calculated by the area method (Nkedi-Kizza et al., 1987). The breakthrough curve of the column sorption test became asymmetric because the sorption reaction in the column was non-equilibrium, as well as the nonlinearity of the sorption behavior. The asymmetric breakthrough curve agreed with the analytical solution of the advection-dispersion equation, assuming Freundlich-type sorption behavior (Nkedi-Kizza et al., 1987; Maraqa et al., 2001).

In addition to the shape of the Freundlich model, the asymmetry breakthrough curves have been reported in which the stabilizing agent of MgO was applied to evaluate fluorine sorption (Kato et al., 2021). The asymmetry has been pointed out to be the influence of slow chemical reactions, such as precipitation, not considered in the advection-dispersion equation.

6.3 Methodologies for determination of partition coefficients from breakthrough curves using four different ways

6.3.1 Overview of approaches

This study was conducted, as shown in Fig. 6.2. First, column sorption test results were simulated. Numerical analysis of advection-dispersion analysis parametrically created breakthrough curves. Herein, K_f, n, and C were considered as parameters when breakthrough curves are created. Next, partition coefficients, K_d were determined from the created breakthrough curves using four different methods: a) Area method, b) Fitting the Henry-type advection-dispersion equation (ADE) to the breakthrough curves, c) Fitting the Henry-type ADE to the breakthrough curves until $C/C_0 = 0.5$, and d) calculate K_d by making the horizontal axis of the breakthrough curve dimensionless with PVF and the vertical axis with C/C_0 and calculating the retardation factor R from the point of $C/C_0 = 0.5$, as shown in Section 6.2.1.

6.3.2 Theory of numerical analysis

Column sorption tests and contaminant's migration in the attenuation layer were simulated using the equilibrium sorption model shown in equations (6.1) and (6.2) and the advection-dispersion equation. Solute transport in column sorption tests was expressed by the one-dimensional advection-dispersion equation (6.3). For retardation factor R (-) in equation (6.3), equation (6.4) was used when linear sorption was assumed, while equation (6.5) was used when nonlinear sorption was assumed.

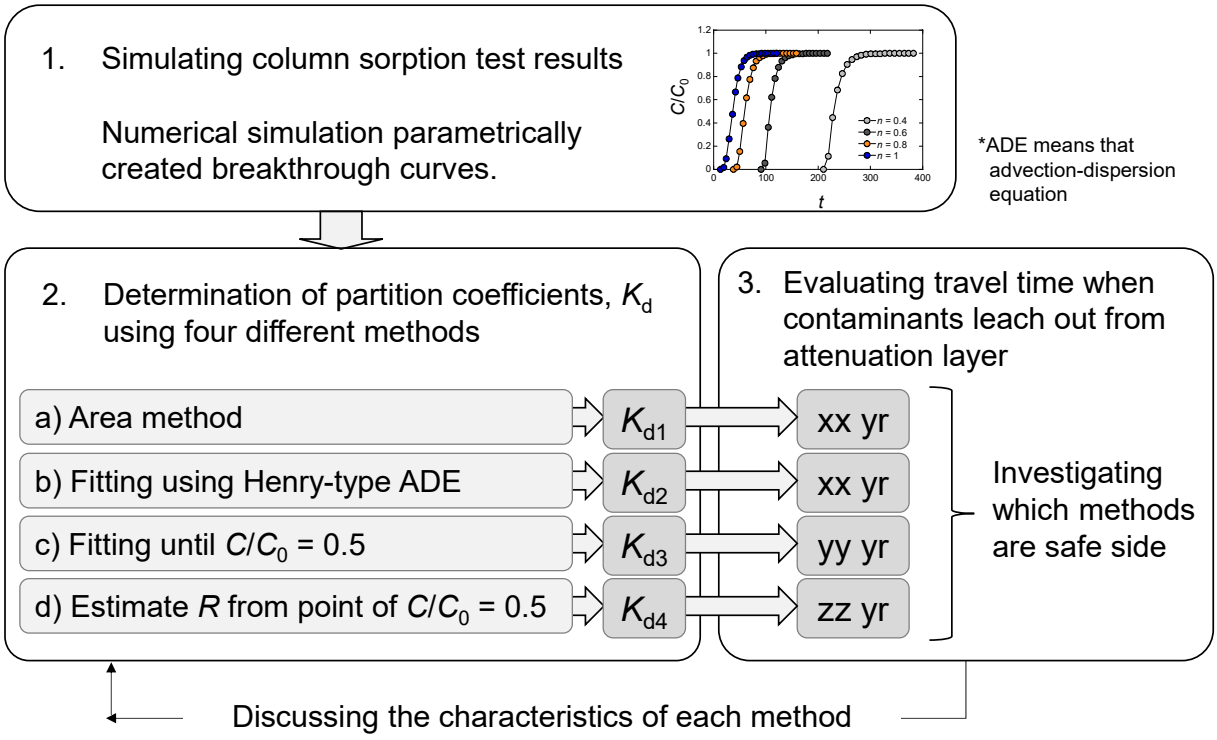

Figure 6.2 Approaches overview of this research.

$$R\frac{\partial C}{\partial t}=D\frac{\partial^2 C}{\partial x^2}-v\frac{\partial C}{\partial x} \tag{6.3}$$

$$R=1+\frac{\rho_{\mathrm{d}}K_{\mathrm{d}}}{\theta} \tag{6.4}$$

$$R=1+\frac{\rho_{\mathrm{d}}K_{\mathrm{f}}nC^{n-1}}{\theta} \tag{6.5}$$

$$D=D_{\mathrm{e}}+\lambda|v| \tag{6.6}$$

Here, t is time (s), D is dispersion coefficient (cm^2/s), x is depth (cm), v is the pore water velocity (cm/s), θ is volumetric water content (-), ρ_{d} is the dry density of the soil (g/cm^3), D_{e} is the molecular diffusion coefficient (cm^2/s), and λ is the dispersion length (cm). Note that equation (6.6) shows that D in equation (6.3) can be expressed by a diffusion term (the first term in equation (6.6)) and an advection term (the second term in equation (6.6)). In this study, diffusion was assumed to be negligibly small compared to advection in the sandy ground, which was assumed to be used in the attenuation layer method. Therefore, $D = \lambda \times |v|$ was assumed.

This study used equation (6.7) as the initial condition when performing numerical analysis on solute transport. Use the constant flux boundary shown in equation (6.8) for the boundary condition on the inflow side. In contrast, for the boundary condition on the outflow side, use the concentration gradient = 0 at L (cm) for the finite length of soil, as shown in equation (6.9) (van Genuchten et al., 1984; Toride et al., 2006). Herein, C_0 is the inflow concentration (mg/L).

$$C_{(x,0)}=0 \tag{6.7}$$

$$-D\frac{\partial C}{\partial x}+vC=vC_0 \tag{6.8}$$

$$\frac{\partial C_{(L,t)}}{\partial x}=0 \tag{6.9}$$

When analyzed in three dimensions, solute transport in the attenuation layer becomes a realistic but complex numerical simulation. This study briefly evaluated the relationship between the magnitude of the partition coefficients obtained from column sorption tests. Also, the travel time for contaminants starting to be discharged from the attenuation layer was evaluated. Therefore, like the column sorption test, the simulation for the travel time of the attenuation layer was analyzed using a simple one-dimensional advection-dispersion

equation. In this study, solute transport analysis was performed using one-dimensional soil moisture, heat, and solute transport prediction program, HYDRUS-1D (Simunek et al., 2008). In addition to forward analysis, HYDRUS-1D also has a function that allows inverse estimating parameters by fitting numerical solutions to a series of plots (experimental data). This inverse analysis function was applied in this study.

6.3.3 Parametrically created breakthrough curves

A column sorption test using a column with a height of 10 cm and an inner diameter of 5 cm was simulated. Tables 6.1 and 6.2 show the considered parameters in the simulation. Considering permeability, sandy soil is used as the parent material of the attenuation layer. Since the dispersion length, λ, in sandy soil was reported to be 0.1 to 0.7 cm, this study set it at 0.5 cm (Public Work Research Institute Japan, 2012). The effective porosity n_e was determined to be 0.4 (void ratio, e =0.67). This value corresponds to where the column is filled with sandy soil by applying the ISO testing protocols (ISO 21268-3, 2019).

Breakthrough curves described by the Freundlich-type numerical solution were simulated using a parametric study. As shown in Table 6.2, breakthrough curves focused on three parameters based on K_f = 100 (mg/kg)/(mg/L)^n and n = 1. Arsenic (As) was assumed to be the target because As is frequently reported among geogenic contaminants (e.g., Tabelin et al., 2018; Ito and Katsumi, 2020). The conditions of K_f = 100 (mg/kg)/(mg/L)^n and n = 1 mean that the effluetn concentration C of the attenuation layer with a layer thickness of 30 cm exceeds the SCCL environmental standard value for As after 100 years, C = 0.01 mg/L was confirmed in advance through preliminary analysis (refer to Section 6.3.5). The value of n was determined based on previous studies' batch sorption test results (sorption isotherms) (Tastuhara et al., 2015; Nakamura et al., 2017; Mo et al., 2020). The coefficient of the Freundlich model was set to n= 0.4, 0.6, 0.8, and 1, considering the range of possible values.

The initial concentration of contaminants was also treated as a parameter because shortening the period of the column test can accelerate the time for a breakthrough by changing the initial concentration C_0.

Table 6.1 Fixed parameters in the numerical analysis of creating breakthrough curves

	Value	Unit
Inner diameter of the column, d	5	cm
Height of the column, h	10	cm
Soil particle density, ρ_s	2.65	g/cm^3
Dry density, ρ_d	1.6	g/cm^3
Effective porosity, n_e	0.40	-
Saturated volumetric water content, θ_s	0.40	-
Flow rate, r	36	mL/h
Dispersion length, λ	0.5	cm
Darcy velocity, K_s	44	cm/day

In the column sorption test, the equilibrium concentration C of the effluent approaches the inflow concentration C_0, and finally, $C = C_0$. Therefore, this study treated C_0 in the column test as C. As shown in Figure 6.3, since the magnitude of the sorption isotherm reversed when C = 1 mg/L, C = 0.1, 1, and 10 mg/L were decided as the parameters.

Effluents are collected at arbitrary time intervals in column sorption tests. Therefore, the total number of plots in the breakthrough curve should vary from test to test. The number of plots of breakthrough curves was unified in this study. From the breakthrough curve created by numerical analysis, the area where C/C_0 increases from 0.01 to 1 was focused. Then, 20 plots were extracted at equal intervals from the column test results. A program code using Visual Basic language in Visual Studio 2019 was created to extract 20 plots. The extracted plots were used in Section 6.3.4. The appearance of the created program is shown in Figure 6.4 and Appendix 1. This program reads the plots of the breakthrough curve created with Hydrus 1D as input data and extracts 20 plots as outputs. Herein, C/C_0 represents the concentration at the top of the column, where x = 10 cm.

Table 6.2 Input parameters in the numerical analysis of creating breakthrough curves

	Value	Unit
Coefficient of Freundlich model, K_F	50, 100, 200	$(mg/kg)/(mg/L)^n$
Coefficient of Freundlich model, n	0.4, 0.6, 0.8, 1	-
Equilibrium concentration, C	0.1, 1, 10	mg/L

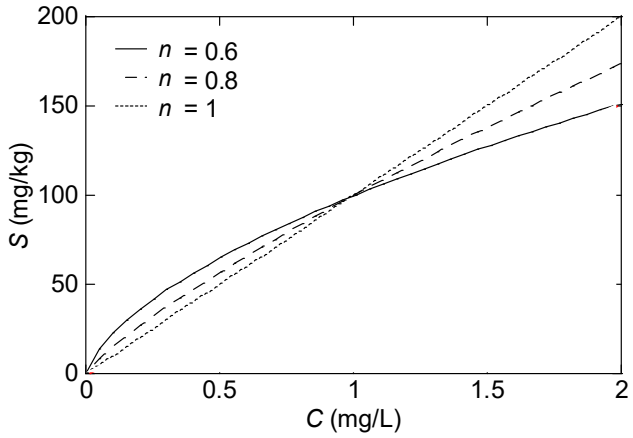

Figure 6.3 An example of that the magnitude of the sorption isotherm reversed when C = 1 mg/L.

(a)

```
            'C(j)を順に読んでいって、0.01*Cmaxを超えたら、その時のTime(j)をT01に記録する

            C01 = 0.01 * Cmax

            j = 1

            Do
                If C(j) > C01 Then
                    T01 = Time(j)
                    Exit Do
                Else
                End If
                j = j + 1
            Loop

            T01 = Time(j)

            'C(j)を順に読んでいって、0.99*Cmaxを超えたら、その時のTime(j)をT99に記録する

            C99 = 0.99 * Cmax

            j = 1

            Do
                If C(j) = Cmax Then
                    T99 = Time(j)
                    Exit Do
                Else
                End If
                j = j + 1
            Loop

            deltaT = (T99 - T01) / 17
            Tsample = T01 - deltaT
            j = 1
            k = 1

            'k = 21になったらDoLoopを抜ける
            Do
                If k = 21 Then
                    Exit Do
                Else
                    If Time(j) > Tsample Then
                        Time1(i, k) = Time(j)
                        Cont1(i, k) = C(j)
                        k = k + 1
                        Tsample = Tsample + deltaT
                    End If
                End If
                j = j + 1
            Loop
        Next i

        'この時点でファイルNo. iのデータポイントが、Time1(i,1～20)とCont(i,1～20)に収納された
```

(b)

Figure 6.4 A program code written by Visual Basic to extract 20 plots at equal intervals from breakthrough curves: (a) a part of the program code, (b) an application form to conduct the program.

6.3.4 Obtaining partition coefficients using four different ways

From breakthrough curves created by the numerical analysis in Section 6.3.3, K_d was obtained using four different methods. Then, the obtained K_d were compared. An image of the four methods is shown in Fig. 6.5.

a) K_{d1}: Partition coefficient determined by the area method

Many previous studies have applied the area method (e.g., Maraqa et al., 1998; Chotpantarat et al., 2011). This method obtains the partition coefficient by calculating the area surrounded by the breakthrough curve and the Y-axis. In previous studies, R was estimated by calculating the area surrounded by the breakthrough curve, the Y-axis, and $C/C_0 = 1$, and then K_d was obtained from equation (6.4). In this study, this method was slightly modified. As shown in Figure 6.5, the amount of sorbed contaminants onto the solid phase S (mg/kg) is determined by the area surrounded by the breakthrough curve, the Y axis, and $C/C_0 = 1$. Strictly speaking, the area should be determined by integration. However, for simplicity, S was calculated using the piecewise quadrature method for the 20 points extracted by forward analysis of advection-dispersion analysis, as shown in equation (6.10) and Fig. 6.6 a) in this study.

$$S = \frac{1}{M}\sum_{i}^{20}\left(C_{\text{input}} - C_{i-1}\right)\left(V_i - V_{i-1}\right) = \frac{1}{M}\sum_{i}^{20}\left(C_{\text{input}} - C_{i-1}\right) r\left(t_i - t_{i-1}\right) \tag{6.10}$$

Here, S is the sorbed amount (mg/kg), M is the mass of the attenuation layer material packed in the column (kg), and C_i is the concentration of effluent sampled No. i (mg/L) (i = 1 to 20, where Ci = 0 = 0), C_{input} is the influent concentration to the column (mg/L), and V_i is the volume of the effluent No. i (L) (where, $V_i = 0 = 0$, $t_i = 0 = 0$), r is the flow rate (L/h).

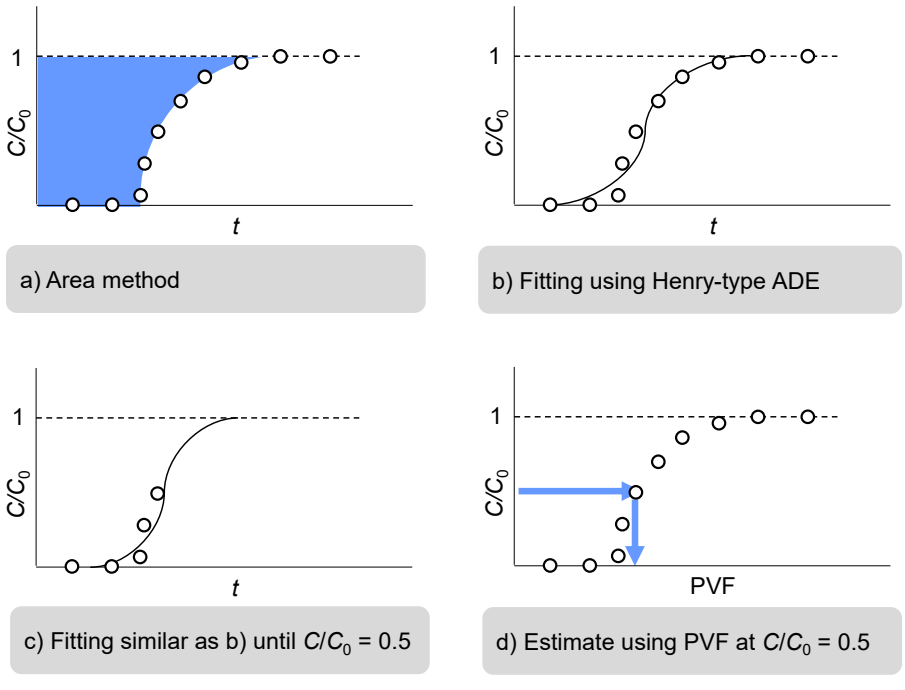

Figure 6.5 An image of the four methods obtaining partition coefficients.

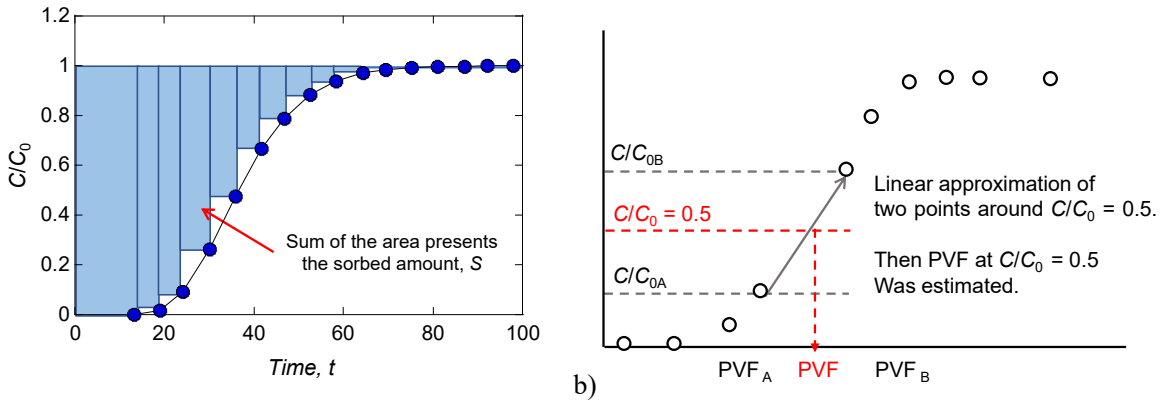

Figure 6.6 An image of the procedure to determine K_d: a) an example of the piecewise quadrature method to calculate the sorbed mass of S for K_{d1}, b) estimating PVF at $C/C_0 = 0.5$ when K_{d4} was calculated.

When performing piecewise quadrature, area No. i was calculated by calculating the midpoint t_i between the plots of the breakthrough curve. Area was calculated using the length from the midpoint to the next midpoint. Furthermore, if the pores of the specimen are saturated with water before the column sorption test, the sorbed amount might be overestimated by one pore volume. Therefore, calculating S from the breakthrough curve was corrected by subtracting the time for one pore volume (2.2 h in this study) from t_i. As mentioned in Section 6.2.2, K_d is a coefficient expressing the linear relationship between S and the equilibrium concentration C (mg/L) of the liquid phase. The K_d value is calculated by dividing S by C, as shown in equation (6.1). In the column sorption test, the effluent concentration terminates C. In this study, K_d determined by this method was called K_{d1} and compared with partition coefficients determined by other methods to examine whether K_{d1} was on the safe side.

b) K_{d2}: Partition coefficient determined by fitting using numerical solution of advection-dispersion equation

The partition coefficient was determined by fitting a Henry-type numerical solution (assuming linear sorption) to a parametrically created Freundlich-type breakthrough curve (assuming non-linear sorption). In this study, fitting was performed to minimize the sum of squared residuals of the relative concentrations of the Freundlich-type and Henry-type numerical solutions (e.g., Hioki and Aoki, 2007). The partition coefficient obtained using this method was called K_{d2}. Herein, exact values for the parameters shown in Table 6.1 were used.

c) K_{d3}: Partition coefficient determined by fitting until $C/C_0 = 0.5$

In Section 6.3.4 b), fitting was performed assuming the breakthrough curve plot was obtained until $C/C_0 = 1$. On the other hand, when the column test period is limited, especially in practice, tests might be terminated before the breakthrough curve reaches $C/C_0 = 1$, and fitting might be conducted. Therefore, in this study, a similar operation as in Section 6.3.4 b) was carried out by extracting plots of breakthrough curves up to the point where $C/C_0 = 0.5$ and performing inverse analysis. A program code to extract 14 equally spaced points from the breakthrough curve plot was prepared, and K_{d3} was calculated.

d) K_{d4}: Partition coefficient estimated by PVF at $C/C_0 = 0.5$

As shown in Fig. 6.5, in the breakthrough curve of the column sorption test, the pore volumes of flow (PVF) at $C/C_0 = 0.5$ corresponds to R (Maraqa et al., 1998). Therefore, the partition coefficient can be calculated from equation (6.4) since R can be obtained. In this study, the partition coefficient determined in this way is called K_{d4}. The PVF is the value obtained by dividing the permeated solution's total volume by the specimen's pore volume, as shown in equation (6.11).

$$PVF = \frac{rt}{V_v} \tag{6.11}$$

Here, r (mL/h) is the flow rate of permeation, t (h) is time, and V_v (cm^3) is the pore volume. 1 PVF means a permeated water volume equal to the specimen's pore volume. As shown in Fig. 6.6 b), the value of PVF at $C/C_0 = 0.5$ was interpolated by linear approximation of two points before and after $C/C_0 = 0.5$.

When the breakthrough curve reaches $C/C_0 = 0.5$, K_d can be calculated. Therefore, method d) is simple and has the advantage of shortening the test period. On the other hand, when applying d), the shape of the breakthrough curve must be point symmetric (Nkedi-Kizaa et al., 1987). Therefore, an unrealistic K_d might be obtained when d) was applied to the asymmetric Freundlich-type breakthrough curve.

6.3.5 Evaluating travel time when contaminants leach out from attenuation layer

In order to investigate the influence of K_d obtained in Section 6.3.4 on contaminant migration, forward analysis was performed using obtained K_{d1} to K_{d4}, and a one-dimensional attenuation layer model analysis was conducted. As shown in Fig 6.7, the travel time when contaminants reached the bottom of the attenuation layer was compared. The thickness of the layer was set to 30 cm based on the previous research (Gathuka et al., 2021). Generally, the attenuation layer is constructed higher than the groundwater level. Strictly speaking, performing seepage flow and advection-dispersion analysis under unsaturated conditions is necessary. However, analysis was performed under saturated conditions as a primary study here. The analysis conditions are shown in Tables 3 and 4.

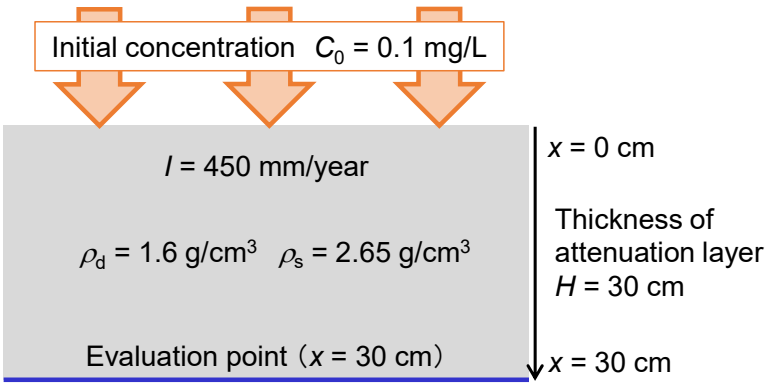

Figure 6.7 A one-dimensional attenuation layer model assumed in this research.

Table 6.3 Fixed parameters in the numerical analysis of travel time in the attenuation layer.

	Value	Unit
Attenuation layer thickness, H	30	cm
Initial concentration of the target contaminants, C	0.1	mg/L
Dispersion length, λ	0.5	cm
Rainfall intensity, P	1500	mm/year
Infiltration to the attenuation layer, I	450	mm/year
Soil particle density, ρ_s	2.65	g/cm^3
Dry density, ρ_d	1.6	g/cm^3
Effective porosity, n_e	0.40	-
Saturated volumetric water content, θ_s	0.40	-
Darcy velocity, K_s	0.123	cm/day

Table 6.4 Input parameters in the numerical analysis of travel time in the attenuation layer.

	Value	Unit
Coefficient of Freundlich model, K_F	50, 100, 200	(mg/kg)/(mg/L)^n
Coefficient of Freundlich model, n	0.4, 0.6, 0.8	-
Initial concentration, C_0	0.1	mg/L

The leaching concentration of geogenic contaminants is approximately several times exceeding the SCCL environmental standards (Ito and Katsumi, 2020). Based on this background, the initial concentration of contaminants, especially the arsenic concentration C assumed in this study, was set at C = 0.1 mg/L, ten times higher than the environmental standard. Previous studies evaluated the leaching behavior of geogenic contaminants using column tests (e.g., Nakamura et al., 2014; Naka et al., 2016). The leaching concentration of geogenic contaminants had been reported to tend to decrease as the liquid-solid ratio in the test increased, that is, as the testing duration increased. Therefore, considering the leaching behavior of geogenic contaminants, the analysis conditions of this study, which continue to provide a constant As concentration of C = 0.1 mg/L, can be on the safe side. For other parameters, the infiltration, I, was set to I = 450 mm/year, assuming that 30% of the annual rainfall intensity of 1500 mm infiltrates into the attenuation layer.

As the input parameters, K_{d1} to K_{d4} obtained from each K_f, n, and C in Section 6.3.4 were used. This study defined the time when the concentration at the bottom of the attenuation layer reached C = 0.01 mg/L, exceeding the SCCL environmental standard, as the breakthrough time T (year). Each breakthrough time was compared. No difference occurs in the case of n = 1 because of $K_f = K_d$. Therefore, n = 0.4, 0.6, and 0.8 were considered. The breakthrough time when using K_{d1} was set as T_1, K_{d2} as T_2, K_{d3} as T_3, and K_{d4} as T_4. When comparing breakthrough times, the breakthrough time obtained by Freundlich-type forward analysis (numerical solution including K_f and n) assuming nonlinear sorption was used as the standard breakthrough

time, T_F. For example, if $T_2 / T_F < 1$, the evaluation of the attenuation layer performance using K_{d2} obtained through fitting presents on the safe side.

6.4 Results

6.4.1 Partition coefficients obtained from four different methods

Table 6.5 shows the partition coefficients obtained from four methods (see Section 6.3.4 a) ~ d)). Since the unit of K_F is long, the unit of "(mg/kg)/(mg/L)^n" is shown at the bottom of Table 6.5. Figure 6.5 shows the K_{d2}, K_{d3}, and K_{d4} to K_{d1} ratio for the partition coefficients determined by each method when K_f = 100 (mg/kg)/(mg/L)^n. As shown in Fig. 6.8 a), when n = 0.4, the obtained K_{d2}, K_{d3}, and K_{d4} were in the range of 0.91 to 1.28 times compared to K_{d1}. As shown in Fig. 6.8 b), when n = 0.6, the range was 0.94 to 1.20 times, and as shown in Fig. 6.8 c), when n = 0.8, it was in the range of 0.96 to 1.06 times. Herein, the results are compared to the previous research. Breakthrough curves were obtained in column sorption tests using organic compounds as solutes (Bouchard et al., 1988). The breakthrough curve with a linear sorption model resulted in K_{d4}/K_{d1} values of approximately 1.06 to 1.10. On the other hand, when the breakthrough curve differed from the linear sorption model, the value of K_{d4}/K_{d1} was 0.69, which was about 30% smaller than K_{d1} (Bouchard et al., 1988). Similarly, the difference between K_{d1} and K_{d4} tended to increase as the value of n increased, and the nonlinearity increased in this study (see Table 6.5).

As shown in Fig 6.8 d), when n = 1, only K_{d1} was large in the obtained partition coefficients, and the $K_{d2} \sim K_{d4}$ were equally 0.95 times smaller. The four partition coefficients did not match even when n = 1, which is the Henry-type breakthrough curve because the asymmetry occurs in the numerical solution due to the influence of the degree of dispersion. The previous research obtained the similar result (Bouchard et al., 1988).

Within the parameters considered in this study, when n = 0.4, 0.6, and 0.8, K_{d2} was the most conservative compared to other partition coefficients. On the other hand, K_{d3} had a larger value compared to K_{d1}. The evaluation may be on the dangerous side when the fitting is performed using C/C_0 from 0 to 0.5. Also, except when n = 1, $K_{d3} > K_{d4}$.

Table 6.5 Partition coefficients K_{d1}, K_{d2}, K_{d3}, and K_{d4} obtained from four different methods.

Case	K_f *	n	C (mg/L)	K_{d1} (L/kg)	K_{d2} (L/kg)	K_{d3} (L/kg)	K_{d4} (L/kg)
1	50	0.4	0.1	316	288	395	309
2		0.6		152	143	181	148
3		0.8		84.9	81.0	89.7	81.6
4		1.0		52.8	50.0	50.0	50.3
5		0.4	1	79.9	72.5	100	78.2
6		0.6		59.6	55.9	71.1	57.9
7		0.8		53.6	51.2	56.4	51.4
8		1.0		52.8	50.0	50.0	50.2
9		0.4	10	20.7	18.6	25.6	20.1
10		0.6		23.4	21.8	27.5	22.5
11		0.8		34.0	32.3	35.5	32.5
12		1.0		52.8	50.0	50.0	50.2
13	100	0.4	0.1	643	584	812	632
14		0.6		304	287	366	297
15		0.8		168	162	177	163
16		1.0		105	100	100	100
17		0.4	1	161	147	201	158
18		0.6		119	112	142	116
19		0.8		106	102	112	102
20		1.0		105	100	100	100
21		0.4	10	40.4	37.3	51.7	40.0
22		0.6		46.1	43.8	54.9	45.3
23		0.8		66.8	64.4	70.7	64.7
24		1.0		105	100	100	100
25	200	0.4	0.1	1303	1185	1651	1280
26		0.6		607	570	726	592
27		0.8		338	323	356	325
28		1.0		210	200	200	201
29		0.4	1	327	296	411	321
30		0.6		238	223	279	232
31		0.8		213	204	225	205
32		1.0		210	200	200	201
33		0.4	10	80.7	73.0	101	79.1
34		0.6		92.8	87.4	110	90.2
35		0.8		135	129	142	129
36		1.0		210	200	200	201

*The unit of K_f is (mg/kg)/(mg/L)^n.

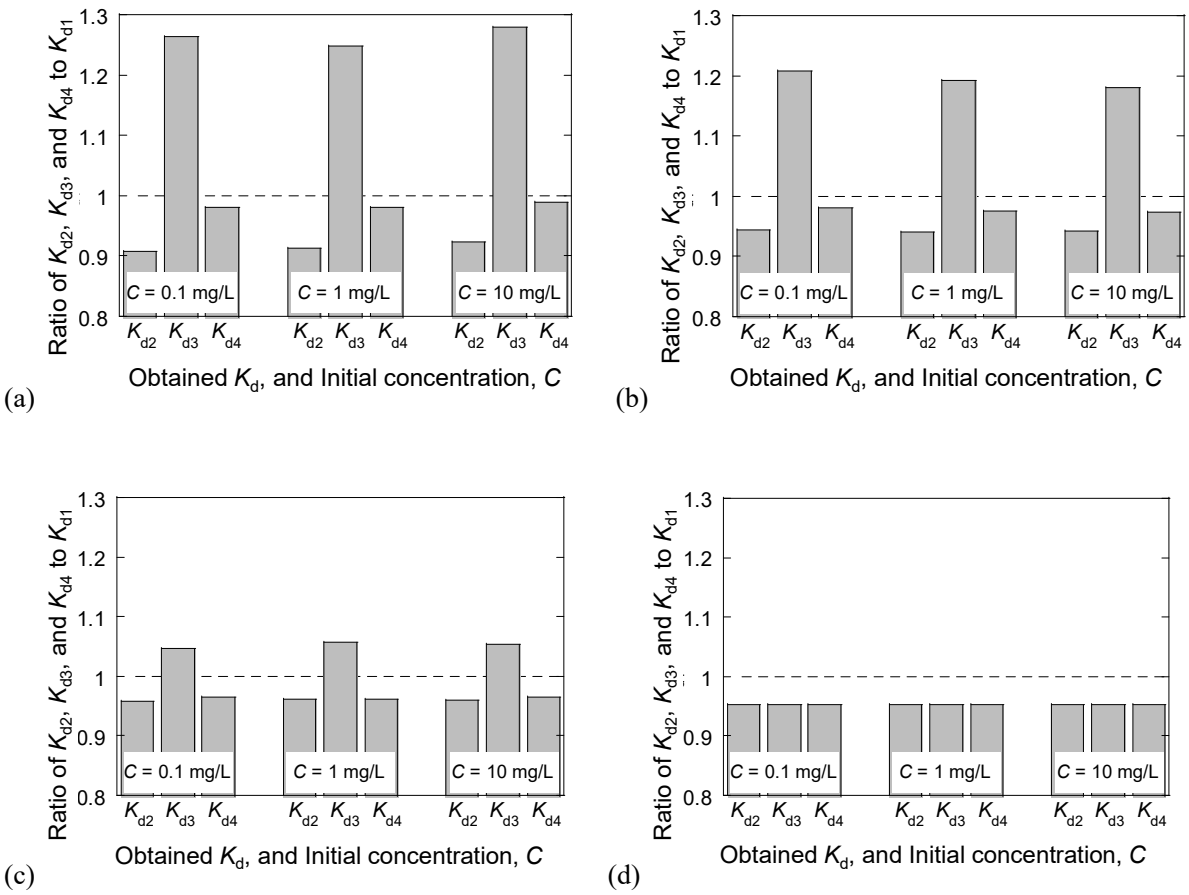

Figure 6.8 Ratio of partition coefficients obtained when K_f = 100 (mg/kg)/(mg/L)^n: (a), (b), (c), and (d) present the cases of n = 0.4, 0.6, 0.8, and 1, respectively.

6.4.2 Effects of breakthrough curve shape on partition coefficients

The influence of the shape of the breakthrough curve (Freundlich-type coefficient, K_f or n) obtained in the column sorption test on the obtained partition coefficients is discussed. As shown in Table 6.5, the ratio of partition coefficients was K_f = 50, 100, 200 (mg/kg)/(mg/L)^n, 0.90 to 1.28 times when n = 0.4, 0.90 to 1.28 times when n = 0.6, and 0.95 to 1.06 times when n = 0.8 were obtained. Therefore, it was confirmed that the ratio of partition coefficients does not depend on the difference in K_f.

On the other hand, as shown in Fig. 6.8, the smaller the value of n, the more significant the difference in K_d, making it clear that the difference mainly depends on the value of n. If n = 1, the calculated four partition coefficients are almost identical, while as the value of n decreases from 1 to 0.8, 0.6, and 0.4, the shape of the breakthrough curve obtained from the column test gradually four partition coefficients differ because the shape of breakthrough curves differs from the shape of the numerical solution of the Henry type advection-dispersion equation. This result was similar to the previous study comparing K_{d1} and K_{d4} (Bouchard et al., 1988). Similarly, for K_{d2} and K_{d3} obtained by fitting, the smaller n, the more significant difference between K_{d2} and K_{d3}.

6.4.3 Effects of equilibrium concentration of contaminants on partition coefficients

When obtaining K_d from a column sorption test, due to the limitation of the testing time, a larger initial solute concentration of C might be applied to make the breakthrough time earlier and shorten the test period. Therefore, this section summarizes the trends of C and the obtained K_d.

Focus on Cases 13 to 16 in Table 6.5. Using the same K_d obtaining method and the same K_f and n, when the C was relatively small at 0.1 mg/L, a more significant partition coefficient was obtained as the n value was smaller. On the other hand, focusing on Cases 21 to 24 in Table 6.5, when C was 10 mg/L, the smaller n, the smaller K_d obtained. For example, when K_f= 100 (mg/kg)/(mg/L)^n, n = 0.4, and C = 0.1 mg/L, K_{d2} = 584 L/kg was obtained, while K_{d2} = 37.3 L/kg was obtained at C = 10 mg/L. As a result, there is a difference in K_d values of approximately 16 times. In the Freundlich-type sorption model, the obtained K_d value decreases as the C value increases. Therefore, the obtained K_d depends on the initial concentration. Regardless of the determination method of K_d, the partition coefficient value obtained by increasing the inflow concentration becomes smaller. Therefore, as this study considers, K_d on the safe side is obtained in the Freundlich-type breakthrough curve as the initial concentration increases during the column sorption test.

6.4.4 Evaluating the performance of attenuation layer using obtained partition coefficients

Differences in the travel time of contaminants to reach the bottom of the attenuation layer were investigated using the obtained partition coefficients, as shown in Fig. 6.8. As shown in Section 6.3.5, an advection-dispersion analysis was performed using K_{d1} to K_{d4} listed in Table 6.5 using the one-dimensional attenuation layer model. The partition coefficients obtained in Section 6.4.1 were always the smallest for K_{d2} and the largest for K_{d3}. Therefore, for the breakthrough time, T_2, determined by K_{d2}, was always the minimum, while T_3, determined by K_{d3}, was always the maximum.

Mention specific values of breakthrough time, T are presented. When K_f = 50 (mg/kg)/(mg/L)^n and n = 0.4, the breakthrough times T_F, T_2, and T_3 calculated using Freundlich-type numerical solutions were 314, 245, and 336 years, respectively. When K_f = 50 (mg/kg)/(mg/L)^n and n = 0.6, T_F, T_2, and T_3 were 140, 122, and 154 years, respectively. When K_f was doubled, K_f = 100 (mg/kg)/(mg/L)^n, and n = 0.6, T_F, T_2, and T_3 became 283, 244, and 311 years, respectively. The breakthrough time T was approximately proportional to the value of K_f. As K_f increased, T also increased. This study obtained the minimum T when K_f = 50 (mg/kg)/(mg/L)^n and n = 0.8, and T_F, T_2, and T_3 were 78.8, 69.2, and 76.5 years, respectively.

When a batch sorption test against arsenic was carried out by adding a stabilizing agent of a calcium carbonate and magnesium oxide composite material to decomposed granite soil at a dry mass ratio of 5%, the K_f value was 430 (mg/kg)/(mg/ L)^n, approximately n = 0.6 (Mo et al., 2020). Since the K_f considered in this study is smaller than the range of values obtained in sorption tests for stabilizing agents, the K_f values are likely to be even larger in attenuation layers with stabilizing agents added. Although the knowledge of column sorption tests using stabilizing agents is insufficient, based on the results of one-dimensional advection and dispersion analysis in this study, T_1 to T_4 are estimated to be approximately 500 to 1000 years.

The difference in travel time for contaminants to reach the bottom of the attenuation layer is compared. Figure 6.9 shows the results of calculating T_F / T_F, T_2 / T_F, and T_3 / T_F for each case. Figure 6.9 a) b) shows the results when n = 0.4, 0.6. Breakthrough time T was estimated using K_d calculated in four ways. When n = 0.4, T was 0.78 to 1.2 times as much as T_F, while when n = 0.6, T was 0.85 to 1.1 times as much as T_F. Regardless of the value of K_f, T_2 / T_F < 1, T_3 / T_F > 1. Under the analysis conditions assumed this time, if K_{d2} is obtained by fitting a Henry-type numerical solution to all plots of the breakthrough curve, the evaluation can be on the safest side. On the other hand, if only plots with C/C_0 up to 0.5 are obtained and fitting is performed, the evaluation can be on the dangerous side. Furthermore, as shown in Fig. 6.9 c), when n = 0.8, T was estimated to be 0.88 to 0.97 times larger than T_F. When n = 0.8, T_2 / T_F, T_3 / T_F < 1. The risk assessment is safe, regardless of which partition coefficient is used.

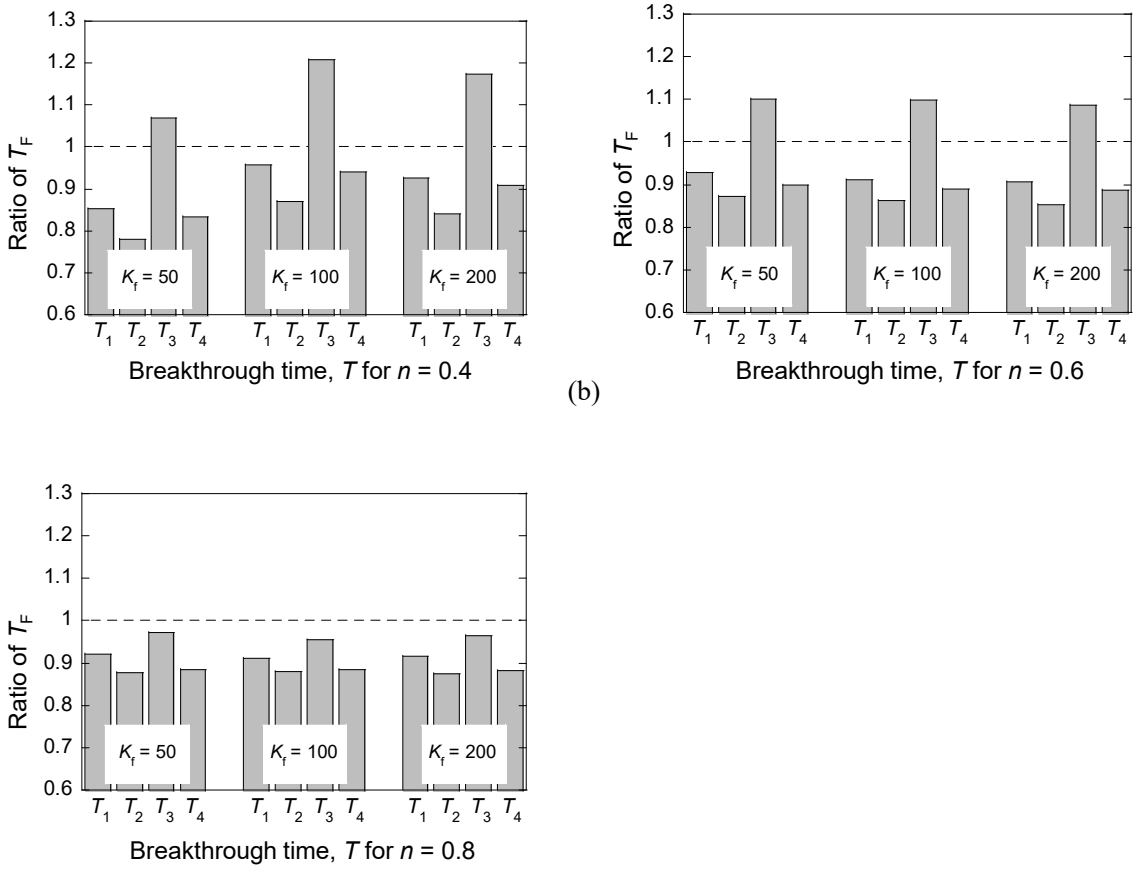

Figure 6.9 Ratio of the breakthrough time (T_1 / T_F, T_2 / T_F T_3 / T_F, and T_4 / T_F): (a), (b), and (c) present the cases of n = 0.4, 0.6, and 0.8, respectively.

6.5 Discussion

6.5.1 Characteristics of four different methods obtaining partition coefficients

In this study, when K_d was obtained using the four methods from the Freundlich-type breakthrough curves, partition coefficients of 0.91 to 1.27 times were obtained, and the difference was within 40%. The smallest partition coefficient, K_{d2}, was obtained through fitting. Suppose a column sorption experiment is conducted, and a breakthrough curve that fits the Freundlich-type numerical solution is obtained. In that case, it is desirable to evaluate the performance of the attenuation layer using K_{d2} calculated by fitting the Henry-type numerical solution.

On the other hand, if the breakthrough curve is obtained only up to the point $C/C_0 = 0.5$, when calculating the partition coefficients by fitting, as in the case where K_{d3} is approximately 30% larger than K_{d1} and K_{d4}, a significant value of the partition coefficient is obtained. Therefore, the risk assessment could be on the dangerous side. In such cases, it is desirable to use K_{d4}, which obtains the retardation factor, R, from the point of $C/C_0 = 0.5$, to evaluate the performance of the attenuation layer because the method can be simply conducted. The difference between K_{d1}, determined by the area method, and K_{d4}, determined by R from the $C/C_0 = 0.5$ point of the breakthrough curve, remains within 10%. Therefore, K_{d1} and K_{d4} are almost the same regardless of the method.

6.5.2 Relationship between obtained partition coefficients and breakthrough time

If the breakthrough curve obtained from the column sorption experiment fits a Freundlich-type numerical solution and the degree of nonlinearity is large, such as when the value of n is 0.4 or 0.6, it is on the safe side when evaluated using K_{d2}, while using K_{d3} was on the dangerous side. Therefore, when $n < 0.6$, it is desirable to perform the column sorption test up to $C/C_0 = 1$ and obtain K_{d2} by fitting. On the other hand, if $n > 0.8$, the column sorption test can be ended at $C/C_0 = 0.5$, and the evaluation using K_{d4} is on the safe side. When $n > 0.8$, there is much room to choose the method of obtaining K_d depending on the test implementation situation.

This paragraph discusses why the magnitude relationship between T_2 / T_F, T_3 / T_F, and 1 differs when n values are 0.4, 0.6, and 0.8. The reason is the difference in shape between the numerical solution of the Freundlich-type and Henry-type advection-dispersion equation. The Henry type has a point-symmetrical shape, while the Freundlich type depends on C. Therefore, the Freundlich is a model in which the sorption performance is high as C is small, while the sorption performance decreases rapidly as C increases (Nkedi-Kizza et al., 1987). As shown in Fig. 6.9, this tendency becomes more noticeable as n, which affects nonlinearity among Freundlich-type coefficients, becomes smaller. The Freundlich-type numerical solution under the condition of $C = 0.1$ mg/L can ensure longer until a breakthrough ($C > 0.01$ mg/L) occurs than the Henry-type. However, once C increases, sorption performance rapidly disappears. Therefore, the results regarding the magnitude of T were obtained under the criteria assumed in this study, "Breakthrough time, T is the time when $C = 0.01$ mg/L," and if the criteria changes, the breakthrough time must change. It should be noted that relationships change depending on the concentration levels.

6.5.3 Effects of differences in Freundlich-type parameters

This paragraph focuses on the sorption model, especially the differences in the Freundlich-type coefficients K_f and n. n is an index indicating the heterogeneity of the adsorption performance of soil and adsorption materials (Sposito, 1980). In this study, the smaller n in the breakthrough curve, the more significant differences in the partition coefficients obtained by the four methods. This is because the smaller n becomes, the more asymmetrical the shape of the breakthrough curve becomes. Therefore, the more heterogeneity in the sorption performance of soils or stabilizing agents, the more care must be taken in obtaining the partition coefficient. In particular, if the fitting is performed before all breakthrough curve plots are obtained, the evaluation can be dangerous when n = 0.4, 0.6, as in T_3 in Fig. 6.9 a) b). This is likely because the shape of the Freundlich-type numerical solution differs significantly from the Henry-type numerical solution due to the influence of the heterogeneity of the soil and stabilizing agent.

6.5.4 Future works

In this study, the discussion proceeded on the assumption that the breakthrough curve obtained from column sorption experiments has an asymmetric shape, especially when a Freundlich-type numerical solution can express it. However, as mentioned in Section 6.2.3, when the influence of reactions not considered in the advection-dispersion equation (e.g., reactions other than adsorption/desorption) is significant, an asymmetric breakthrough curve different from the Freundlich equation is obtained, as reported in the previous research (Kato et al., 2021). In particular, some stabilizing agents applied in the attenuation layer have slow chemical kinetics against contaminants, and column tests are assumed to be conducted in non-equilibrium conditions. Therefore, further discussion is required regarding the method for obtaining K_d.

In this analysis, arsenic was assumed to be the target contaminant. The SCCL environmental standard values for other heavy metals such as selenium, lead, and cadmium are C = 0.01 mg/L, the same as arsenic. Therefore, the concentrations of these four chemicals leaching from excavated soils are expected to be approximately the same so that the present findings can be applied to geogenic selenium, lead, and cadmium. On the other hand, the SCCL environmental standard values for fluorine and boron are C = 0.8 and 1 mg/L, respectively. Since the leaching concentration of geogenic contaminants is often approximately 2 to 3 times exceeding the SCCL environmental standard (Ito and Katsumi, 2020), the leaching concentration of fluorine and boron is expected to exceed C = 1 mg/L. As shown in Fig. 6.3, when n changes, the magnitude of the Freundlich-type sorption isotherm changes around C = 1 mg/L. Therefore, fluorine and boron might be inconsistent with the trends considered in this analysis. In addition, for simplicity, an advection-dispersion analysis was carried out under the condition that a constant leaching concentration flows into the attenuation layer. However, it has been reported that, in reality, the leaching of geogenic contaminants does not usually continue at a constant concentration but often decreases (e.g., Nakamura et al., 2014; Naka et al., 2016). In the future, the results of column leaching tests should be combined with numerical analysis under conditions where the initial concentration changes over time to design the attenuation layer closer to reality.

6.6 Summary and Conclusions

In this study, breakthrough curves according to the Freundlich model were created parametrically using a numerical solution of the advection-dispersion equation. Then, four methods obtained the partition coefficient from the resulting breakthrough curves. The obtained partition coefficients were compared to examine the effects of differences in the determining method, differences in the Freundlich-type coefficients K_f, n, and differences in the initial concentration C when performing the sorption test. Furthermore, using the obtained partition coefficients, the travel time of contaminants was simulated when the contaminant reached the bottom of the 30-cm attenuation layer and determined the partition coefficient for evaluating a safe attenuation layer. The results support the following conclusions:

1. The partition coefficients were within a maximum difference of 40% for the four determination methods.
2. In the case of a breakthrough curve following a Freundlich-type model, fitting all plots where the relative concentration changes from 0 to 1 was safe. On the other hand, when fitting only to the plot where the relative concentration changes from 0 to 0.5, a larger partition coefficient will be obtained, resulting in a dangerous evaluation.
3. When obtaining the partition coefficient from the Freundlich-type breakthrough curve, since n determines the shape of the sorption model, the smaller n, the more significant the difference in the obtained partition coefficients.
4. The Freundlich-type breakthrough curve is concentration-dependent. Therefore, the lower the concentration, the higher the sorption performance, and the higher partition coefficient obtained. If a column sorption experiment is performed with a higher concentration of geogenic contaminants than expected in the field, a smaller partition coefficient can be obtained, resulting in a safer performance evaluation.
5. By performing a column sorption test until the relative concentration reaches 1, obtaining the partition coefficient through the fitting, and performing a one-dimensional advection-dispersion analysis, the evaluation is on the safer side than the numerical analysis that inputs Freundlich-type coefficients.

References for Chapter 6

Arima, T., Sato, D., Igarashi, T., Tamoto, S, and Tatsuhara, T., 2011. Reduction and retardation of arsenic and boron leached from excavated rocks by volcanic ash adsorption layer. *Journal of the Japan Society of Engineering Geology* 52(3), 88–96 (in Japanese). https://doi.org/10.5110/jjseg.52.88.

Bouchard, D.C., Wood, A.L., Campbell, M.L., Nkedi-Kizza, P. and Rao, P.S.C., 1988. Sorption nonequilibrium during solute transport. *Journal of Contaminant Hydrology* 2(3), 209–223. https://doi.org/10.1016/0169-7722(88)90022-8.

Chotpantarat, S., Ong, S.K., Sutthirat, C. and Osathaphan, K., 2011. Competitive sorption and transport of Pb^{2+}, Ni^{2+}, Mn^{2+}, and Zn^{2+} in lateritic soil columns. *Journal of Hazardous Materials* 190, 391–396. https://doi.org/10.1016/j.jhazmat.2011.03.058.

Gathuka, L.W., Kato, T., Takai, A., Flores, G., Inui, T., and Katsumi, T., 2021. Effect of acidity on the attenuation performance of sandy soil amended with granular calcium-magnesium composite. *Soils Foundations* 61(4), 1099–1111. https://doi.org/10.1016/j.sandf.2021.05.007.

Gathuka, L.W., Kasai, H., Kato, T., Takai, A., Inui, T., and Katsumi, T., 2022. Evaluating the arsenic attenuation of soil amended with calcium–magnesium composites of different particle sizes. *Soils Foundations* 62(3), 101130. https://doi.org/10.1016/j.sandf.2022.101130.

Hioki K., and Aoki, K., 2007. An inverse problem study of geoenvironmental parameters based on the results of column tests. *Doboku Gakkai Ronbunshuu (JSCE Journal)* C 63(1), 34–46 (in Japanese). https://doi.org/10.2208/jscejc.63.34.

Igarashi, T., and Shimogaki, H., 1998. Migration characteristics of boron by batch and column methods, *Journal of Groundwater Hydrology* 40(2), 121–132 (in Japanese). https://doi.org/10.5917/jagh1987.40.121.

ISO 21268-3, 2019. Soil Quality—Leaching Procedures for Subsequent Chemical and Ecotoxicological Testing of Soil and Soil Materials—Part 3: Up-Flow Percolation Test. International Standardization Organization.

Itaya Y., and Kuninishi, K., 2020. Development of selenium insolubilized material eluted from tunnel excavation rock. *Japanese Geotechnical. Journal* 15(3), 435–440 (in Japanese). https://doi.org/10.3208/jgs.15.435.

Ito, H., and Katsumi, T., 2020. Leaching characteristics of naturally derived toxic elements from soils in the western Osaka area: Considerations from the analytical results under the Soil Contamination Countermeasures Act. *Japanese Geotechnical. Journal* 15(1), 119–130 (in Japanese). https://doi.org/10.3208/jgs.15.119.

Kato, T., Gathuka, L.W., Okada, T., Takai, A., Katsumi, T., Imoto, Y., Morimoto, K., Nishikata, M., and Yasutaka, T., 2021. Sorption-desorption column tests to evaluate the attenuation layer using soil amended with a stabilizing agent. *Soils Foundations* 61(4), 1112–1122. https://doi.org/10.1016/j.sandf.2021.05.004.

Katsumi, T., 2017. Use of excavated soils with natural contamination. *Japanese Geotechnical Society Magazine*. 65 (11/12), 1–3 (in Japanese).

Maraqa, M. A., Zhao, X., Wallace, R. B. and Voice, T. C., 1998. Retardation coefficients of nonionic organic compounds determined by batch and column techniques. *Soil Science Society of America Journal* 62, 142–152. https://doi.org/10.2136/sssaj1998.03615995006200010019x.

Maraqa, M. A., 2001. Effects of fundamental differences between batch and miscible displacement techniques on sorption distribution coefficient. *Environmental Geology* 41, 219–228. https://doi.org/10.1007/s002540100386.

Martínez-Lladó, X., Valderrama, C. M. Rovira, Martí, V., Giménez, J., and De Pablo, J., 2011. Sorption and mobility of Sb(V) in calcareous soils of Catalonia (NE Spain): batch and column experiments. *Geoderma* 160, 468–476. https://doi.org/10.1016/j.geoderma.2010.10.017.

Ministry of Land, Infrastructure, and Transport, Japan, 2023. Technical Manual on the Countermeasure Against Soils and Rocks Containing Naturally Occurring Heavy Metals in Construction Works. https://www.mlit.go.jp/sogoseisaku/region/recycle/d11pdf/recyclehou/manual/shizenyurai2023.pdf (accessed 29 November 2023) (in Japanese).

Ministry of Environment, Japan, 1995. Environmental Agency Notification No.46: Leaching Test Method for Soils. http://www.env.go.jp/kijun/dojou.html (in Japanese) (accessed 27 October 2021).

Mo, J., Flores, G., Inui, T., and Katsumi, T., 2020. Hydraulic and sorption performances of soil amended with calcium-magnesium composite powder against natural arsenic contamination. *Soils and Foundations*, 60(5), 1084–1096. https://doi.org/10.1016/j.sandf.2020.05.007.

Naka, A., Yasutaka, T., Sakanakura, H., Kalbe, U., Watanabe, Y., Inoba, S., Takeo, M., Inui, T., Katsumi, T., Fujikawa, T., Sato, K., Higashino, K., and Someya, M., 2016. Column percolation test for contaminated soils: key factors for standardization, *Journal of Hazardous Materials* 320, 326–340. https://doi.org/10.1016/j.jhazmat.2016.08.046.

Nakamura, K., Ysutaka, T., Fujikawa, T., Takeo, M., Sato, K., Watanabe, Y., Inoba, S., Tamoto, S., and Sakanakura, H., 2014. Up-flow column tests to evaluate heavy metal leaching for standardization. *Japanese Geotechnical. Journal* 9(4), 697–706 (in Japanese). https://doi.org/10.3208/jgs.9.697.

Nakamura, K., Yasutaka, T., Kuwatani, T. and Komai, T., 2017. Development of a predictive model for lead, cadmium and fluorine soil—water partition coefficients using sparse multiple linear regression analysis. *Chemosphere* 186, 501–509. https://doi.org/10.1016/j.chemosphere.2017.07.131.

Nkedi-Kizza, P., Rao, P.S.C. and Hornsby, A.G., 1987. Influence of organic cosolvents on leaching of hydrophobic organic chemicals through soils. *Environmental Science and Technology* 21, 1107–1111, 1987. https://doi.org/10.1021/es00164a011.

Nishikata, M., Yasutaka, T., Morimoto, K., and Imoto, Y., 2022. Evaluation of water contact influence on adsorbents by water immersion pretreatment and serial batch tests. *Japanese Geotechnical. Journal* 17(2), 195–204 (in Japanese). https://doi.org/10.3208/jgs.17.195.

Plassard, F., Winiarski, T., and Petit-Ramel, M., 2000. Retention and distribution of three heavy metals in a carbonated soil: comparison between batch and unsaturated column studies. *Journal of Contaminant Hydrology* 42, 99–111. https://doi.org/10.1016/S0169-7722(99)00101-1.

Public Work Research Institute Japan, 2012. Manual for dealing with ground contamination encountered during construction work (revised edition), 130–135.

Šimůnek, J., van Genuchten, M. Th. and Šejna, M., 2008. Development and applications of the HYDRUS and STANMOD software packages, and related codes. *Vadose Zone Journal* 7(2), 782–797. https://doi.org/10.2136/vzj2007.0077.

Sposito, G., 1980. Derivation of the Freundlich equation for ion exchange reactions in soils. *Soil Science Society of America Journal* 44, 652–655. https://doi.org/10.2136/sssaj1980.03615995004400030045x.

Tabelin, C.B., Igarashi, T., Villacorte-Tabelin, M., Park, I., Opiso, E.M., Ito, M., and Hiroyoshi, N., 2018. Arsenic, selenium, boron, lead, cadmium, copper, and zinc in naturally contaminated rocks: a review of their sources, modes of enrichment, mechanisms of release, and mitigation strategies. *Science of the Total Environment* 645, 1522–1553. https://doi.org/10.1016/j.scitotenv.2018.07.103.

Tatsuhara, T., Jikihara, S., Tastumi, T., and Igarashi, T., 2015. Effects of the layout of adsorption layer on immobilizing arsenic leached from excavated rocks. *Japanese Geotechnical. Journal* 10(4), 635–640 (in Japanese). https://doi.org/10.3208/jgs.10.635.

Toride, N, Sakai, M., and Saito, H., 2006. Boundary conditions for the convective-dispersive solute transport in soils. *Journal of the Japanese Society of Soil Physics* 10, 75–84 (in Japanese). https://doi.org/10.34467/jssoilphysics.104.0_75.

van Genuchten, M. Th. and Parker, J.C., 1984. Boundary conditions for displacement experiments through short laboratory columns. *Soil Science Society of America Journal* 48, 703–708. https://doi.org/10.2136/sssaj1984.03615995004800040002x.

Wang, X. and Liu, X., 2005. Sorption and desorption of radioselenium on calcareous soil and its solid components studied by batch and column experiments. *Applied Radiation and Isotopes* 62, 1–9. https://doi.org/10.1016/j.apradiso.2004.05.081.

Chapter 7

Practical Implications

7.1 Proposal to determine leaching concentrations of geogenic contaminants

Chapter 3 conducted the batch leaching tests focusing on temperature effect, leaching kinetics, and shaking conditions. As for the temperature effect, the results imply that the impact of the temperature on the leaching behavior is not so significant. Considering the results, if a solute transport analysis is conducted to predict the risks of geogenic contamination to the surrounding ground to utilize excavated materials as geomaterial and to assess the effectiveness of the countermeasures (e.g., Tabelin et al., 2014), the leaching concentrations of geogenic contaminants could be up to five times higher than the regulatory limit under elevated temperatures. For this reason, leachate concentrations several times the regulatory limit are enough to account for in the analysis.

Leaching kinetics is revealed to be one of the crucial parameters. In previous studies, the leaching of toxic metals and metalloids occurs mainly via the dissolution of the minerals in the rocks or the desorption from the soil particles (Tabelin et al., 2018). The dissertation indicates that geogenic arsenic and boron leaching is more significant through the dissolution of the minerals by combining temperature-changing batch leaching tests and zeta potential analysis. Since the leaching reaction of geogenic contaminants might not be equilibrium at less than 24 hours of soil-water contact because the dissolution of minerals takes time, batch leaching tests of more than 24 hours are recommended to obtain the equilibrium concentrations, C_{eq}. If batch tests are finished under non-equilibrium conditions, the obtained concentration might be dangerous. Although the leaching concentration of geogenic contaminants is not as high as that of anthropological contamination (Katsumi 2017, Ito and Katsumi, 2020), the equilibrium should be carefully examined to prevent soil-groundwater contamination without realizing it. If batch leaching tests cannot be conducted due to the limitation of testing time and a 6-hours batch test is conducted, the equilibrium concentration should be estimated higher than the 6-hours test.

Shaking conditions are also essential parameters. Since unrealistic leaching behavior was obtained under shaking conditions, the leaching behavior should be evaluated under nonshaking conditions. This dissertation implies that the friability of the natural soils is considered to give such an unrealistic prediction. When the excavated soils are applied for the leaching tests, the gentle shaking test or nonshaking test should be suitable.

This chapter illustrates the proposal to determine leaching concentrations of geogenic contaminants, considering the findings obtained in this research. When the testing time is enough, batch leaching tests under

the longer soil-water contact time are recommended because the burden of the leaching concentration should not be underestimated. Similar to the results of Chapter 3, the leaching concentration of iron (Fe) and sulfide ion (SO_4^{2-}) from rocks obtained in the mine were not equilibrium even for 100 hours (Igarashi et al., 2002). The leaching concentration of As from rocks containing pyrite might not be equilibrium for short testing time. Therefore, when the testing time is insufficient, and a 6-hour batch leaching test is conducted, the concentration should be assumed to be several times higher. Also, since the friability of the specimen might affect the leaching behavior, the shaking condition should be further discussed. The nonshaking condition might be suitable for the leaching test using friable excavated rock materials, while the time for equilibrium might be longer than the shaking condition. As explained in the first paragraph, since temperature effects are not supposed to be significant, when the excavated soils might be utilized under temperature fraction especially supposed to be higher temperature (e.g., 40°C), leaching concentration obtained under room temperature (20°C) should be considered several times higher to safely evaluate the burden of the leaching concentration of the toxic chemicals.

Chapter 4 performed column leaching tests to discuss the interpretation of concentration profiles. Since the concentration trends of the readily soluble chemicals, such as selenium (Se), provided a monotonous decrease, showed a maximum value of approximately 0 PVF, and showed half of the maximum value of less than 1 PVF, their leaching was considered to diminish immediately. On the other hand, arsenic (As) and fluorine (F) concentrations showed initial increases and consequent decreases. Therefore, their leaching continued after 10 PVF. Since monotonous decreasing leaching contaminants show a maximum concentration of approximately 0 PVF, a more realistic risk analysis can be carried out to obtain the maximum concentration, C_{max}, from column leaching tests. Column tests should be carried out at least 2 PVF when the trends in concentrations are investigated.

This dissertation proposes to conduct the column leaching tests regardless of the time limitation. Since column leaching tests can screen whether the leaching diminishes immediately or not, even in short testing time, column tests should be conducted for precise evaluation. Suppose the contaminants are readily soluble chemicals since long-term countermeasures might not be required. In that case, countermeasures such as the active geocomposite (e.g., Zhang et al., 2023) can be suitable, and the excavated soils can be utilized. The utilization should be carefully discussed, considering the concentrations of geogenic contaminants that might leach for a long time. Since the leaching concentration of such chemicals is difficult to determine in column tests, this dissertation proposes to use the equilibrium concentration, C_{eq}, as one index obtained from the batch tests to design the attenuation layer.

7.2 Evaluating sorption performance of the attenuation layer

Sorption-desorption column tests describe in Chapter 5 showed that since breakthroughs ($C/C_0 > 0.05$) occurred after approximately 1, 20, and 50 PVF for stabilizing agent contents of 1, 5, and 10%, respectively, the amendment using the stabilizing agent can be one effective countermeasures against geogenic contamination, as shown in the previous studies (e.g., Morishita and Wada, 2013; Itaya and Kuninishi, 2020;

Mo et al., 2020; Gathuka et al., 2021; Nishikata et al., 2022). However, when the one-dimensional advection-dispersion equation modelled the breakthrough curves obtained from the column sorption tests, the predictions gave unrealistic estimates, especially for the breakthrough point where $C/C_0 = 0.05$. These results have a crucial meaning for the design of the attenuation layer. If the sorption performance of the stabilizing agent or soil materials by batch tests, since results are arranged by sorption isotherms regardless of the mechanisms of the chemical reactions between soil-water-chemicals, as shown in Fig. 6.1, the breakthrough point must be predicted by the model following the conventional advection-dispersion analysis, as shown in Chapter 6. However, this dissertation elucidated that the breakthrough curves for the soil amended with the stabilizing agent might be difficult to be predicted by the conventional analytical model due to the reactivity of the stabilizing agent. When the sorption performance of the soil materials is evaluated, the breakthrough curves are well predicted because the significant sorption mechanism is considered a relatively quick reaction, such as the adsorption onto the surface of the soil particle (e.g., Igarashi and Shimogaki 1998; Wang and Liu, 2005; Martínez-Lladó et al., 2011). Soil is the natural origin material and has weathered over many years, while the stabilizing agent is the artificially manufactured material. The reactivity of the stabilizing agent is enhanced against contamination (Wada and Morishita, 2013). When the risk assessment, such as the advection-dispersion analysis, is conducted, the difference must be carefully considered. Until now, in the ground improvement field where the stabilizing agent is mixed with soil, the agent is usually added to enhance the stiffness of the soft clay, the resilience against liquefaction, etc. Therefore, fewer studies focus on the soil's seepage and solute transport, as amended with the stabilizing agent. As a future work, the improved solute transport model should be established.

Since the model has yet to be established, the practical solution is to investigate the possibility where geogenic contaminants once stabilized in the attenuation layer are released and mix in a safe amount of stabilizing agent. Chapter 5 presented that, for the 1% agent content, approximately 20% of the sorbed mass, S_s, was desorbed, but the percentage of desorbed mass, S_d, was much smaller for the higher agent contents. The difference between the sorbed and desorbed masses was the immobilized fraction, S_s - S_d. For the 5% agent content, S_s - S_d = 4.0 mg/g, and most fluoride was immobilized in the soil-agent mixture. Considering the results mentioned above, the immobilized fraction, S_s - S_d, obtained from the sorption-desorption column tests can be one index for the design of the attenuation layer.

In Chapter 6, towards the discussion of the design of the attenuation layer, breakthrough curves, which are assumed to be obtained from column sorption tests, are simulated using numerical analysis. Four different methods to obtain partition coefficients, K_d, from breakthrough curves were investigated to discuss the evaluation of the attenuation layer. As a result of the numerical analysis using the advection-dispersion equation, K_d values were determined within approximately 40% differences. The partition coefficient, K_d, obtained using inverse analysis to fit the numerical solution provided the lowest determination. As a result, Chapter 6 suggests that when K_d is determined from column sorption test results, inverse analysis (fitting) from $0 < C/C_0 < 1$ is the best way for the breakthrough curves described by the Freundlich-type sorption model. However, the applicability of the breakthrough curves, such as those obtained from Chapter 5, has yet to be clarified.

Findings from Chapters 5 and 6 imply the difficultness of the attenuation layer design. Although

the schematic diagram of the attenuation layer seems simple, as shown in Figs. 4.10 and 5.1, the fate and transport of the geogenic contaminants are complicated due to the limitation of the solute transport model for the soil amended with the stabilizing agent. Also, since the reactivity of the stabilizing agent might affect the attenuation layer's hydraulic performance and physical properties, the geotechnical aspects should be further studied. Further, considering the leaching behavior of geogenic contaminants shown in Chapters 3 and 4, the leaching concentration should be changed over time. Therefore, the boundary condition of the initial concentration, C_0, should be considered the dynamic parameter. To summarize, the attenuation layer is a simple method, but the design is complex and imperfect. When the countermeasures against geogenic contaminated soils are considered, proper countermeasures, including the full containment or just compaction described in Section 2.3.1 (e.g., Wasaki and Yamawaki, 2012) should be discussed considering the levels of the leaching concentration, the surrounding environment, and the stability of the embankment. Mutual considerations for utilizing excavated soils with geogenic contamination with environmental safety are discussed below.

7.3 Linkage among considerations towards material recycling of excavated soils and rocks with geogenic contamination

Figure 7.1 illustrates mutual relations between contents obtained in each chapter. As explained above, since column leaching tests with even short testing time (e.g., up to 2 PVF) can categorize the leaching behavior of geogenic contaminants, this dissertation highly recommends carrying out the column leaching test. As shown in Chapter 4, when the purpose of the column test is to determine the readily soluble chemicals, a smaller specimen scale than that regulated in the international standard (ISO 21268-3, 2019) can be applied. Considering the specimen saturation step, the column leaching test can be terminated within two days. Therefore, although testing time is really limited under onsite conditions, this 2-day duration for the column tests may be acceptable.

After the column leaching test, readily soluble chemicals are categorized, as shown in Fig. 7.1. Since the leaching behavior of non-readily soluble chemicals is difficult to predict, this dissertation proposes to conduct nonshaking batch tests with different soil-water contact time because of equilibrium concentration, C_{eq} should be obtained to design the countermeasures. As mentioned in Section 7.1, longer soil-water contact time is preferable because the leaching reaction of geogenic contaminants from natural soils is supposed to be relatively slow. On the other hand, for the readily soluble chemicals, since the maximum concentration, C_{max} is obtained from the column mentioned above, the leaching test can be applied because the chemical reaction of the readily soluble chemical is considered to be immediately equilibrium. Therefore, the step of batch leaching tests can be skipped.

Two countermeasures are considered in this dissertation regarding utilizing excavated soils with geogenic contamination with readily soluble chemicals. The countermeasures should be selected depending on the space of the stockyard and time limitations. If enough stockyard space and time are available onsite, pre-washing the excavated soils using rainfall or sprayed groundwater is one possible countermeasure. Since

the readily soluble chemicals leach out immediately up to 2 PVF if leached water is collected at the stockyard, the excavated soils might be utilized as the clean soils. On the other hand, if the space of the stockyard and time are limited, countermeasures that perform the sorption performance against the target contaminants should be installed beneath the excavated soils. Since the readily soluble chemicals leach out immediately, the short-term countermeasures are enough. Herein, methods such as the active geocomposite (e.g., Zhang et al., 2023) or the attenuation layer are promising ways in terms of workability and economics.

The leaching mass, S, should be calculated to estimate the leaching burden and design the countermeasures for non-readily soluble chemicals. Using obtained C_{eq} and L/S, S is calculated as shown in Fig. 7.1. Herein, L/S is decided based on the seepage expected to infiltrate the embankment during the embankment in use and the amount of excavated soils. When the leaching burden is expected to be high, appropriate countermeasures such as geomembrane or clay liner should be applied to prevent soil-ground water contamination because Chapters 5 and 6 elucidated how the design of the attenuation layer is complex. Although using excavated soils with geogenic contamination should proceed more, environmental safety should also be considered. On the other hand, when the leaching concentration is not significant, simple countermeasures such as the attenuation layer or using sorption performance of the original ground can be promising, considering workability and economics.

Figure 7.1 mentions a high or low leaching burden, but the criteria for which concentration is high have yet to be established. The leaching concentration of geogenic contaminants is affected by the type of earthen materials (e.g., soils, rocks), contained minerals (e.g., pyrite, calcite), the environment of the site (e.g., infiltration, weathering, redox condition) and so on (e.g., Tabelin et al., 2018; Tang et al., 2023). Towards the design of the way utilizing excavated soils and rocks with geogenic contamination, the applicability of the attenuation layer and other countermeasures should be further discussed from the perspective of geoenvironmental engineering and geology, geotechnical engineering, and so on.

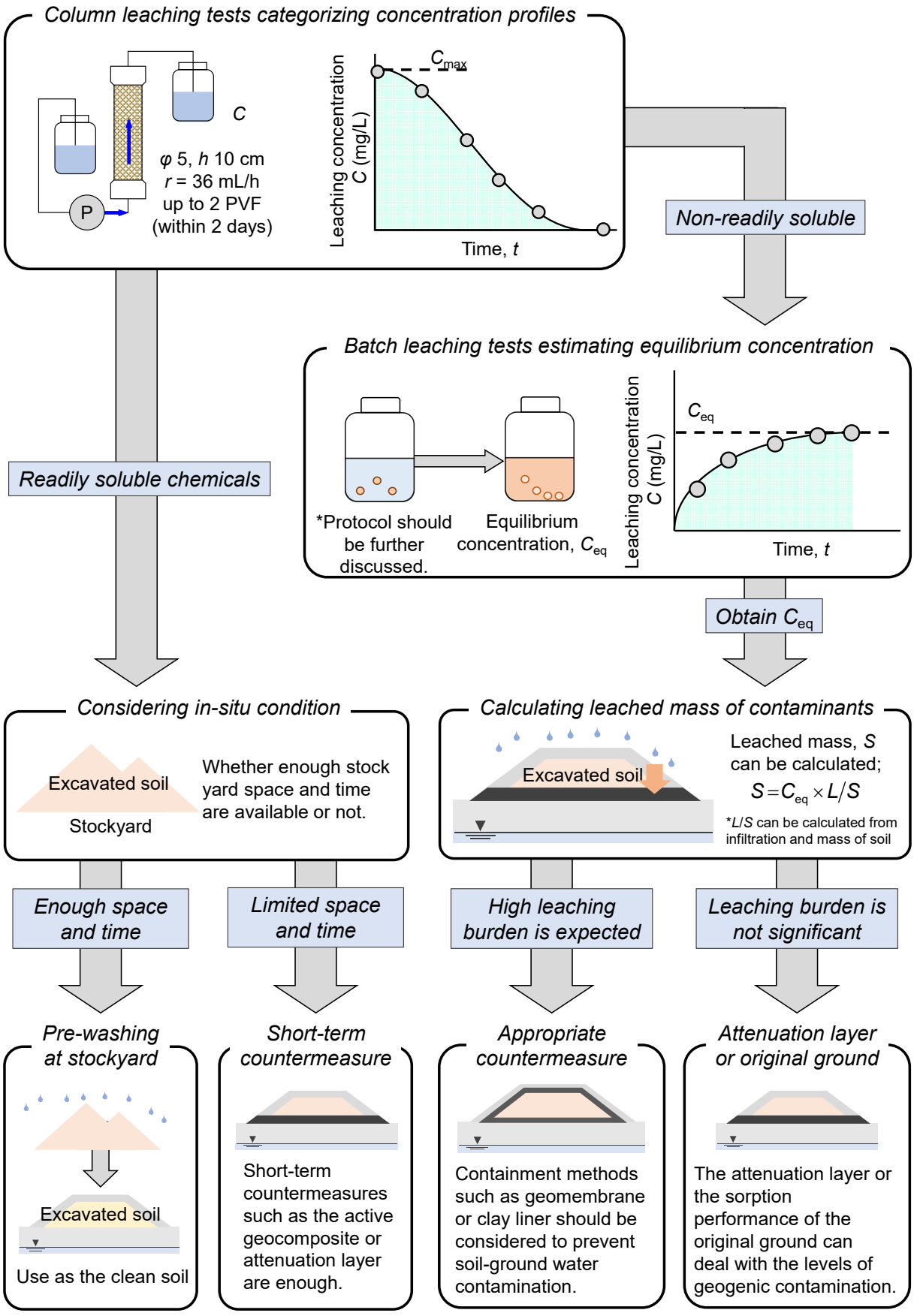

Figure 7.1 Linkage among considerations towards material recycling of surplus soil.

References for Chapter 7

Gathuka, L.W., Kato, T., Takai, A., Flores, G., Inui, T., and Katsumi, T., 2021. Effect of acidity on the attenuation performance of sandy soil amended with granular calcium-magnesium composite. *Soils Foundations* 61(4), 1099–1111. https://doi.org/10.1016/j.sandf.2021.05.007.

Igarashi, T., Izutsu, T., and Oka, Y., 2002. Evaluation of pyrite dissolution rates by two-step leaching model. *Journal of the Japan Society of Engineering Geology* 43(4), 208–215 (in Japanese). https://doi.org/10.5110/jjseg.43.208.

Igarashi, T., and Shimogaki, H., 1998. Migration characteristics of boron by batch and column methods, *Journal of Groundwater Hydrology* 40(2), 121–132 (in Japanese). https://doi.org/10.5917/jagh1987.40.121.

ISO 21268-3, 2019. Soil Quality—Leaching Procedures for Subsequent Chemical and Ecotoxicological Testing of Soil and Soil Materials—Part 3: Up-Flow Percolation Test. *International Standardization Organization*.

Itaya Y., and Kuninishi, K., 2020. Development of selenium insolubilized material eluted from tunnel excavation rock. *Japanese Geotechnical. Journal* 15(3), 435–440 (in Japanese). https://doi.org/10.3208/jgs.15.435.

Ito, H., and Katsumi, T., 2020. Leaching characteristics of naturally derived toxic elements from soils in the western Osaka area: Considerations from the analytical results under the Soil Contamination Countermeasures Act. *Japanese Geotechnical. Journal* 15(1), 119–130 (in Japanese). https://doi.org/10.3208/jgs.15.119.

Katsumi, T., 2017. Use of excavated soils with natural contamination. *Japanese Geotechnical Society Magazine*. 65 (11/12), 1–3 (in Japanese).

Martínez-Lladó, X., Valderrama, C. M. Rovira, Martí, V., Giménez, J., and De Pablo, J., 2011. Sorption and mobility of Sb(V) in calcareous soils of Catalonia (NE Spain): batch and column experiments. *Geoderma* 160, 468–476. https://doi.org/10.1016/j.geoderma.2010.10.017.

Morishita, T. and Wada, S., 2013. Hydration reaction of magnesium oxide in soil. In: *Proceedings of the 48th Symposium on Japanese Geotechnical Society*, Kyoto, Japan (in Japanese).

Mo, J., Flores, G., Inui, T., and Katsumi, T., 2020. Hydraulic and sorption performances of soil amended with calcium-magnesium composite powder against natural arsenic contamination. *Soils and Foundations*, 60(5), 1084–1096. https://doi.org/10.1016/j.sandf.2020.05.007.

Nishikata, M., Yasutaka, T., Morimoto, K., and Imoto, Y., 2022. Evaluation of water contact influence on adsorbents by water immersion pretreatment and serial batch tests. *Japanese Geotechnical. Journal* 17(2), 195–204 (in Japanese). https://doi.org/10.3208/jgs.17.195.

Tabelin, C.B., Igarashi, T., Arima, T., Sato, D., Tatsuhara, T., and Tamoto, S., 2014. Characterization and evaluation of arsenic and boron adsorption onto natural geologic materials, and their application in the disposal of excavated altered rock, Japan. *Geoderma* 213, 163–172. https://doi.org/10.1016/j.geoderma.2013.07.037.

Tabelin, C.B., Igarashi, T., Villacorte-Tabelin, M., Park, I., Opiso, E.M., Ito, M., and Hiroyoshi, N., 2018.

Arsenic, selenium, boron, lead, cadmium, copper, and zinc in naturally contaminated rocks: a review of their sources, modes of enrichment, mechanisms of release, and mitigation strategies. *Science of the Total Environment* 645, 1522–1553. https://doi.org/10.1016/j.scitotenv.2018.07.103.

Tang, J., Sakanakura, H., Takai, A., and Katsumi, T., 2023. Effect of dry-wet cycles on leaching behavior of recovered soil collected from tsunami deposits containing geogenic arsenic. *Soils and Foundations* 63(1), 101271. https://doi.org/10.1016/j.sandf.2022.101271.

Wada, S., and Morishita, T., 2013. Stabilization of heavy metals contaminated soils by magnesium oxide and related chemical and mineralogical reactions. *Journal of the Clay Science Society of Japan* 51, 107–117 (in Japanese). https://doi.org/10.11362/jcssjnendokagaku.48.1_9.

Wang, X. and Liu, X., 2005. Sorption and desorption of radioselenium on calcareous soil and its solid components studied by batch and column experiments. *Applied Radiation and Isotopes* 62, 1–9. https://doi.org/10.1016/j.apradiso.2004.05.081.

Wasaki, K. and Yamawaki S., 2012. A design and construction of gneiss including tge heavy metal and pyrite in Shin Tomei expressway. *Japanese Geotechnical Society Magazine*. 60 (7), 10–13 (in Japanese).

Zhang, Y., Kinoshita, Y., Kato, T., Takai, A., and Katsumi, T., 2023. Attenuation performance of geosynthetic sorption sheets against arsenic subjected to compressive stresses. *Geotextiles and Geomembranes* 51(4), 179–190. https://doi.org/10.1016/j.geotexmem.2023.06.004.

Chapter 8

Conclusions and Future Directions

8.1 Conclusions

This dissertation presents various issues of the utilization of excavated soils with geogenic contamination. Towards fulfilling material recycling of the excavated soils with geogenic contamination, both evaluate the contaminants' leaching behavior and the countermeasures' performance.

In Chapter 1, this dissertation's objectives and contents were explained in conjunction with general information related to this research. The general information includes fundamentals of material recycling of surplus soils with geogenic contamination, a simple overview of the problem of geogenic contamination and the attenuation layer method.

Chapter 2 presents a literature review regarding soil utilization, evaluating the leaching behavior of geogenic contaminants and countermeasures against geogenic contamination. The current status of soil utilization in Japan was explained, and material recycling was emphasized. Regarding the leaching behavior of geogenic contaminants, various testing methods and parameters that previous research focused on were presented. The characteristics of the attenuation layer method were mainly explained for the countermeasures, and how to currently evaluate the sorption performance was shown.

In Chapter 3, The leaching behavior of arsenic and boron is evaluated through two types of excavated rocks with geogenic contamination under different temperatures. Excavated rocks with geogenic contamination are expected to be usable for embankments after appropriate countermeasures have been taken against the risks brought about by geogenic contamination. The leaching behavior might change because of changes in the ground temperature. However, the effects of temperature on the leaching behavior of such rocks have not been well examined. Herein, batch leaching tests at temperatures between 5 and 60°C were performed under shaking and nonshaking conditions. Mudstone and shale rock were crushed into particles smaller than 2 mm, which were required for the tests. The tests were carried out for durations ranging from 6 h to 15 days because changes in leaching kinetics also require careful evaluation.

After conducting the nonshaking tests for 15 days at 40°C, the mudstone sample leached arsenic and boron at concentrations of ~0.7 mg/L and ~1.0 mg/L, respectively. The arsenic and boron concentrations were about 20 and 40% higher than those of the sample leached at a temperature of 20°C. Elevated temperatures were seen to increase the leaching kinetics of the toxic elements. For the shale rock sample, the leaching rate for arsenic was 7.7×10^{-2}/h at 40°C, which was approximately 2.5 times greater than the value at 30°C. The nonshaking tests showed higher leaching amounts of arsenic and boron than the shaking tests,

especially at elevated temperatures. As unrealistic estimations should be avoided, nonshaking tests are suggested. Moreover, nonshaking tests lasting longer than 6 h are necessary due to the relatively slow dissolution of minerals.

In Chapter 4, up-flow column percolation tests were conducted to discuss the rigor interpretations and the engineering applications, adequate descriptions of which have been limited. Two types of marine sediments were tested using the two different sizes of columns (ϕ 5 cm× h 10 or 30 cm) with a flow rate of 12 or 36 mL/h. Trends in concentrations with pore volumes of flow (PVF) were examined.

As a result of column leaching tests, since the concentration trends of selenium provided a monotonous decrease and showed the maximum value of approximately 0 PVF, and showed half of the maximum value less than 1 PVF, their leaching was considered to diminish immediately. On the other hand, arsenic and fluorine concentrations showed initial increases and consequent decreases, therefore their leaching continued after 10 PVF. Since monotonous decreasing leaching contaminants show the maximum concentration of approximately 0 PVF, a more realistic risk analysis can be conducted to obtain the maximum concentration from column tests. To investigate the trends in concentrations, column tests should be carried out at least 2 PVF.

In Chapter 5, sorption-desorption column tests using acrylic columns (ϕ 5 cm × h 10 cm) were employed to evaluate the sorption performance of an attenuation layer against geogenic contamination. The attenuation layer material was silica sand amended with 1, 5, or 10% of a stabilizing agent. The main component of the agent was magnesium oxide. The sorption behavior of the materials was determined by a fluoride solution (C_0 = 80 mg/L F^-), while the desorption behavior was determined by distilled water.

As a result of sorption-desorption column tests, breakthroughs (C/C_0 > 0.05) occurred after approximately 1, 20, and 50 PVF for stabilizing agent contents of 1, 5, and 10%, respectively. The one-dimensional advection-dispersion equation modelled the breakthrough curves obtained from the tests. The predictions gave unrealistic estimates, especially for the breakthrough point where C/C_0 = 0.05. For the 1% agent content, approximately 20% of the sorbed mass, S_s, was desorbed, but the percentage of desorbed mass, S_d, was much smaller for the higher agent contents. The difference between the sorbed and desorbed masses was defined as the immobilized fraction, S_s - S_d. For the 5% agent content, S_s - S_d = 4.0 mg/g. The results suggest that when silica sand is amended with magnesium oxide as an agent, the mixture can immobilize the fluoride in the attenuation layer.

In Chapter 6, towards the discussing the design of the attenuation layer, breakthrough curves which are assumed to be obtained from column sorption tests are simulated using numerical analysis. Four different methods to obtain partition coefficients from breakthrough curves are discussed to investigate the evaluation of attenuation layer. The one-dimensional advection-dispersion analysis was conducted considering attenuation layer of 30 cm thickness using these obtained partition coefficients, K_d.

As a result of the numerical analysis using advection-dispersion equation, K_d values were determined within approximately 40% differences. The partition coefficient, K_d obtained using inverse analysis to fit numerical solution provided the lowest determination, and earlier breakthrough than the parameters determined by Freundlich parameters.

In Chapter 7, the interpretation of results was described, taking into consideration practical

implications. Based on the findings obtained from Chapters 3 and 4, one consideration of determining leaching concentrations of geogenic contaminants was presented. Herein, the combination of the short-term column leaching tests up to liquid-to-solid ratio (L/S) of 2 and nonshaking batch leaching tests were proposed to categorize whether the leaching behavior were judged as the readily soluble chemical and investigate the equilibrium concentration. Also, the limitation of conventional risk assessment using the advection-dispersion analysis is shown based on the findings obtained from Chapter 5. Considering the difficulty of predicting breakthrough curves of soil amended with the stabilizing agent, immobilized fraction can be one of the indices for the attenuation layer design. Based on the results in Chapters 5 and 6, this dissertation stated that the applicability of the attenuation layer should be carefully discussed. In this chapter, mutual relations between the results were finally discussed.

8.2 Future directions

Herein, the issues regarding evaluating leaching behavior, performance of the attenuation layer, and earthen cover are presented. Also, since future work on the utilization of excavated soils with geogenic contamination soils should be extended from the geoenvironmental engineering field, the issues regarding geotechnical aspects and regulatory science are mentioned.

Regarding the leaching behavior of geogenic contaminants, first of all, further research simulating the reality is required. Chapter 3 evaluated the leaching behavior under a liquid-to-solid ratio of 10. If the conditions of the liquid-to-solid ratio differ, the equilibrium concentration might be affected. Tests under small liquid-to-solid ratio closer to the in-situ condition are necessary. In addition, the effect of the friability of rocks should be evaluated to simulate the leaching behavior more precisely. Pre-crushing of the specimen is considered as one way. Although the effect of temperature, soil-water contact time, and shaking conditions were investigated in this dissertation, some parameters still need to be well investigated. As explained in Chapter 2, since the leaching behavior of several contaminants, such as arsenic or selenium, is affected by the redox conditions because their chemical species changes, the leaching test simulating the redox condition is necessary. Also, the scale effects of the leaching tests should be investigated. Chapter 4 compared the difference in height of 10 and 30 cm, which was not significant in this study. However, since the final goal is to discuss the utilization of excavated soils with geogenic contamination as geomaterials for the embankment, the scale effect between lab-scale test (e.g., 30 cm) and practical condition (e.g., 5 m) should be investigated. The on-site embankment tests and the embankment monitoring (already exist) are desirable to be conducted. In this dissertation, batch leaching tests were conducted in Chapter 3, while column tests were conducted in Chapter 4. As a direction of evaluating the behavior of geogenic contaminants, although a complex protocol test such as a column leaching test can obtain more information than a simple test such as a batch test, only a short-term batch test can be conducted in some construction sites due to the time limitation. The relation between the batch test (closed-type test) and the column test (flowthrough-type test) should be elucidated for the practical field. In the future, simple parameters obtained from batch tests are expected to predict the concentration profiles of column tests. In addition, the number of investigations needs to be increased.

Chapters 3 and 4 discussed the leaching behavior using two different excavated earthen materials, but the samples should be increased to obtain a generalized finding.

Issues regarding the sorption performance of the attenuation layer are presented here. First, the sorption testing methods should be standardized. Currently, each material company will conduct the sorption test so that its stabilizing can perform the highest sorption performance. Namely, the batch testing conditions, such as liquid-to-solid ratios, agent-water contact time, and specimen preparation ways differ. Also, various flow rates, scale of the column, and mixing ratios are applied in the column tests. Therefore, when the attenuation layer is designed, constructors have difficulty selecting the stabilizing agent because the sorption performance of the stabilizing agent is difficult to compare. This background prevents the spread of the attenuation layer method. Second, the results of column sorption tests using stabilizing agents should be accumulated. As mentioned in Chapter 5, the breakthrough curves using the reactive stabilizing agent are challenging to predict using the conventional advection-dispersion equations. In order to establish the solute transport model accounting for the soil-water-chemical reaction where the stabilizing agent is mixed, the parameters such as column heights, initial concentrations, and types of the stabilizing agent should be investigated in the column sorption tests. Third, the competition of the sorption reaction should be carefully examined. Since natural soils and rocks contain not only geogenic contaminants but also other elements (e.g., sodium (Na), magnesium (Mg), potassium (K), calcium (Ca), and sulfide (S)), as shown in Chapter 3, the sorption performance should be evaluated using the solution which contains not only the target contaminants but also other significant ions for closer evaluation to reality. One possible way is sorption tests using the leachate of the leaching tests. Fourth, since a slight amount of the stabilizing agent is mixed with the parent material, how to mix the stabilizing agent homogeneously should be investigated to increase the geoenvironmental reliability of the attenuation layer.

The function of the earthen cover should be featured. As shown in the schematic diagrams of the attenuation layer method, the cover soil layer is usually considered to be installed. Since the covered soil layer is well compacted to prevent infiltration to the embankment, most rainfall can be considered not to seepage into the embankment. However, the current leaching tests are conducted with a relatively sizeable liquid-to-solid ratio. Further, since embankments have a relatively steep slope (e.g., 30°) and greening, some rainfall can be the surface flow and does not permeate the embankment. Therefore, contaminants are easier to leach from the solid (soil), and a very conservatively high leaching burden might be estimated because of this testing condition. Towards a more realistic design of the attenuation layer, the function of the cover layer preventing the infiltration should be more attention for the utilization of the surplus soils.

Geotechnical aspects must be discussed, such as evaluating the hydraulic performance and physical properties of the embankment and the attenuation layer. As shown in Chapter 7, the impact of the stabilizing agent's reactiveness on the solute transport analysis prediction was pointed out. This impact may influence the hydraulic conductivity and strength of the attenuation layer and embankments. If the stabilizing agent hydrates, the ground may be stiff. The hydraulic conductivity of the attenuation layer may decrease, and the embankment becomes weak because the saturation degree increases. Further, if pore water containing geogenic contaminants cannot permeate into the attenuation layer, the pore water may leach out from the side of the embankment. Also, the degree of compaction should be discussed because the state of compaction

affects both the stability and permeability of the embankment. Geotechnical aspects should be considered in the design of the attenuation layer to ensure both environmental safety and stability of the earth's structure.

Finally, the necessity of both laboratory and regulatory science is presented here. When the risk communication achieves the consensus to use excavated soils with geogenic contamination that slightly exceed the environmental standard regulated by SCCL, the use of the excavated soils with geogenic contamination can proceed. A mature, comprehensive understanding of geogenic contamination from perspectives such as geology, law, social study, and geotechnical, geoenvironmental, and environmental engineering is expected.